

Drawing a Map of Elections*

Stanisław Szufa^{1,2}, Niclas Boehmer³, Robert Brederick⁴, Piotr Faliszewski¹, Rolf Niedermeier⁵, Piotr Skowron⁶, Arkadii Slinko⁷, and Nimrod Talmon⁸

¹AGH University, {faliszew,szufa}@agh.edu.pl

²CNRS, LAMSADE, Université Paris Dauphine – PSL, s.szufa@gmail.com

³Hasso Plattner Institute, University of Potsdam, niclas.boehmer@hpi.de

⁴Institut für Informatik, TU Clausthal, robert.bredereck@tu-clausthal.de

⁵Technische Universität Berlin, Algorithmics and Computational Complexity

⁶University of Warsaw, p.skowron@mimuw.edu.pl

⁷University of Auckland, a.slinko@auckland.ac.nz

⁸Ben-Gurion University, talmonn@bgu.ac.il

Abstract

Our main contribution is the introduction of the map of elections framework. A map of elections consists of three main elements: (1) a dataset of elections (i.e., collections of ordinal votes over given sets of candidates), (2) a way of measuring similarities between these elections, and (3) a representation of the elections in the 2D Euclidean space as points, so that the more similar two elections are, the closer are their points. In our maps, we mostly focus on datasets of synthetic elections, but we also show an example of a map over real-life ones. To measure similarities, we would have preferred to use, e.g., the isomorphic swap distance, but this is infeasible due to its high computational complexity. Hence, we propose polynomial-time computable positionwise distance and use it instead. Regarding the representations in 2D Euclidean space, we mostly use the Kamada-Kawai algorithm, but we also show two alternatives. We develop the necessary theoretical results to form our maps and argue experimentally that they are accurate and credible. Further, we show how coloring the elections in a map according to various criteria helps in analyzing results of a number of experiments. In particular, we show colorings according to the scores of winning candidates or committees, running times of ILP-based winner determination algorithms, and approximation ratios achieved by particular algorithms.

1 Introduction

Alongside theoretical research, experimental studies are in the very heart of *computational social choice* [29]. Computational aspects of elections, such as the problems of winner determination [42, 64, 89, 97], identifying and analyzing various forms of manipulation [5, 43, 73, 81, 88, 124] or control [31, 59, 128], measuring candidate performance [18, 27, 33], and preference elicitation [11, 90, 107] are nowadays often investigated through experiments. For example, researchers evaluate running times of algorithms [65, 125, 127], or test what approximation ratios appear in practice [81, 116]. It is also common to test non-computational properties of elections and voting rules—for instance to evaluate how frequently a given phenomenon occurs (e.g., how frequently a given voting

*This paper merges results from an AAMAS-2020 paper [120], an IJCAI-2021 paper [19], and the PhD thesis of Szufa [119]. In particular, most of Sections 4 and 5, as well as significant fragments of Section 6, were not published in either of the two conference papers, or were published in very rudimentary forms. Code and data for the paper are available at <https://github.com/Project-PRAGMA/Journal---Drawing-a-Map-of-Elections>.

rule is manipulable [59, 73, 125], or how frequently particular candidates win [55]; naturally, the cited papers are just a few examples). Yet, designing convincing experiments is not easy and, in particular, it is not clear what election data to use.

The main contribution of this paper is setting up the “map of elections” framework, which allows one to build and visualize election datasets, and helps in planning and evaluating experiments. Further, we argue that the framework is useful by showcasing a number of its applications. We focus on ordinal elections, i.e., on the setting where an election consists of a set of candidates and a collection of voters that rank the candidates from the most to the least desirable ones. For results regarding approval elections we point the reader to the follow-up work of Szufa et al. [121].

1.1 Motivating Example

Imagine we are interested in the Harmonic Borda [63] (HB) multiwinner voting rule. Under this rule we are given an ordinal election and an integer k , and the rule chooses a committee of k candidates that minimizes the sum of dissatisfaction scores assigned by the voters; it is a variant of the classic proportional approval voting rule, PAV [82, 122] (see Section 5.2.1 for a detailed definition). Finding a winning committee under this rule is NP-hard [117], but such a committee can be computed, e.g., using ILP solvers (i.e., solvers for integer linear programming problems). We want to assess how quickly an ILP solver can compute the winning committees.

Ideally, we would want to try all elections of a given size. For example, elections with 100 candidates and 100 voters are common in the multiwinner literature [38, 55, 64]; see also the overview of Boehmer et al. [26]. Naturally, this is infeasible. Instead, a natural approach is to generate elections according to several standard distributions, referred to as *statistical cultures*, and test the algorithms on them.¹ Indeed, many of the above-cited papers focus on some subset of the following four models (see Section 2 for detailed descriptions of the distributions):

1. The impartial culture (IC) model, where all votes are generated uniformly at random and independently (this is one of the most popular models in experiments, often used as a baseline for other experiments [59, 73, 81, 116, 125, 127]).
2. The Polya-Eggenberger urn model [13, 95], which proceeds similarly to the impartial culture one, but already generated votes have increased probability of being generated again—as specified by a “contagion” parameter—and, hence, the model introduces correlations. The model is quite common in various experiments [59, 65, 81, 116, 125].
3. The Mallows model [92], and its mixtures, where the probability of generating a vote depends on its similarity to a preselected central one (a dispersion parameter controls the concentration of the generated votes). Mallows model is particularly natural for settings with some sort of a ground truth [12, 30, 73, 97, 116].
4. The Euclidean model [57, 58], where candidates and voters are drawn as points in a Euclidean space and the closer a candidate is to a voter, the more this voter appreciates this candidate, is also common in recent experiments [30, 55, 65, 84]; the way of generating the ideological positions of the candidates and voters is the parameter of the model.

However, which of these models should we use and how should we set their parameters? Perhaps we should also use some other models as well, possibly generating elections that are single-peaked [16],

¹It would also be natural to consider real-life elections (e.g., from Preflib [93], or those collected by Boehmer and Schaar [17], currently also included in Preflib). However, many sources of real-life elections lead to data over relatively few candidates (often just three or four [94, 123], although elections with 15 and more candidates are not uncommon either). Accordingly, such elections would not suffice for our experiments (yet, they are useful in other cases; see, e.g., the works of Brandt et al. [30] and Ayadi et al. [4]).

single-crossing [99, 112], group-separable [76, 77], or that are structured in some other way? Intuitively, we would like to have a set of elections that would be as varied as possible for our experiment, so that, on the one hand, we would not spend too much time on very similar elections—for which we expect nearly identical results of the experiments—and, on the other hand, we would not miss interesting families of elections—for which the results would be hard to predict.

Unfortunately, researchers working on elections only recently started to ask and carefully answer questions like the ones given above, though, of course, there are examples of older experimental papers that address these issues in detail; see, e.g., the work of Brandt et al. [30]. This view is supported by a recent analysis by Boehmer et al. [26] of over 160 papers that include numerical experiments on elections and were published between 2009 and 2023 in the IJCAI, AAAI, and AAMAS conference series. In particular, the authors found that in about half of the papers that considered ordinal elections (of which there were a bit over 120), researchers only used a single data source.² While the situation has been improving over time and in recent papers researchers do use more varied data, the process is slow³ and principled advice on how experiments should be conducted is missing.

As reported by Boehmer et al. [26], nearly two-thirds of papers that include experiments on elections rely on synthetically generated data, without looking at any elections based on real-life data. While this is natural—real-life data relevant to a particular setting is not easy to come by—it reinforces the need for a good understanding of how elections generated synthetically relate to each other and to elections occurring in practice. Indeed, many papers do not seem to be making informed decisions on which data sources to include and either rely on intuitions or on copying approaches of previous authors working on similar topics (see the discussion of election sizes in the work of Boehmer et al. [26], where the authors discuss typical application scenarios).

Our main motivation behind the map of elections framework is to help with solving the issues mentioned above. In particular, the maps help with analyzing and using diverse data sources and with relating synthetic elections to real-life ones.

1.2 Maps of Elections

Our main idea is that given a set of elections we may arrange them as points on a plane, so that the Euclidean distances between the points would indicate the similarity between the corresponding elections. Such points form a map, which can then be colored in a number of ways. For example, each color may correspond to the statistical culture (or, a real-life dataset) from which the given election comes, or to some feature of the election. We show two examples of such maps and the former type of coloring in Figure 1. In Section 5, we show a number of colorings of the latter type, including ones related to the motivating example from Section 1.1.

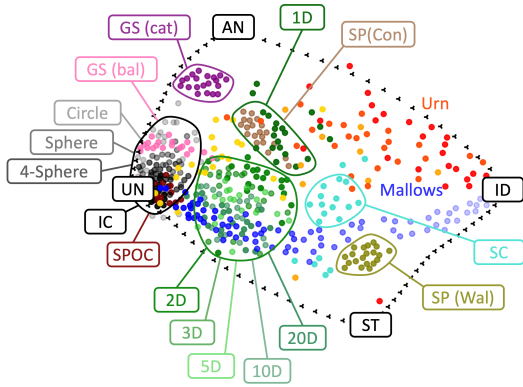
Preparing a map requires three main components: (1) the set of elections that we want to work with, (2) the way of measuring similarities between the elections, and (3) the way of embedding points on the plane that respects these similarities. We describe and evaluate these components in detail in Section 3 and Section 4. Below we give a quick overview.

Election Datasets and Compass. We mostly focus on synthetic elections, generated from various statistical cultures, such as those mentioned in the motivating example above. Specifically, we build several election datasets, where each of them consists of 480 elections that come from several well-known cultures, with various parameter settings,⁴ with each dataset involving a different number of

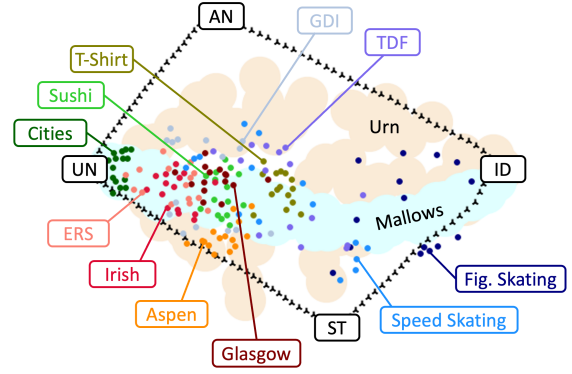
²If one’s paper were to address a specific practical problem only using real-life data from the relevant data source can be justified. However, many of these papers relied on the highly unrealistic impartial culture model, which may put some doubt on the relevance and generalizability of their results.

³According to Boehmer et al. [26], in 2023 still about half of the papers studying ordinal elections used only one or two data sources.

⁴We additionally use 84 elections that help us navigate through the map.



(a) A map of synthetic elections.



(b) A map of various real-life elections.

Figure 1: Two examples of maps of elections. Each point on each of the maps represents an election with 10 candidates and 100 voters. Elections on the left were generated using various statistical cultures (as reflected by their colors), whereas those on the right were derived from real-life data (after appropriate preprocessing). We define various statistical cultures in Section 2.3. Maps of synthetic elections are discussed in detail in Section 4, whereas the map of real-life elections is discussed in Section 6; the maps will become fully comprehensible only after reading these sections. The maps include four special points (UN, ID, ST, AN), to which we refer as the “compass,” and their connecting paths. The map on the right also includes pale blue and orange areas, which represent places where Mallows and urn elections would land, respectively.

candidates. The idea is that if one wants to perform some computational experiment on elections, a priori it is not clear which models are most interesting to consider. Our datasets contain elections sampled from many different ones, so that one could use these datasets for initial studies and only then decide which models to use in follow-up, more focused experiments. That said, our choices are, of course, somewhat arbitrary and one may as well prefer other combinations of models and their parameters. We complement our results on the synthetic models by also considering elections derived from real-life data, available in Preflib [93] or collected by Boehmer and Schaar [17] (the latter ones are now included within Preflib).

In addition to the base content, all our datasets also include a number of elections that help in navigating the maps. In particular, these elections include what we call “the compass,” that is, four elections that capture four different types of (dis)agreement among the voters:

1. The identity election, ID, which models perfect agreement and contains voters that all have the same preference order.
2. The uniformity election, UN, which models perfect lack of agreement (or, chaos) and contains voters with all possible preference orders.
3. The stratification election, ST, which models partial agreement, where voters agree that half of the candidates are better than those in the other half, but lack agreement on anything else.
4. The antagonism election, AN, which models a conflict where half of the voters have one preference order and the other half has the opposite one.

Besides the compass elections themselves, we also include *paths* of intermediate elections in between them. For example, a path from ID to AN can be seen as consisting of elections where, initially, all voters agree on a single preference order, but as we move toward AN, more and more voters report the opposite one.

Similarities Between Elections. To measure the similarity of our elections, we need a notion of a distance. Furthermore, this distance needs to be both neutral and anonymous—i.e., independent of the names of both the candidates and the voters. Indeed, we want to compare elections generated from statistical cultures, where this information is random, as well as elections that come from different real-life datasets, whose candidates and voters are unrelated. Such distances were studied by Faliszewski et al. [70], who—in particular—proposed the isomorphic variants of the swap and Spearman distances, which satisfy our requirements. However, while these distances have many attractive features [22], they also are NP-hard to compute, which makes them difficult to use on elections with more than a few candidates. Since we want our framework to be scalable, we provide a new distance, which we call *positionwise*. This distance is less precise than the isomorphic ones, but still satisfies our desiderata, is computable in polynomial time, and appears to give meaningful results.

Briefly put, the key idea of the positionwise distance is to not work directly on elections and votes, but to use an aggregate representation. Specifically, given an election with m candidates, its *frequency matrix* is an $m \times m$ matrix where the columns correspond to the candidates, the rows correspond to the positions in the votes, and the entries give fractions of the votes where a given candidate was ranked on a given position. Positionwise distance measures the distance between such matrices. An added benefit of using frequency matrices is that we show a nearly 1-to-1 correspondence between them and elections with a given number of voters. Consequently, instead of working directly with our compass elections, it is often more convenient to work with their matrices. Generally, we often speak of matrices and elections interchangeably.

Embedding Algorithms. There is a number of algorithms that given a set of objects and distances between each pair of these objects find their embedding as points on a plane (or, other Euclidean space), so that the Euclidean distances between the points resemble those between the objects that they represent. (getting perfect embedding is often impossible; as an example, consider embedding 10 points on a plane, where each pair is supposed to be at the same distance). These algorithms may either focus on obtaining embeddings that are more visually pleasing, or may strive for as high accuracy as possible.

In most of our visualizations, we use the Kamada-Kawai algorithm [78], which belongs to the latter group and which gave the most accurate embeddings according to a number of criteria (another example of such an algorithm is the Multidimensional Scaling algorithm, MDS, [44, 83], but it did not perform as well). A brief idea of the Kamada-Kawai algorithm is that it considers the points to be embedded as vertices in the 2D space that are connected with springs. Each spring has its resting length corresponding to the desired distance (the positionwise distance in our case) between its two endpoints, but typically it is either stretched or compressed. The algorithm iteratively moves the vertices to minimize the energy of the system. The original algorithm uses the Newton-Raphson method for this purpose, but we use the faster optimization method presented by Barzilai and Borwein [7]. For a comparison of the two variants of the Kamada-Kawai algorithm with the two optimization methods, see the work of Pospisil et al. [109]; we point to the work of Sapała [114] for the implementation that we use.

We note that in some cases the force-directed algorithm of Fruchterman and Reingold [71], which belongs to the group of algorithms that prioritize creating a visually pleasing embedding, also can be useful. In particular, it produces embeddings where the election points are more spread over the plane, which in some circumstances can help with the analysis of the map; such a more spread map still shows the main relations between various elections, but the points do not overlap and it is easier to see their colors. We conduct a quantitative comparisons of the different embeddings produced by these algorithms in Appendix B.

1.3 Use Cases for the Maps

There is a number of ways in which maps of elections can help in conducting numerical experiments. Below we give three general types of experiments where maps can be helpful:

Finding Relations Between Elections. By their very nature, maps arrange elections in 2D space, so that similar elections are close to each other. By examining a map and comparing the positions of particular elections to each other and to the characteristic compass elections, we learn about their nature and properties. For example, in Section 4 we form a dataset of elections generated from various statistical cultures and find how they relate to each other by drawing a map where each election has a color that specifies the statistical culture from which it was generated. Among other findings, we observe how the Conitzer and Walsh models for generating single-peaked elections produce elections that are quite different from each other, and how the Conitzer model is similar to the 1D Euclidean model. This type of experiment also allowed Boehmer et al. [19, 24] to discover that the dispersion parameter in the Mallows model may need normalization, and to propose such a normalization. Perhaps most importantly, by looking at positions where elections land on the maps, we get a better understanding as to which areas of the election space are not covered by our datasets. This encourages forming more diverse datasets for further experiments (indeed, we form such a dataset in Section 4). Further, experiments where we analyze the positions of elections on the map allow us to learn about real-life data. For example, while there are statistical cultures that generate highly polarized elections—i.e., elections close to the antagonism compass election—real-life elections rarely fall in the respective region of the map (see Section 6). By analyzing the proximity of real-life elections to those generated from statistical cultures, we may also learn which cultures (have a chance to) generate realistic data. We show some results in this direction in Section 6; in a follow-up paper, Boehmer et al. [20] pursue this direction more systematically.

Visualizing Election Properties. Given a dataset of elections, we may want to learn something about some of their features, such as the Borda scores of their winners (see Section 5.1), the running times an ILP solver takes to compute their winners according to some NP-hard voting rules (see Section 5.2), or many others. In this case, we color the elections on the map according to a given feature. This way we obtain a comprehensible bird’s eye view at the results for all the elections, without resorting to computing averages or other statistics (naturally, these statistics are also important—the maps simply offer a different perspective and an ability to spot issues that otherwise would not be as readily visible). In the most beneficial case, we learn that the considered features closely depend on elections’ positions on the map. For example, in Section 5.1 we find that Borda scores of the winners tend to increase as we move from the uniformity compass election toward the identity one. In Section 5.2 we see a similar phenomenon for the running time required to find Harmonic Borda winners using an ILP solver. Another possibility is that we would spot some pattern regarding the considered feature and statistical cultures present on the map. For example, in Section 5.2 we observe that an ILP formulation for computing the results of the Dodgson rule tends to require a close-to-fixed amount of time for elections from all our statistical cultures (for a given fixed size of elections) except for two, where on one it is much faster and on the other it is much slower. Maps that include diverse statistical cultures facilitate such observations because they include varied data⁵ and allow one to see the results “all at once.” An experiment of the type described here was recently provided by Contet et al. [41], where the map was used to analyze the sizes of explanations regarding why a particular candidate won in a given election.

⁵As shown by Boehmer et al. [26], many computational social choice papers that include experiments on elections limit their attention to a small collection of statistical cultures. When performing experiments on such limited data it is very easy to overlook such phenomena as described here.

Comparing Algorithm Performance. The third use case is when we want to compare, e.g., how two different algorithms perform on elections from a given dataset. As an example, in Section 5.3 we take two approximation algorithms for the NP-hard Chamberlin–Courant multiwinner voting rule [39] and compute the approximation ratios they achieve on our elections. Then, we color the elections on the map according to the algorithm that performed better (with the blue color for one algorithm and red for the other) and its performance (the better is the achieved approximation ratio, the darker is the color). Such an experiment is particularly useful for areas of the map where, on average, both algorithms perform similarly but where on particular elections one of the algorithms is notably better than the other one: Various colorings of the map allow us to spot such places more easily than using basic statistics (such as the average approximation ratio on elections from a given statistical culture). Recently, a similar visualization was used by Delemazure and Peters [45], who analyzed two different ways of generalizing the STV voting rule to elections where voters can express indifferences.

We want to stress that, in principle, all the experiments and types of experiments that we described above could be performed without maps and without the visualizations that they offer, possibly letting one reach the same conclusions and spotting the same phenomena as using the maps. The main advantage of using the maps is that it may be significantly easier to make relevant observations and reach particular conclusions. We also stress that the researchers can take advantage of our maps even without including the actual plots in their papers. For example, they may run their initial experiments using our diverse, synthetic datasets, analyze the maps to see where interesting phenomena happen, and then focus only on those areas. Indeed, this is how the map framework was used, e.g., in the works of Boehmer et al. [18] and Boehmer et al. [21]. That said, the maps also have a number of drawbacks and there are challenges that one faces when using them. We describe them throughout the paper and summarize them in Section 7.

1.4 Related Work

To the best of our knowledge, this paper is the first to provide a principled framework for analyzing and visualizing election datasets. In this respect, we are not aware of previous works to which we can directly compare our approach. Nonetheless, we do build on numerous ideas that were already present in the literature, and we continued working on the topic. Below we review both our follow-up works and other related literature.

The Map Framework. This paper is based on two conference papers, where the first one proposed the map framework and showed its usefulness through initial experiments [120], and the second one added, e.g., the compass elections, analysis of position and frequency matrices, and studies of real-life data [19]. The paper is also based on fragments of the PhD thesis of Stanisław Szufa [119]. Both conference papers also included content that we decided to omit—sometimes to maintain focus, sometimes because further research showed that our initial ideas were misguided, and sometimes because they deserved more detailed treatment than we could have provided here. We also show some additional results, not present in either of the two papers. Indeed, most of Sections 4 and 5 present new material; Section 6.3 also is new. Yet, on the whole, the current paper can largely be seen as a union of the two initial works and fragments of the PhD thesis. Next we give an overview of the follow-up papers that regard the framework.

Boehmer et al. [20] extended the map framework by observing that the positionwise distance can be applied not only to elections, but also to distributions over votes—such as impartial culture, the Mallows distribution, or various distributions of single-peaked votes—by measuring distances between the expected frequency matrices of such distributions. They have provided a number of ways of computing

such matrices and have shown that they can be used for learning parameters of the models that, e.g., are as close as possible to various real-life elections. In this sense, their work put a principled layer over the analysis of real-life elections that we provide in Section 6.4.

The work of Boehmer et al. [20] can also be seen as presenting one more argument—on top of low computational complexity and apparent usefulness—for using the positionwise distance in the map framework. Yet, a priori, it is not really clear if the positionwise distance really is making a good compromise between computational complexity and expressivity. Perhaps an even simpler distance would give equally good (or, only slightly worse) results? Or, maybe, the results given by the positionwise distance are too far off and we should seek a different approach? This issue was addressed by Boehmer et al. [22], who compared several distances and analyzed their properties. In the end, they concluded that the compromise offered by the positionwise distance indeed is appealing. However, if one considers small enough elections or has sufficient computing power, using the isomorphic swap distance certainly *is* preferable, as done, e.g., by Faliszewski et al. [67], who explain the positions of elections on the map—generated according to the isomorphic swap distance—using the notions of agreement, diversity, and polarization among the voters. Boehmer et al. [23] have shown a number of downsides and difficulties that may arise when using the positionwise distance, but they also concluded that on typical datasets, such as those that we use in this paper, the issues are not significant.

Maps of elections already proved useful in planning and conducting several experiments and we mentioned some such examples in Section 1.3.

While our work focuses on ordinal elections, in principle the map framework can be applied to any type of objects, provided that one can find an appropriate distance and, possibly, a set of compass points to navigate the map. So far, this was done by Szufa et al. [121] for the case of approval elections (i.e., elections where each vote is a set of candidates that a given voter finds appealing), by Boehmer et al. [25] for the case of the stable roommates problem (in this problem we have a group of people who have ordinal preferences over the other ones, regarding who to be teamed-up with), and by Faliszewski et al. [68] for the case of approval-based multiwinner voting rules. Further, Faliszewski et al. [67] have used the same approach for visualizing particular votes within a single election.

Distances. There is a number of works in computational social choice that use various forms of distances, either between votes or between whole elections. For example, this is the case in the distance rationalizability framework [54, 74, 96, 102, 115] (see also the overview of Elkind and Slinko [53]) or in various works that use distances to define forms of manipulating elections [3, 10, 48, 103] or to analyze the space of elections [104, 105]. The main difference between these works and ours is that they consider distances between elections with the same candidate sets, whereas we allow these sets to differ (although we do require them to be of the same cardinality). We point the readers interested in an encyclopedic listing of various kinds of distances to the work of Deza and Deza [49].

Election Data. Our datasets mostly consist of synthetic data, generated according to a number of prominent (and not-so-prominent) statistical cultures. We describe these cultures and give appropriate references in Section 2.3. In Section 6, we also draw a map of real-world elections. In this map, we include elections from all datasets from Preflib⁶ that contain at least ten candidates and in which votes are not heavily incomplete (see Appendix C for an overview of the Preflib datasets that we considered and the reasons for rejecting many of them). These elections include the now-classic Sushi preferences collected by Kamishima [79], elections from the city councils of Aspen and Glasgow [106], and surveys regarding costs of living and populations of a number of cities [37]. Moreover, we included three datasets capturing sports competitions, collected by Boehmer and Schaar [17]. Naturally, there is also a number of other sources of real-life data that one might use, but which we do not include in our experiments

⁶We refer to the contents of Preflib prior to extending it with the datasets collected by Boehmer and Schaar [17].

(also, oftentimes, these elections have below ten candidates). For example, there are extensive datasets from field experiments held during French presidential elections [8, 9, 28, 86] and during German state and federal ones [2].

Embedding Algorithms. There is a number of algorithms that one could use to obtain an embedding of points in space in a way that attempts to respect their prescribed distances. For example, one could consider the Principal Component Analysis [98], t -Distributed Stochastic Neighbor Embeddings (t -SNE) [46, 47], or Locally Linear Embeddings [50, 129]. We have tried these algorithms, but the results were highly unsatisfactory on our data. Instead, we focus on the algorithm of Kamada and Kawai [78] (as adapted by Sapala [114]), which work by simulating a system of springs. In Appendix B we also compare it to the algorithms of Fruchterman and Reingold [71] and to (metric) Multidimensional Scaling [44, 83], which also perform well.

2 Preliminaries

We write \mathbb{R}_+ to denote the set of non-negative real numbers. For an integer n , we write $[n]$ to denote the set $\{1, \dots, n\}$. Given a vector $x = (x_1, \dots, x_m)$, we interpret it as an $m \times 1$ matrix, i.e., we use column vectors. For a matrix X , we write $x_{i,j}$ to refer to the entry in its i -th row and j -th column. For two finite sets C and D of the same cardinality, we write $\Pi(C, D)$ to denote the set of bijections from C to D .

2.1 Elections

An election is a pair $E = (C, V)$, where $C = \{c_1, \dots, c_m\}$ is a set of candidates and $V = (v_1, \dots, v_n)$ is a collection of voters. Each voter v_i has a preference order, i.e., a ranking of the candidates from the most to the least desirable one. To simplify notation, v_i refers both to the voter and to his or her preference order; the exact meaning will always be clear from the context. We write $v: a \succ b$ to indicate that voter v ranks candidate a ahead of candidate b , and we write $\text{pos}_v(c)$ to denote the position of candidate c in v 's preference order (the top-ranked candidate has position 1, the next one has position 2, and so on). For an election $E = (C, V)$ and two candidates $a, b \in C$, we write $M_E(a, b)$ to denote the fraction of voters in V who prefer a to b . By $d_{\text{swap}}(v, u)$ we denote the swap distance between votes u and v (over the same candidate set C), i.e., the minimum number of swaps of adjacent candidates needed to turn vote u into vote v . By $d_{\text{Spearman}}(v, u)$ we denote the Spearman's distance between v and u . It is defined as $d_{\text{Spearman}}(v, u) = \sum_{c \in C} |\text{pos}_v(c) - \text{pos}_u(c)|$.

Let C and D be two equal-sized candidate sets. If v is a preference order over C and δ is a bijection in $\Pi(C, D)$, then by $\delta(v)$ we mean a preference order obtained from v by replacing each candidate $c \in C$ with candidate $\delta(c) \in D$. Similarly, for an election $E = (C, V)$, where $V = (v_1, \dots, v_n)$, by $\delta(V)$ we mean $(\delta(v_1), \dots, \delta(v_n))$, and by $\delta(E)$ we mean $(\delta(C), \delta(V)) = (D, \delta(V))$.

2.2 Structured Preferences

Our datasets will include elections where the voters' preferences have some particular structure, such as *single-peaked* or *single-crossing* ones (or several others). Such elections have been frequently studied and used in the literature [56] to model various features observed in real-life scenarios. Further, many problems that are intractable in the general case become solvable in polynomial time for structured elections (see the overview by Elkind et al. [56] for a detailed discussion of structured domains, including motivations as well as their axiomatic and algorithmic properties).

Single-peaked preferences, introduced by Black [16], capture settings where it is possible to order the candidates in such a way that as we move along this order, then each voter's appreciation for the candidates first increases and then decreases (one example of such an order is the classic left-to-right

spectrum of political opinions; another one regards preferences over temperatures in an office). Recently, Peters and Lackner [108] introduced the notion of preferences single-peaked on a circle, where instead of ordering the candidates as a line, we arrange them cyclically (such preferences may appear, e.g., when choosing a video-conference time and the voters are in different time zones).

Definition 2.1 (Black [16], Peters and Lackner [108]). *Let C be a set of candidates and let $c_1 \triangleleft c_2 \triangleleft \dots \triangleleft c_m$ be a strict, total order over C , referred to as the societal axis. Let v be a preference order over C . We say that v is single-peaked with respect to \triangleleft if for each $\ell \in [m]$ the set of the ℓ top-ranked candidates according to v forms an interval within \triangleleft . We say that v is single-peaked on a circle (SPOC) with respect to \triangleleft if for each $\ell \in [m]$, the set of the ℓ top-ranked candidates either forms an interval within \triangleleft or a complement of an interval. An election is single-peaked (is single-peaked on a circle) if there is an axis such that each voter's preference order is single-peaked (single-peaked on a circle) with respect to this axis.*

We note that if an election is single-peaked then each voter ranks one of the two extreme candidates from the societal axis last. Elections single-peaked on a circle are not restricted in this way.

Example 2.1. *Consider the candidate set $\{a, b, c, d\}$ and the axis $a \triangleleft b \triangleleft c \triangleleft d$. The Vote $b \succ c \succ a \succ d$ is single-peaked with respect to \triangleleft (sets $\{b\}$, $\{b, c\}$, $\{a, b, c\}$, and $\{a, b, c, d\}$ form intervals within \triangleleft), whereas $b \succ a \succ d \succ c$ is single-peaked on a circle with respect to \triangleleft , but is not single-peaked ($\{a, b, d\}$ is not an interval within \triangleleft). The Vote $a \succ c \succ b \succ d$ is not even single-peaked on a circle with respect to \triangleleft .*

Single-crossingness is based on a similar principle as single-peakedness, but with respect to the voters. The idea is that we can order the voters in such a way that for each pair of candidates a and b , as we move along this order, the relative preference over a and b changes at most once (in the left-to-right political spectrum example, one could think that voters are ordered from the extreme-left one to the extreme-right one, initially the voters prefer the more left-wing candidate, and then they switch to the more right-wing one). Single-crossing preferences were introduced by Mirrlees [99] and Roberts [112] to capture preference orders that arise in the context of taxation.

Definition 2.2 (Mirrlees [99], Roberts [112]). *An election $E = (C, V)$ is single crossing if it is possible to order the voters in such a way that for each pair of candidates $a, b \in C$, the set of voters that prefer a to b either forms a prefix or a suffix of this order.*

We say that a set of preference orders \mathcal{D} is a *single-crossing domain* if every election where each voter has a preference order from \mathcal{D} is single-crossing. For a discussion and analysis of single-crossing domains, we point the reader to the work of Puppe and Slinko [111].

Example 2.2. *Consider the candidate set $C = \{a, b, c, d\}$ and the following votes:*

$$\begin{array}{ll} v_1: a \succ b \succ c \succ d, & v_5: c \succ b \succ d \succ a, \\ v_2: b \succ a \succ c \succ d, & v_6: c \succ d \succ b \succ a, \\ v_3: b \succ c \succ a \succ d, & v_7: d \succ c \succ b \succ a. \\ v_4: b \succ c \succ d \succ a, & \end{array}$$

The election $E = (C, V)$, where $V = (v_1, \dots, v_7)$ is single-crossing. Since deleting or cloning voters cannot turn a single-crossing election into one that is not single-crossing, we see that $\mathcal{D} = \{v_1, \dots, v_7\}$ is a single-crossing domain. Note that E is also a single-peaked election with respect to $a \triangleleft b \triangleleft c \triangleleft d$.⁷

⁷We want to remark that this is merely a coincidence, as there are single-peaked elections that are not single-crossing and the other way around. For instance, $(C, \{d \succ a \succ b \succ c, d \succ c \succ b \succ a\})$ is single-crossing but not single-peaked, whereas $(C, \{a \succ b \succ c \succ d, a \succ b \succ d \succ c, b \succ a \succ d \succ c, b \succ a \succ c \succ d\})$ is single-peaked with respect to $c \succ a \succ b \succ d$ but not single-crossing.

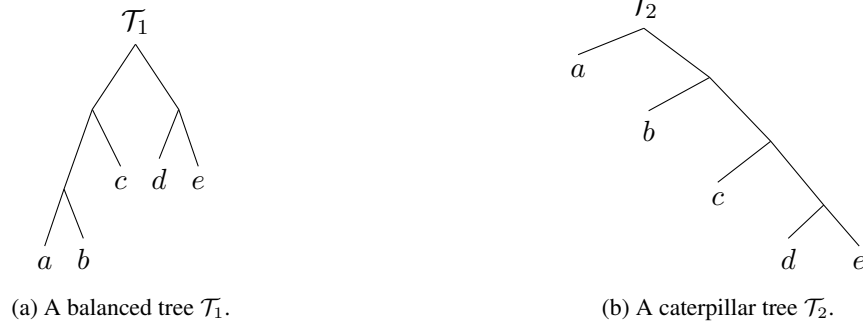


Figure 2: Trees from Example 2.3.

We are also interested in group-separable elections, introduced by Inada [76, 77]. Inada's original definition says that an election is group-separable if each subset A of at least three candidates from this election can be partitioned into two nonempty subsets, A' and A'' , such that every voter either ranks all members of A' ahead of all members of A'' or the other way round. The intuition is that for every candidate set A , some candidates have one feature (say, those in A') and the others have an opposite one (those in A''). Some voters prefer one variant of the feature and some prefer the other. Indeed, these features are organized hierarchically in a tree, as captured in a tree-based definition of group-separable elections, provided by Karpov [80]. For examples of this feature-based interpretation, as well as for computational properties of group-separable elections, see the work of Faliszewski et al. [66]. While these definitions are equivalent, we will find the tree-based one more convenient and present it in the following.

Fix a candidate set C and consider an ordered, rooted tree \mathcal{T} with $|C|$ leaves, where each node either is a leaf or has at least two children, ordered in a sequence (for the sake of simplicity, we will speak of these children as ordered from left to right). Further, each leaf has a unique candidate from C as a label. We refer to such trees as C -based. A frontier of \mathcal{T} is the preference order obtained by reading the labels of the leaves from left to right. A preference order v is *consistent* with \mathcal{T} if we can obtain v as a frontier of \mathcal{T} by reversing the order of children of (some of) the internal nodes.

Definition 2.3 (Inada [76, 77], Karpov [80]). *An election $E = (C, V)$ is group-separable if there is a C -based tree \mathcal{T} such that every vote from V is consistent with \mathcal{T} .*

We are particularly interested in the following two types of group-separable elections:

1. We say that an election is *balanced group-separable* if it is group-separable with respect to a complete binary tree (where every level except possibly the last one is filled with nodes).
2. We say that an election is *caterpillar group-separable* if it is group-separable with respect to a binary caterpillar tree (in such a tree, every node is either a leaf or has exactly two children, of which at least one is a leaf).

Example 2.3. Consider the candidate set $C = \{a, b, c, d, e\}$, the following votes

$$\begin{aligned}
 v_1: a \succ b \succ c \succ d \succ e, & \quad v_2: b \succ a \succ c \succ d \succ e, & \quad v_3: e \succ d \succ c \succ a \succ b, \\
 v_4: a \succ b \succ d \succ e \succ c, & \quad v_5: b \succ c \succ e \succ d \succ a, & \quad v_6: b \succ c \succ d \succ e \succ a,
 \end{aligned}$$

and the trees \mathcal{T}_1 and \mathcal{T}_2 from Figure 2 (we see that \mathcal{T}_1 is balanced while \mathcal{T}_2 is caterpillar). Vote v_1 is consistent with both trees as it is their frontier. Votes v_2 and v_3 are consistent with \mathcal{T}_1 but not \mathcal{T}_2 (in particular, because for consistency with \mathcal{T}_2 candidate a has to be either ranked first or last), where v_4 , v_5 , and v_6 are consistent with \mathcal{T}_2 but not \mathcal{T}_1 (in particular, because for consistency with \mathcal{T}_1 candidates a , b , and c must be ranked consecutively).

Finally, we consider Euclidean preferences, discussed in detail, e.g., by Enelow and Hinich [57, 58], which are defined geometrically: Each candidate and each voter corresponds to a point in a Euclidean space and voters form their preferences by ranking the candidates with respect to their distance.

Definition 2.4. *Let t be a positive integer. An election $E = (C, V)$ is t -Euclidean if it is possible to associate each candidate and each voter with his or her ideal point in t -dimensional Euclidean space \mathbb{R}^t in such a way that the following holds: For each voter v and each two candidates $a, b \in C$, v prefers a to b if and only if v 's point is closer to the point of a than to the point of b .*

It is well known that 1-dimensional Euclidean elections are both single-peaked and single-crossing. We also note that in a 2-dimensional Euclidean election where the ideal points are arranged on a circle, the voters have SPOC preferences.

2.3 Statistical Cultures

Below we describe a number of ways of generating random elections (i.e., statistical cultures). For each of the models we either describe explicitly how an election with m candidates and n voters is generated, or we describe the process of generating a single vote (and then it is implicit that this process is repeated n times to obtain an election).

Impartial Culture and Related Models. Under the impartial culture model (IC), every preference order is sampled with the same probability. That is, to generate a vote we choose a preference order uniformly at random. Under impartial anonymous culture (IAC), we require that each *voting situation* appears with the same probability (a voting situation specifies how many votes with a given preference order are present in a profile; thus IAC generates anonymized preference profiles uniformly at random). The Impartial Anonymous Neutral Culture (IANC) model additionally abstracts away from the names of the candidates [60]. For elections with 100 candidates, which are our main focus, these three models are nearly the same, so we only consider IC.

Pólya-Eggenberger Urn Model. The Pólya-Eggenberger urn model [13, 95] is parametrized with a nonnegative number α , known as the level of contagion, and proceeds as follows: Initially, we have an urn with one copy of each of the $m!$ possible preference orders. To generate a vote, we draw a preference order from the urn uniformly at random (this is the generated vote), and we return it to the urn together with additional $\alpha m!$ copies. For larger α s the generated votes are more correlated. For $\alpha = 0$ the model is equivalent to IC, for $\alpha = 1/m!$ it is equivalent to IAC, and for $\alpha = \infty$ it produces unanimous elections.

Mallows Model. The Mallows model [92] is parameterized by the dispersion parameter $\phi \in [0, 1]$ and the center preference order v (we choose it uniformly at random and then use it for all the generated votes). We generate each vote independently at random, where the probability of generating vote u is proportional to $\phi^{d_{\text{swap}}(v,u)}$. For $\phi = 1$, the model is equivalent to impartial culture, whereas for $\phi = 0$ all generated votes are identical to the center v . See the work of Lu and Boutilier for an effective algorithm for sampling from the Mallows model [91]. Instead of using the dispersion parameter directly, we will use its normalized variant, which we discuss in Section 4.1; we also point the reader to the recent work of Boehmer et al. [24] for a comparison of the two Mallows parameterizations.

Single-Peaked Models. We consider two ways of generating single-peaked elections, one studied by Walsh [126] and one studied by Conitzer [40]; thus we refer to them as the *Walsh model* and the *Conitzer model*. Under both models, we first choose the axis (uniformly at random). To generate a vote, we proceed as follows:

1. Under Walsh's model, we choose a single-peaked preference order (under the given axis) uniformly at random. Walsh [126] provided a sampling algorithm for this task.
2. To generate a vote under the Conitzer model for the axis $c_1 \triangleleft c_2 \triangleleft \dots \triangleleft c_m$, we first choose some candidate c_i (uniformly at random) to be ranked on top (so, at this point, c_i is the only ranked candidate). Then, we perform $m - 1$ steps as follows: Let $\{c_j, c_{j+1}, \dots, c_k\}$ be the set of the currently ranked candidates. We choose the next-ranked candidate from the set $\{c_{j-1}, c_{k+1}\}$ uniformly at random (if $j = 1$ or $k = m$ then this set contains a single element and randomization is not needed).

The Conitzer model is sometimes referred to as the *random peak* model, whereas the Walsh model can be dubbed as *impartial culture over single-peaked votes*.

To generate a single-peaked on a circle vote, we use the Conitzer model, except that we take into account that the axis is cyclical (consequently, each SPOC vote is equally likely to be generated and, hence, we could also refer to this model as impartial culture over SPOC votes, or as the Walsh model for SPOC elections).

Single-Crossing Models. We would like to generate single-crossing elections uniformly at random, but we are not aware of an efficient sampling algorithm. Thus, to generate a single-crossing election, we first generate a single-crossing domain \mathcal{D} and then draw n votes from it uniformly at random. To generate this domain for a candidate set $C = \{c_1, \dots, c_m\}$, we use the following procedure:

1. We let v be a preference order $c_1 \succ c_2 \succ \dots \succ c_m$ and we output v as the first member of our domain.
2. We repeat the following steps until we output $c_m \succ c_{m-1} \succ \dots \succ c_1$: (a) We draw candidate c_j uniformly at random and we let c_i be the candidate ranked right ahead of c_j in v (if c_j is ranked on top, then we repeat); (b) If $i < j$ then we swap c_i and c_j in v and output the new preference order.
3. We randomly permute the names of the candidates.

Our domains always have cardinality $(1/2)m(m-1) + 1$. We believe that studying the process of sampling single-crossing elections (uniformly at random) in more detail is an interesting direction for future research. The approach given here is quite ad hoc, and we use it due to the lack of better alternatives.

Group-Separable Model. Given a candidate set C and a C -based tree \mathcal{T} , we generate each vote independently as follows: For each of the internal nodes in \mathcal{T} , we reverse the order of its children with probability $1/2$. The frontier of the resulting tree is the generated vote. This process generates each vote compatible with a given tree with the same probability and, hence, it is a form of impartial culture over group-separable votes. We consider either balanced trees or caterpillar trees.

Euclidean Models. To generate a t -Euclidean election, we choose the ideal points for the candidates and the voters, and then derive the voters' preferences as in Definition 2.4. Given $t \in \{1, 2, \dots\}$, we consider the following two ways of generating the ideal points:

1. In the t -dimensional hypercube model (t D-Hypercube), we choose all the ideal points uniformly at random from $[-1, 1]^t$.
2. In the t -dimensional hypersphere model (t D-Hypersphere), we choose all the ideal points uniformly at random from the t -dimensional hypersphere centered at $(0, \dots, 0)$, with radius 1.

For $t \in \{1, 2, 3\}$, we refer to t D-Hypercube models as 1D-Interval, 2D-Square, and 3D-Cube, respectively. Similarly, by Circle and Sphere we mean the t D-Hypersphere models for $t \in \{2, 3\}$.

For the urn and Mallows models it is not completely clear what values of the contagion and dispersion parameters to use. In our later discussion we will suggest how to pick the parameter values to cover a broad spectrum of elections that can be generated from these models. For the other models, either there are no parameters to set, or we proposed particular approaches above (such as using uniform distributions on the hypercubes and hyperspheres for Euclidean elections, or the particular type of trees for group-separable elections). These choices are, of course, somewhat arbitrary, but we believe that they, at least, cover some possible extreme approaches.

2.4 (Isomorphic) Distances Between Elections

For a given set X , a pseudometric over X is a function $d: X \times X \rightarrow \mathbb{R}_+$ such that for each $x, y, z \in X$ it holds that (1) $d(x, x) = 0$, (2) $d(x, y) = d(y, x)$, and (3) $d(x, z) \leq d(x, y) + d(y, z)$. In our case, we take X to be the set of all elections with a given number of candidates and a given number of voters. As our goal is to compare elections generated from statistical cultures, where the names of the candidates or the voters are chosen randomly, we require distances to be invariant under permutations of the names of candidates and voters. We refer to such distances as neutral/anonymous (*neutrality* refers to invariance with respect to permuting candidate names and *anonymity* has an analogous meaning for the case of voters).

Recently, Faliszewski et al. [70] introduced several pseudometrics between elections that satisfy our basic anonymity/neutrality conditions. The main idea is that given two elections, we find mappings between their candidates and between their voters, and then we sum up the distances between the matched pairs of votes assuming the candidate mapping (using, e.g., the swap distance or the Spearman’s distance); we seek mappings that give the smallest final distance. These distances are known as the isomorphic swap distance and the isomorphic Spearman distance. The names stem from the underlying distance between the votes and the fact that two elections are isomorphic—i.e., one can be obtained from the other by renaming the candidates and reordering the voters—if and only if their distances are equal to zero. While these distances are intuitively very appealing—they capture even the smallest differences in the structure between elections and have very natural interpretations—they are NP-hard to compute, hard to approximate, and the known FPT algorithms are too slow [70].

3 Positionwise Distance and the Backbone Map

In this section we define our main tool, the positionwise distance, and apply it to form our first map. The idea of the positionwise distance is that given two elections we first derive their aggregate representations (as position matrices) and then compute the distances between these representations. This way we lose some precision as compared to the isomorphic swap or Spearman distances (e.g., because some nonisomorphic elections have the same aggregate representations and, hence, are at positionwise distance zero) but we gain efficient, polynomial-time computability. In this section we first define and analyze the position and frequency matrices, i.e., the aggregate representations that we use and which facilitates the low computational complexity of our distance,⁸ and then we define the positionwise distance and provide the basic setup for the map of elections. Finally, we reflect on why we believe that positionwise distance is a good choice for our maps (for elections with larger numbers of candidates).

⁸Indeed, just using an aggregate representation does not need to lead to a polynomial-time computable distance. In one of the conference papers on which this paper is based we have studied a distance based on the weighted pairwise majority matrix, which turned out to be NP-complete to compute [120]. For more details on this distance, see the work of Boehmer et al. [22].

3.1 Position and Frequency Matrices

Given an election, its position matrix specifies for each candidate how many voters rank him or her at each possible position. Frequency matrices are defined analogously, but focus on the fractions of votes instead of absolute vote counts. Formally, let $E = (C, V)$ be an election, where $C = \{c_1, \dots, c_m\}$ and $V = (v_1, \dots, v_n)$. For a candidate $c \in C$ and position $i \in [m]$, we write $\#pos_E(c, i)$ to denote the number of voters in election E that rank c on position i , and by $\#pos_E(c)$ we mean the vector:

$$(\#pos_E(c, 1), \#pos_E(c, 2), \dots, \#pos_E(c, m)).$$

A *position matrix* of election E , denoted $\#pos(E)$, is the $m \times m$ matrix that has vectors $\#pos_E(c_1), \dots, \#pos_E(c_m)$ as its columns.⁹ Frequency matrices are defined analogously: For a candidate c and a position $i \in [m]$, let $\#freq_E(c, i)$ be $\frac{\#pos_E(c, i)}{n}$, let vector $\#freq_E(c)$ be $(\#freq_E(c, 1), \dots, \#freq_E(c, m))$, and let each *frequency matrix* of election E , denoted $\#freq(E)$, consist of columns $\#freq_E(c_1), \dots, \#freq_E(c_m)$. In other words, a frequency matrix is a position matrix normalized by the number of voters.

Note that in each position matrix, each row and each column sums up to the number of voters in the election. Similarly, in each frequency matrix, the rows and columns sum up to one (such matrices are called bistochastic). For a positive integer m , we write $\mathcal{F}(m)$ [$\mathcal{P}(m)$] to denote the set of all $m \times m$ frequency [position] matrices.

Example 3.1. Consider an election $E = (C, V)$, where $C = \{a, b, c, d\}$, $V = (v_1, v_2, v_3)$, and the voters have the following preference orders:

$$v_1: a \succ b \succ c \succ d, \quad v_2: a \succ c \succ b \succ d, \quad v_3: d \succ b \succ c \succ a.$$

The position and frequency matrices of this election are:

$$\#pos(E) = \begin{matrix} & \begin{matrix} a & b & c & d \end{matrix} \\ \begin{matrix} 1 \\ 2 \\ 3 \\ 4 \end{matrix} & \begin{bmatrix} 2 & 0 & 0 & 1 \\ 0 & 2 & 1 & 0 \\ 0 & 1 & 2 & 0 \\ 1 & 0 & 0 & 2 \end{bmatrix} \end{matrix} \quad \text{and} \quad \#freq(E) = \begin{matrix} & \begin{matrix} a & b & c & d \end{matrix} \\ \begin{matrix} 1 \\ 2 \\ 3 \\ 4 \end{matrix} & \begin{bmatrix} 2/3 & 0 & 0 & 1/3 \\ 0 & 2/3 & 1/3 & 0 \\ 0 & 1/3 & 2/3 & 0 \\ 1/3 & 0 & 0 & 2/3 \end{bmatrix} \end{matrix}.$$

Naturally, two distinct elections can have identical position matrices (this issue was recently studied in detail by Boehmer et al. [23], who has shown that counting the number of non-isomorphic elections with a given position matrix is $\#P$ -complete, but it is possible to deduce some nontrivial properties of the elections with a given matrix).

Example 3.2. Consider election $E' = (C, U)$, where $C = \{a, b, c, d\}$, $U = (u_1, u_2, u_3)$, and the voters have preference orders:

$$u_1: a \succ b \succ c \succ d, \quad u_2: a \succ b \succ c \succ d, \quad u_3: d \succ c \succ b \succ a.$$

This election has the same position (and frequency) matrix as E in Example 3.1. However, E and E' are not isomorphic because all votes in E are different, whereas E' contains two identical ones.

⁹Technically, due to different possible orderings of the candidates, an election may have several different position matrices; for our purposes we typically assume some arbitrary order because the positionwise distance will internally reorder the candidates as needed.

3.2 Distances Among Vectors

For our new distance, we will need distances among vectors. Given two vectors, $x = (x_1, \dots, x_t)$ and $y = (y_1, \dots, y_t)$, their ℓ_1 -distance is:

$$\ell_1(x, y) = |x_1 - y_1| + |x_2 - y_2| + \dots + |x_t - y_t|.$$

To define the *earth mover's distance* (EMD) [113], we additionally require that the entries of these vectors are nonnegative and sum up to the same value. Then their earth mover's distance, denoted $\text{emd}(x, y)$, is defined as the lowest total cost of operations that transform vector x into vector y , where each operation is of the form “subtract δ from position i and add δ to position j ” and costs $\delta \cdot |i - j|$. Such an operation is legal if the current value at position i is at least δ .

It is well-known that $\text{emd}(x, y)$ can be computed in polynomial time using a simple greedy algorithm. For each vector $z = (z_1, \dots, z_t)$, let \hat{z} be its prefix-sum vector, i.e., $\hat{z} = (z_1, z_1 + z_2, \dots, z_1 + z_2 + \dots + z_t)$. Then, we have that $\text{emd}(x, y) = \ell_1(\hat{x}, \hat{y})$ [113].

3.3 Positionwise Distance

We are now ready to define the positionwise distance. Its main underlying principle is that the most valuable information about each candidate can be extracted from the positions that this candidate occupies in the voters' preference rankings.

Definition 3.1. Let $E = (C, V)$ and $F = (D, U)$ be two elections with m candidates each (we do not require that $|V| = |U|$). Let δ be a bijection in $\Pi(C, D)$. We define:

$$\delta\text{-POS}(E, F) := \sum_{c \in C} \text{emd}(\# \text{freq}_E(c), \# \text{freq}_F(\delta(c))).$$

The positionwise distance between E and F , denoted $\text{POS}(E, F)$, is defined as:

$$\text{POS}(E, F) := \min_{\delta \in \Pi(C, D)} \delta\text{-POS}(E, F).$$

We refer to δ as the candidate matching that implements (or, witnesses) the distance between E and F .

In other words, the positionwise distance is the sum of the earth mover's distances between the frequency vectors of the candidates from the two elections, with candidates/columns matched optimally according to σ . The positionwise distance is invariant to renaming the candidates and reordering the voters.

Example 3.3. Consider election E from Example 3.1 and election $F = (D, U)$ with candidate set $D = \{x, y, z, w\}$ and voter collection $U = (u_1, u_2, u_3)$, where the voters have preference orders:

$$u_1: x \succ y \succ z \succ w, \quad u_2: y \succ x \succ w \succ z, \quad u_3: w \succ z \succ x \succ y.$$

These elections have the following frequency matrices:

$$\# \text{freq}(E) = \begin{matrix} & \begin{matrix} a & b & c & d \end{matrix} \\ \begin{matrix} 1 \\ 2 \\ 3 \\ 4 \end{matrix} & \begin{bmatrix} 2/3 & 0 & 0 & 1/3 \\ 0 & 2/3 & 1/3 & 0 \\ 0 & 1/3 & 2/3 & 0 \\ 1/3 & 0 & 0 & 2/3 \end{bmatrix} \end{matrix}, \quad \# \text{freq}(F) = \begin{matrix} & \begin{matrix} x & y & z & w \end{matrix} \\ \begin{matrix} 1 \\ 2 \\ 3 \\ 4 \end{matrix} & \begin{bmatrix} 1/3 & 1/3 & 0 & 1/3 \\ 1/3 & 1/3 & 1/3 & 0 \\ 1/3 & 0 & 1/3 & 1/3 \\ 0 & 1/3 & 1/3 & 1/3 \end{bmatrix} \end{matrix}.$$

Let us consider a mapping σ such that $\sigma(a) = y$, $\sigma(b) = x$, $\sigma(c) = z$, and $\sigma(d) = w$. We see that:

$$\begin{aligned} \text{emd}(\# \text{freq}_E(a), \# \text{freq}_F(\sigma(a))) &= \text{emd}((2/3, 0, 0, 1/3), (1/3, 1/3, 0, 1/3)) = 1/3, \\ \text{emd}(\# \text{freq}_E(b), \# \text{freq}_F(\sigma(b))) &= \text{emd}((0, 2/3, 1/3, 0), (1/3, 1/3, 1/3, 0)) = 1/3, \\ \text{emd}(\# \text{freq}_E(c), \# \text{freq}_F(\sigma(c))) &= \text{emd}((0, 1/3, 2/3, 0), (0, 1/3, 1/3, 1/3)) = 1/3, \\ \text{emd}(\# \text{freq}_E(d), \# \text{freq}_F(\sigma(d))) &= \text{emd}((1/3, 0, 0, 2/3), (1/3, 0, 1/3, 1/3)) = 1/3. \end{aligned}$$

Hence, for this mapping, the positionwise distance is $1/3 + 1/3 + 1/3 + 1/3 = 4/3$. This mapping is, indeed, optimal. To see this, note that each column of $\#freq(E)$ includes the value $2/3$, whereas the largest value in each column of $\#freq(F)$ is $1/3$. Hence, the smallest possible EMD distance between a column of $\#freq(E)$ and a column of $\#freq(F)$ is at least $1/3$. Consequently, we have $POS(E, F) = 4/3$.

Remark 3.1. To obtain the normalized positionwise distance between two elections with m candidates each (where m is divisible by 4), we divide their positionwise distance by $\frac{1}{3}(m^2 - 1)$. This normalization factor is the largest positionwise distance between two elections with m candidates [22]. Proposition 3.5 and the discussion below will make this normalization more intuitive.

Definition 3.1 calls for some explanations. First, let us mention that we could have used any other distance between vectors instead of EMD and, indeed, Boehmer et al. [22] evaluate the effects of using ℓ_1 (and conclude that the practical differences are not huge, but still EMD is preferable). We use EMD because it captures the idea that being ranked on the top position is more similar to being ranked on the second position than to being ranked on the bottom one.

The second issue is that we could have used position matrices instead of the frequency ones. The difference would only be technical. Indeed, if we used position matrices then we would have to assume that the elections have the same numbers of voters (in our maps this holds anyway) and the obtained distances would be multiplied by this number of voters. We use frequency matrices because of their increased flexibility (this will become clear, e.g., in Section 3.5).

The third issue is that we should formally argue that the positionwise distance is, indeed, a pseudometric. We do so in the next proposition.

Proposition 3.1. *The positionwise distance is a pseudometric.*

Proof. We show that the positionwise distance satisfies the triangle inequality (the other requirements for being a pseudometric are easy to verify). Consider three elections with candidate sets of equal size, $E_1 = (C_1, V_1)$, $E_2 = (C_2, V_2)$, and $E_3 = (C_3, V_3)$. Let δ and σ be the candidate matchings that minimize the EMD distances between E_1 and E_2 and between E_2 and E_3 , respectively. We have that:

$$\begin{aligned} POS(E_1, E_3) &\leq \sum_{c \in C_1} \text{emd}(\#freq_{E_1}(c), \#freq_{E_3}(\sigma(\delta(c)))) \\ &\leq \sum_{c \in C_1} \text{emd}(\#freq_{E_1}(c), \#freq_{E_2}(\delta(c))) \\ &\quad + \sum_{c \in C_2} \text{emd}(\#freq_{E_2}(\delta(c)), \#freq_{E_3}(\sigma(\delta(c)))) \\ &= POS(E_1, E_2) + POS(E_2, E_3). \end{aligned}$$

The first inequality follows from the definition of the positionwise distance, the second one from the fact that EMD is a metric. \square

Last but not least, a crucial feature of the positionwise distance is that we can compute it in polynomial time. In short, doing so reduces to finding a minimum-cost matching in a certain weighted bipartite graph.

Proposition 3.2. *There is a polynomial-time algorithm for computing the positionwise distance.*

Proof. Let $E = (C, V)$ and $F = (D, U)$ be two elections where $|C| = |D|$. The value of $POS(E, F)$ is equal to the minimum-cost matching in the bipartite graph whose vertex set is $C \cup D$ and which has the following edges: For each $c \in C$ and each $d \in D$ there is an edge with the cost equal to the EMD distance between $\#freq_E(c)$ and $\#freq_F(d)$; these weights can be computed independently for each pair of candidates. Such minimum-cost matchings can be computed in polynomial time (see, e.g., the overview of Ahuja et al. [1]). \square

3.4 Recovering Elections from Matrices

Since the positionwise distance works on frequency matrices, it will sometimes be convenient to operate directly on such matrices rather than on the elections that generate them. To this end, we now argue that given a position or a frequency matrix, we can always compute in polynomial time some election that either generates it (for position matrices) or is very close to generating it (for frequency matrices).

First, we observe that each $m \times m$ position matrix has a corresponding m -candidate election with at most $m^2 - 2m + 2$ distinct preference orders. This was shown by Leep and Myerson [87, Theorem 7] (they speak of “semi-magic squares” and not “position matrices” and show a decomposition of a matrix into permutation matrices, which correspond to votes in our setting). Their proof lacks some algorithmic details which we provide in the appendix.

Proposition 3.3 (★). *Given a position matrix $X \in \mathcal{P}(m)$, one can compute in $O(m^{4.5})$ time an election E that contains at most $m^2 - 2m + 2$ different votes such that $\#_{\text{pos}}(E) = X$.*

Next, we consider the issue of recovering elections based on frequency matrices. Given an $m \times m$ bistochastic matrix X and a number n of voters, we would like to find an election E with position matrix nX . This may be impossible as nX may have fractional entries, but we can get very close to this goal. The next proposition shows how to achieve it, and justifies speaking of elections and frequency matrices interchangeably. By $\lfloor nX \rfloor$, we mean the matrix whose each entry is equal to the floor of the corresponding entry of nX .

Proposition 3.4. *Given an $m \times m$ bistochastic matrix X and an integer n , one can compute in polynomial time an election E with n voters whose position matrix P satisfies $|nx_{i,j} - p_{i,j}| < 1$ for each $i, j \in [m]$ and, under this condition, minimizes the value $\sum_{1 \leq i,j \leq m} |nx_{i,j} - p_{i,j}|$.*

Proof. We first design a randomized algorithm that uses dependent rounding. Then we derive a deterministic algorithm, based on computing min-cost flows, which also performs the minimization step (however, we need the former algorithm to explain why the latter always produces a correct result). We start by computing matrix Y where each entry $y_{i,j}$ is equal to:

$$y_{i,j} = nx_{i,j} - \lfloor nx_{i,j} \rfloor.$$

All entries of Y are between 0 and 1, and each row and each column of Y sums up to an integer because the latter property holds both for nX and $\lfloor nX \rfloor$ (although different rows and columns may sum up to different integers). We construct an edge-weighted bipartite graph G with vertex sets $A = \{a_1, \dots, a_m\}$ and $B = \{b_1, \dots, b_m\}$. For each two vertices a_i and b_j , we have a connecting edge of weight $y_{i,j}$. For each vertex $c \in A \cup B$, we let its fractional degree $\delta_G(c)$ be the sum of the weights of the edges incident to it. Then, we invoke the dependent rounding procedure of Gandhi et al. [72, Theorem 2.3] on this graph: Consequently, in polynomial time we obtain an unweighted bipartite graph G' with the same two vertex sets, such that the (standard) degree of each vertex $c \in A \cup B$ in G' is equal to $\delta_G(c)$ (this is property P2 in the paper of Gandhi et al. [72]; note that dependent rounding is computed via a randomized algorithm, but this condition on the degrees is always satisfied, independently of the random bits selected).¹⁰ Using G' , we form an $m \times m$ matrix D such that for each $i, j \in [m]$, $d_{i,j}$ is 1 if G' contains an edge between a_i and b_j , and $d_{i,j} = 0$ otherwise. Finally, we compute matrix $P = \lfloor nX \rfloor + D$.

The entries of P differ from those of nX by less than one, and the rows and columns of P sum up to n (to see it, consider the degrees of the vertices in G'). So, we obtain the desired election by invoking Proposition 3.3 on matrix P .

¹⁰Dependent rounding accepts input exactly in the format that we have and implements exactly the effect that we describe (plus additional guarantees that we do not need).

Next, we provide a fully deterministic algorithm for computing the matrix D (and, consequently, matrix P), which does not invoke dependent rounding and which minimizes the value $\sum_{1 \leq i, j \leq m} |nx_{i,j} - p_{i,j}|$. Consider matrix Y from the first part of the proof and let $Z = \sum_{1 \leq i, j \leq m} y_{i,j}$.

We form a flow network with source s , nodes $v_{i,j}$ for each $i, j \in [m]$, “pre-sink” nodes t_1, \dots, t_m , and sink node t . We have the following edges (unless specified otherwise, all of them have cost 0):

1. For each $i \in [m]$, we have a directed path which starts at the source node s , then goes to $v_{i,1}$, next to $v_{i,2}$, and so on, until $v_{i,m}$. Each edge on this path has capacity equal to $Y_i = \sum_{j=1}^m y_{i,j}$. Recall that this value is an integer and note that Y_i is exactly the number of entries in the i -th row of matrix D that need to have value 1 (the other entries in this row will have value 0).
2. For each $i, j \in [m]$, we have an edge from $v_{i,j}$ to t_j , with capacity one and with cost $1 - 2y_{i,j}$. The intuition is that if a unit of flow goes from $v_{i,j}$ to t_j , then $d_{i,j} = 1$, and if the entire flow that enters $v_{i,j}$ goes to $v_{i,j+1}$, then $d_{i,j} = 0$. The intuition for the cost of the edge is that if $d_{i,j} = 0$ then $p_{i,j} = \lfloor nx_{i,j} \rfloor$ and, consequently, $|nx_{i,j} - p_{i,j}| = |nx_{i,j} - \lfloor nx_{i,j} \rfloor| = y_{i,j}$, which we treat as the “default.” If we send a unit of flow from $v_{i,j}$ to t_j then $d_{i,j} = 1$ and $p_{i,j} = \lfloor nx_{i,j} \rfloor + 1$. Consequently, $|nx_{i,j} - p_{i,j}| = |nx_{i,j} - 1 - \lfloor nx_{i,j} \rfloor| = 1 + \lfloor nx_{i,j} \rfloor - nx_{i,j} = 1 - y_{i,j}$. So the difference between the default value $y_{i,j}$ of $|nx_{i,j} - p_{i,j}|$ that we get for $d_{i,j} = 0$ and its value $1 - y_{i,j}$ that we get for $d_{i,j} = 1$ is $1 - 2y_{i,j}$. Note that $1 - 2y_{i,j}$ may be negative, but this is not an issue for the flow computation as our flow network will not have cycles.
3. Finally, for each $j \in [m]$, we have an edge from t_j to t with capacity $\sum_{i=1}^m y_{i,j}$. This value is an integer and it is the number of entries in the j -th column of matrix D that need to become 1 (instead of being 0).

Next, we compute in polynomial time an integral flow that moves $\sum_{i,j \in [m]} y_{i,j}$ units of flow from s to t at the lowest possible cost (which we denote Z_f ; we use an arbitrary polynomial-time algorithm that accepts negative costs, such as one of those available in the overview of Ahuja et al. [1]). If this flow existed, then we could compute matrix D by setting, for each $i, j \in [m]$, $d_{i,j}$ to be the amount of flow (0 or 1) going from $v_{i,j}$ to t_j . Indeed, by definition of our flow network, for each i we would have that $\sum_{j=1}^m d_{i,j} = Y_i = \sum_{j=1}^m y_{i,j}$ (because a flow of Y_i needs to enter $v_{i,1}$ and when a flow enters some node $v_{i,j}$, then it can either go to t_j or to $v_{i,j+1}$). Due to the capacities on the edges from the pre-sink nodes to the sink, for each $j \in [m]$ we would also have that $\sum_{i=1}^m d_{i,j} = \sum_{i=1}^m y_{i,j}$.

We will now argue that our flow problem has a solution. For this, we reexamine the graphs G and G' constructed in the first part of the proof. Note that the two above-discussed properties of the flow network are equivalent to ensuring that the degrees of the vertices in G' are equal to the fractional degrees in G , as is done by dependent rounding. This means that given graph G' computed by our first algorithm and the matrix D induced by G' , we can compute a capacity-respecting flow for our network by sending one unit of flow from $v_{i,j}$ to t_j if $d_{i,j} = 1$. This flow moves $\sum_{i,j \in [m]} y_{i,j}$ units of flow and accordingly, our flow problem has a solution.

Further, for a flow f implying values $d_{i,j}$, we have that:

$$\sum_{1 \leq i, j \leq m} |nx_{i,j} - p_{i,j}| = \sum_{1 \leq i, j \leq m} |nx_{i,j} - (\lfloor nx_{i,j} \rfloor + d_{i,j})| = Z + Z_f.$$

To see why this is the case, note that if all the values $d_{i,j}$, as well as Z_f , were 0, then the equality would hold by the definition of Z . Now, for each $d_{i,j} = 1$, the left-hand side increases by $1 - 2y_{i,j}$ and, consequently, the whole sum is equal to $Z + Z_f$. Thus minimizing Z_f is equivalent to minimizing $\sum_{1 \leq i, j \leq m} |nx_{i,j} - p_{i,j}|$, which is our goal. \square

Together with the fact that computing a frequency matrix for a given election is straightforward, Proposition 3.4 gives a two-way interface between elections and frequency matrices. In the remainder of the paper, we will also express many (idealized families of) elections by focusing on their frequency matrices and we will often speak of elections and their frequency matrices interchangeably.

3.5 Four Compass Elections/Matrices

In this section we prepare our “compass,” i.e., we identify four special matrices (or, families of elections) that correspond to different types of (dis)agreement among the voters. Importantly, we want our compass to form a backbone of the maps and, consequently, we want them to be at large and close-to-constant distances from each other as we consider different numbers of candidates (so that irrespective of the sizes of the considered elections, the compass matrices could be viewed as fixed points on the maps). We argue as to why our matrices indeed are quite extreme, occupy very different areas in the space of elections, and stay at close-to-fixed distances from each other. As explained in the previous section, we focus on $m \times m$ frequency matrices (or, equivalently, on elections with m candidates).

Identity and Uniformity. The first two matrices are the *identity* matrix, ID_m , with ones on the diagonal and zeros elsewhere, and the *uniformity* matrix, UN_m , with each entry equal to $1/m$:

$$ID_m = \begin{bmatrix} 1 & 0 & \cdots & 0 \\ 0 & 1 & \cdots & 0 \\ \vdots & \vdots & \ddots & \vdots \\ 0 & 0 & \cdots & 1 \end{bmatrix}, \quad UN_m = \begin{bmatrix} 1/m & 1/m & \cdots & 1/m \\ 1/m & 1/m & \cdots & 1/m \\ \vdots & \vdots & \ddots & \vdots \\ 1/m & 1/m & \cdots & 1/m \end{bmatrix}.$$

The identity matrix corresponds to elections where each voter has the same preference order, i.e., they capture perfect agreement among the voters. In contrast, the uniformity matrix captures elections where each candidate is ranked on each position equally often, i.e., where, in aggregate, all the candidates are viewed as equally good. Hence, uniformity elections can be seen as capturing perfect lack of agreement regarding the relative qualities of the candidates.

Uniformity elections are quite similar to the IC ones and, in the limit, indistinguishable from them. Indeed, if we choose each preference order uniformly at random then, in expectation, each candidate would be ranked on each position the same number of times. Yet, for a fixed number of voters, typically IC elections are at some (small) positionwise distance from uniformity.

Stratification. The next matrix, *stratification*, is defined as follows (we assume that m is even):

$$ST_m = \begin{bmatrix} UN_{m/2} & 0 \\ 0 & UN_{m/2} \end{bmatrix}.$$

Stratification matrices correspond to elections where the voters agree that half of the candidates are more desirable than the other half, but, in aggregate, are unable to distinguish between the qualities of the candidates in each group.

Antagonism. For the next matrix, we need one more piece of notation. Let rID_m be the matrix obtained by reversing the order of the columns of the identity matrix ID_m . We define the *antagonism* matrix, AN_m , to be $1/2ID_m + 1/2rID_m$:

$$AN_m = \frac{1}{2} \begin{bmatrix} 1 & 0 & \cdots & 0 & 0 \\ 0 & 1 & \cdots & 0 & 0 \\ \vdots & \vdots & \ddots & \vdots & \vdots \\ 0 & 0 & \cdots & 1 & 0 \\ 0 & 0 & \cdots & 0 & 1 \end{bmatrix} + \frac{1}{2} \begin{bmatrix} 0 & 0 & \cdots & 0 & 1 \\ 0 & 0 & \cdots & 1 & 0 \\ \vdots & \vdots & \ddots & \vdots & \vdots \\ 0 & 1 & \cdots & 0 & 0 \\ 1 & 0 & \cdots & 0 & 0 \end{bmatrix} = \begin{bmatrix} 1/2 & 0 & \cdots & 0 & 1/2 \\ 0 & 1/2 & \cdots & 1/2 & 0 \\ \vdots & \vdots & \ddots & \vdots & \vdots \\ 0 & 1/2 & \cdots & 1/2 & 0 \\ 1/2 & 0 & \cdots & 0 & 1/2 \end{bmatrix}.$$

Such matrices are generated, e.g., by elections where half of the voters rank the candidates in one order, and half of the voters rank them in the opposite one, so there is a clear conflict (however, there are also

many other elections that generate this matrix). In some sense, stratification and antagonism are based on similar premises. Under stratification, the set of candidates is partitioned into halves with different properties, whereas in antagonism the voters are partitioned into such halves. However, the nature of the partitioning is quite different.

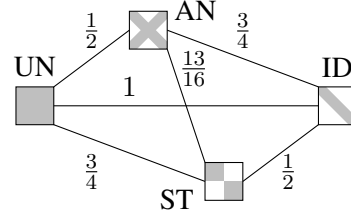
Distances Between the Matrices. We chose the above matrices because they capture natural, intuitive phenomena, seem to occupy very different areas of the space of elections, and their relative distances do not depend strongly on the numbers of candidates. To see that the latter two points hold, let us calculate their positionwise distances (for the calculations, see Appendix A).

Proposition 3.5 (★). *If m is divisible by 4, then it holds that:*

1. $\text{POS}(\text{ID}_m, \text{UN}_m) = \frac{1}{3}(m^2 - 1)$,
2. $\text{POS}(\text{ID}_m, \text{AN}_m) = \text{POS}(\text{UN}_m, \text{ST}_m) = \frac{m^2}{4}$,
3. $\text{POS}(\text{ID}_m, \text{ST}_m) = \text{POS}(\text{UN}_m, \text{AN}_m) = \frac{2}{3}(\frac{m^2}{4} - 1)$,
4. $\text{POS}(\text{AN}_m, \text{ST}_m) = \frac{13}{48}m^2 - \frac{1}{3}$.

To normalize these distances, we divide them by $D(m) = \text{POS}(\text{ID}_m, \text{UN}_m)$, which is the largest positionwise distance between two matrices from $\mathcal{F}(m)$, as shown by Boehmer et al. [22]; recall Remark 3.1.¹¹ For each two matrices X and Y among our four, we let $d(X, Y) := \lim_{m \rightarrow \infty} \text{POS}(X_{4m}, Y_{4m}) / D(4m)$. A simple computation shows the following (see also the drawing on the right; we sometimes omit the subscript m for simplicity):

$$\begin{aligned} d(\text{ID}, \text{UN}) &= 1, \\ d(\text{ID}, \text{AN}) &= d(\text{UN}, \text{ST}) = 3/4, \\ d(\text{ID}, \text{ST}) &= d(\text{UN}, \text{AN}) = 1/2, \\ d(\text{AN}, \text{ST}) &= 13/16. \end{aligned}$$



Importantly, already for fairly small numbers of candidates the normalized distances between the compass matrices become very similar to the above-computed limit values. For example, for $m = 12$ they only differ by a few percent. Hence, the compass matrices indeed can be used to form the backbones of our maps.

Remark 3.2. *Using a combination of brute-force search and ILP solving, for very small values of m , such as 4 or 5, we found sets of matrices that are even further away from each other than the compass ones. Unfortunately, we did not see ways of generalizing these matrices to arbitrary numbers of candidates.*

3.6 Paths Between Election Matrices

Next, we consider convex combinations of frequency matrices. We do so to derive matrices that would be located between the compass ones in the space of elections (as defined by the positionwise distance) and would support our maps' backbones.

¹¹The distance between ID_m and UN_m is also the largest possible under the isomorphic swap distance. Interestingly, the distance between ID_m and AN_m is also the largest possible in this setting, and the distance between AN_m and UN_m seems to approach this largest possible value as the number of candidates grows [22]. This is another reason for including AN_m in our compass.

Given two frequency matrices, X and Y , and $\alpha \in [0, 1]$, one might expect that matrix $Z = \alpha X + (1 - \alpha)Y$ would lie at distance $(1 - \alpha)\text{POS}(X, Y)$ from X and at distance $\alpha\text{POS}(X, Y)$ from Y , so that we would have:

$$\text{POS}(X, Y) = \text{POS}(X, Z) + \text{POS}(Z, Y).$$

However, without further assumptions this is not necessarily the case. Indeed, if we take $X = \text{ID}_m$ and $Y = \text{rID}_m$, then $\text{POS}(X, Y) = 0$, but $Z = 0.5X + 0.5Y = \text{AN}_m$, so $\text{POS}(X, Z) = \text{POS}(\text{ID}, \text{AN}) > 0$ and $\text{POS}(X, Y) \neq \text{POS}(X, Z) + \text{POS}(Z, Y)$. Yet, if we arrange the two matrices X and Y so that their positionwise distance is witnessed by the identity permutation of their column vectors (i.e., by a trivial candidate matching), then their convex combination lies exactly between them.

Proposition 3.6. *Let $X = (x_1, \dots, x_m)$ and $Y = (y_1, \dots, y_m)$ be two $m \times m$ frequency matrices such that $\text{POS}(X, Y) = \sum_{i=1}^m \text{emd}(x_i, y_i)$. Then, for each $\alpha \in [0, 1]$ it holds that $\text{POS}(X, Y) = \text{POS}(X, \alpha X + (1 - \alpha)Y) + \text{POS}(\alpha X + (1 - \alpha)Y, Y)$.*

Proof. Let $Z = (z_1, \dots, z_m) = \alpha X + (1 - \alpha)Y$ be our convex combination of X and Y . We note two properties of the earth mover's distance. Let a, b , and c be three vectors that consist of nonnegative numbers, where the entries in b and c sum up to the same value. Then, it holds that $\text{emd}(a + b, a + c) = \text{emd}(b, c)$. Further, for a nonnegative number λ , we have that $\text{emd}(\lambda b, \lambda c) = \lambda \text{emd}(b, c)$. Using these observations and the definition of the earth mover's distance, we note that:

$$\begin{aligned} \text{POS}(X, Z) &\leq \sum_{i=1}^m \text{emd}(x_i, z_i) = \sum_{i=1}^m \text{emd}(x_i, \alpha x_i + (1 - \alpha)y_i) \\ &= \sum_{i=1}^m \text{emd}((1 - \alpha)x_i, (1 - \alpha)y_i) = (1 - \alpha) \sum_{i=1}^m \text{emd}(x_i, y_i) = (1 - \alpha)\text{POS}(X, Y). \end{aligned}$$

The last equality follows by our assumption regarding X and Y . By an analogous reasoning we also have that $\text{POS}(Z, Y) \leq \alpha\text{POS}(X, Y)$. By putting these two inequalities together, we have that:

$$\text{POS}(X, Z) + \text{POS}(Z, Y) \leq \text{POS}(X, Y).$$

By the triangle inequality, we have that $\text{POS}(X, Y) \leq \text{POS}(X, Z) + \text{POS}(Z, Y)$ and, so, we conclude that $\text{POS}(X, Z) + \text{POS}(Z, Y) = \text{POS}(X, Y)$. \square

Using Proposition 3.6, for each two compass matrices, we can generate a sequence of matrices that form a path between them. For example, matrix $0.5\text{ID} + 0.5\text{UN}$ is exactly at the same distance from ID and from UN . Note that by the proof of Proposition 3.5, it holds that the positionwise distance between any two of our four compass matrices is witnessed by the identity mapping, as required by Proposition 3.6.

3.7 The Backbone Map

Finally, we gather all the tools introduced in this section and form our first map consisting of the four compass matrices and their convex combinations. While it will be very simplistic, it will illustrate how such maps are made.

To form a map, we first need to select a dataset of elections (or, frequency matrices). In our case, we take the four compass matrices and for each two of them, we take 20 path matrices formed as their convex combinations (specifically, for each two compass matrices X and Y and each $\alpha \in \{1/21, 2/21, \dots, 20/21\}$, we have matrix $\alpha X + (1 - \alpha)Y$). Altogether, we have 124 matrices. We generate the matrices for the case of 10 candidates, but for other numbers of candidates the map would look similarly (except for very small candidate sets). Since we are working with frequency matrices only, the number of voters is irrelevant. For each pair of our matrices, we compute their positionwise distance (in the current setting, we could even derive these distances analytically, but generally we invoke the algorithm from

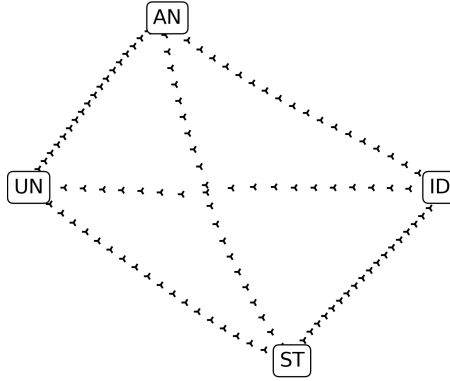


Figure 3: The backbone map, consisting of the four compass matrices and their connecting paths. Each compass matrix is represented by a rectangle with a label. For each two compass matrices we have 20 path matrices, formed as their convex combinations.

Proposition 3.2). Finally, given these distances, we invoke an embedding algorithm (in this case we use Kamada-Kawai algorithm, KK [78, 114]). This algorithm associates each election from the dataset with a point on a 2D plane in such a way that the Euclidean distance between two points resembles the positionwise distance between the corresponding elections as accurate as possible.

We show the result in Figure 3. We can see that the picture is very similar to the fully analytical diagram shown at the end of Section 3.5. Indeed, the compass matrices are located at similar distances as in the diagram. Further, the matrices from each path are equally spaced (since the distance between UN and ID is larger than between, say, UN and AN, the matrices from the former path are more spread, whereas those from the latter are located closer to each other). This reinforces our hope that when there is a good embedding, then KK finds it. In Section 4 we will build a full-fledged map of elections, with a much more diverse dataset, and we will provide stronger arguments for its credibility.

3.8 Why Is Positionwise Distance a Good Choice?

Before we move on to the next section, where we will create our full-fledged maps, let us take a pause to consider why positionwise distance is a good choice for the map framework. To this end, we will largely summarize the results of Boehmer et al. [22], where the authors compared several possible choices of distances.

Ideally, we would prefer to use the isomorphic swap or Spearman distances instead of the positionwise one (recall Section 2.4, where these distances are briefly discussed, and the work of Faliszewski et al. [70]). The reasons for this are as follows. First, these two distances distinguish as many elections as possible while being invariant to renaming the candidates and voters; in other words, under these two distances two elections are at distance zero if and only if they are isomorphic. Second, if we have two elections E and F , then their swap and Spearman distances change at most very mildly if we introduce a small local change to one of them (such as swapping two candidates in some vote). In other words, these distance measures are robust—a small change in the input cannot lead to a large change in the output. The third argument is that both distance measures treat all positions in the votes identically: A swap of two top candidates in some vote affects the distance in qualitatively the same way as swapping two bottom candidates. While there certainly are applications where it would be beneficial to pay attention to tops of the votes more closely than to their bottoms, such an agnostic approach is natural when developing a generic framework that can be used for many different settings and for general comparison of elections. On the negative side, the huge (practical) downside of the isomorphic swap and Spearman

distances is that they are NP-hard to compute. Indeed, Boehmer et al. [22] report that computing a map of elections with 10 candidates and 50 voters based on these two distances took several weeks on a powerful computing cluster. Consequently, generating maps with 100 candidates and 100 voters (or even more), as we do in the following sections, is completely infeasible using these distances.

Let us now compare how the positionwise distance fares against the isomorphic swap and Spearman ones. Foremost, there is a fast, polynomial-time algorithm for computing the positionwise distance. Hence, it is possible to use it for much larger elections than the two isomorphic distances; computing the maps shown in this paper takes at most a few hours on a modern desktop computer and not weeks on a powerful computing cluster. Further, as the positionwise distance operates on frequency matrices, it can directly work on elections with different numbers of voters (although we never use this feature in this paper). On the other hand, applying isomorphic swap and Spearman distances to elections with different numbers of voters would require additional work. The positionwise distance also has a similar robustness property as the swap and Spearman ones: Introducing a small change to one of the elections in its input can only mildly affect the output. Just like the two isomorphic distances, it is also agnostic to which parts of the votes are changed; it treats all the positions in the votes similarly.

The big difference between the positionwise distance and the swap and Spearman ones lies in the equivalence classes they induce. Given an election E , we say that its equivalence class under a distance d consists of all elections that are at distance zero from E under d . Since the positionwise distance is defined over frequency matrices, by definition it has fewer equivalence classes (hence, it is in some sense less precise) than the swap and Spearman distances. However, Boehmer et al. [22] have shown that among all distances that they tried (that are invariant to renaming the candidates and voters), the positionwise distance still has the largest number of equivalence classes, with a fairly large advantage over the other distances, including one defined on top of weighted majority relations of input elections. Hence, while the positionwise distance loses precision as compared to the swap and Spearman distances, the loss is the smallest among distances that were considered for the map framework to date.¹²

Finally, we mention that Boehmer et al. [22] also computed Pearson correlation coefficient (PCC, see Section 4.3.1 for a formal introduction of this measure) between distances computed using the isomorphic swap distance and several other ones. They found that the positionwise distance had the highest correlation (e.g., on a dataset of 340 diverse elections, formed in a similar spirit as the dataset that we describe in the next section, the PCC between the positionwise distance and isomorphic swap distance was 0.745, which means a strong correlation).

Overall, we conclude that the positionwise distance is a good choice for the map framework, for regimes where neither the isomorphic swap nor the isomorphic Spearman ones can be used.

4 Maps of Statistical Cultures

The main goal of this section is to form a map of elections generated using various statistical cultures, to analyze its contents, and to argue that it is accurate and, hence, credible. We consider all the statistical cultures from Section 2.3, but, naturally, we use a limited set of parameters. Specifically, in Section 4.1, we describe the precise composition of our diverse synthetic dataset and present its visualization as a map. Subsequently, in Section 4.2, we analyze where elections generated by different statistical cultures land on the map and which elections end up being placed close to each other and why. Next, in Section 4.3, we verify whether the produced maps are credible in the sense that distances between points on the map accurately reflect the positionwise distances between the corresponding elections.

Overall, this section presents the first use case of the map (*Finding Relations Between Elections*), as presented in Section 1.3.

¹²Note that Boehmer et al. [22] only looked at equivalence classes of very small elections, with a few candidates and voters.

Model	Number of Elections
Impartial Culture	20
Single-Peaked (Conitzer)	20
Single-Peaked (Walsh)	20
SPOC	20
Single-Crossing	20
1D	20
2D	20
3D	20
5-Cube	20
10-Cube	20
20-Cube	20
Circle	20
Sphere	20
4-Sphere	20
Group-Separable (Balanced)	20
Group-Separable (Caterpillar)	20
Urn	80
Mallows	80
Compass (ID, AN, UN, ST)	4
Paths	20×4

Table 1: Composition of the datasets used in Section 4.

4.1 Choosing the Dataset and Drawing the Map

All datasets that we use in this section consist of 480 elections from various statistical cultures—their exact composition is given in Table 1—and we describe the parameters for the urn and Mallows model a bit later. Additionally, we include the four compass matrices and 80 path matrices (20 matrices per path; we omit the paths between UN and ID and between AN and ST, which would cross in the middle of the map and would make it more cluttered). All the elections that we consider include 100 voters and, typically, 100 candidates, but occasionally we consider candidate sets with different cardinalities. We refer to our main dataset as the 100×100 one, but we also consider, e.g., 4×100 , 10×100 or 20×100 datasets, whose elections have, respectively, 4, 10, or 20 candidates and 100 voters. All these datasets consist of elections coming from the same cultures, as described in Table 1. For each number of candidates, we only generate a single dataset. Thus, for example, all maps that depict the 100×100 dataset regard the same 480 elections (plus the 84 matrices for the compass and the paths).¹³

Most of the statistical cultures that we use either do not have parameters, as in the case of, e.g., impartial culture or single-crossing models, or have fairly simple ones, as in the case of, e.g., the Euclidean models for which we only select the dimension.¹⁴ Yet, the choice of the parameters for the urn and

¹³The only exception to this rule appears in Section 4.3 where we generate several different datasets of each size (but with the same composition), to analyze the robustness of the maps that we obtain. Nonetheless, even in that section the figures depict our main 100×100 dataset, that also appears in other sections.

¹⁴Naturally, one could argue that for the Euclidean model we should also view the distribution of the points as a parameter. This certainly is a valid point of view and it would be interesting to consider what types of elections one obtains by varying the distributions of the candidate and voter points, but it goes beyond the scope of this paper. We focus on the simple distributions

Mallows models requires some care:

Urn model. Recall that the urn model has the parameter of contagion α , which takes values between 0 and ∞ . The larger is this parameter, the more similar are the generated elections to the identity one. To generate an urn election, we choose α according to the Gamma distribution with shape parameter $k = 0.8$ and scale parameter $\theta = 1$. This ensures that about half of the urn elections are closer to UN than to ID, and about half are closer to ID than to UN (we have verified this experimentally).

Mallows model. Regarding the Mallows model, we have the central vote v^* and the dispersion parameter ϕ , which takes values between 0 and 1. Using $\phi = 0$ leads to generating ID elections (where all the votes are equal to v^*) and using $\phi = 1$ leads to generating IC ones. Hence, on the surface, it seems natural to choose ϕ uniformly at random from the interval $[0, 1]$. We do not take this approach and, instead, we use the normalization introduced by Boehmer et al. [19].¹⁵ Specifically, they introduced a new parameter $\text{norm-}\phi$, which is converted to the original dispersion parameter as follows: For an election with m candidates and a value of $\text{norm-}\phi \in [0, 1]$, we compute ϕ such that the expected swap distance between a generated vote and the central one (normalized by $m(m-1)/2$, i.e., the largest possible swap distance between two votes) is equal to $\text{norm-}\phi/2$. Consequently, using $\text{norm-}\phi = 0$ still leads to generating identity elections, using $\text{norm-}\phi = 1$ still gives the Impartial Culture model. However, now using $\text{norm-}\phi = x \in [0, 1]$ leads to generating elections whose expected swap distance to ID is an x fraction of the distance between ID and UN, irrespective of the number of candidates (Boehmer et al. [19] observed that the same holds if we use the positionwise distance instead of the isomorphic swap one).¹⁶ The problem with the classic dispersion parameter is that if we fixed it as $\phi = x$, $0 < x < 1$, and generated elections with more and more candidates, their swap distance would decrease relative to the distance between ID and UN [19]. Consequently, using the Mallows model with the classic ϕ parameter selected uniformly at random (for a large number of candidates, such as 100) would lead to a large cluster of elections near ID and far fewer elections near UN. Using values of the $\text{norm-}\phi$ parameter chosen uniformly at random generates Mallows elections that, roughly speaking, are spread uniformly between ID and UN. Hence, we use the latter approach (see also the arguments for the normalized model provided by Boehmer et al. [24]). In the following, whenever we discuss the Mallows model, we use the $\text{norm-}\phi$ parameter.

We have computed the positionwise distance between each pair of elections from the 100×100 dataset (see Figure 4). Next, we have prepared the map of this dataset using the same methodology as in Section 3.7. In particular, this means that we used the Kamada-Kawai embedding algorithm [78]. In Appendix B we compare this map with two other ones, formed using the Fruchterman-Reingold (FR) embedding algorithm [71] and the MDS algorithm [44, 83].

4.2 General Observations

In this section, we describe and analyze the map from Figure 5. We start with some more general observations before we discuss different areas of the map in more detail. One of the most glaring observations

described in Section 2.3.

¹⁵Note that the work of Boehmer et al. [19] is one of the two conference papers on which the current work is based. We omit a detailed discussion of the proposed normalization of the Mallows model here because we consider it to be sufficiently important that it deserves its own paper, focused explicitly on its features and properties (which we intend to write later, and whose conference version already exists [24]). Consequently, here we only refer to the initial definition of the normalization and we briefly explain why we find it useful.

¹⁶The reader may worry that UN is a matrix rather than election. Indeed, for the swap distance, to compute the distance between ID and UN, we would measure a distance between an election where all votes are identical (ID) and an election where each possible vote appears the same number of times (UN).

	ID	UN	AN	ST	IC	SP (Con.)	SP (Wal.)	SPOC	SC	1D	2D	3D	Circle	GS (Bal.)	GS (Cat.)
ID	.	1	.75	.5	.93	.74	.15	.93	.55	.74	.75	.74	.93	.91	.73
UN	1	.	.5	.75	.09	.36	.88	.1	.55	.36	.32	.32	.1	.17	.45
AN	.75	.5	.	.81	.47	.34	.74	.47	.55	.33	.45	.48	.45	.41	.12
ST	.5	.75	.81	.	.68	.53	.4	.68	.36	.54	.49	.48	.69	.69	.76
IC	.93	.09	.47	.68	.06	.3	.81	.07	.47	.3	.25	.25	.08	.14	.41
SP (Con.)	.74	.36	.34	.53	.3	.09	.62	.31	.33	.09	.18	.2	.31	.31	.33
SP (Wal.)	.15	.88	.74	.4	.81	.62	.02	.81	.42	.62	.62	.61	.82	.79	.68
SPOC	.93	.1	.47	.68	.07	.31	.81	.08	.47	.31	.26	.25	.09	.14	.41
SC	.55	.55	.55	.36	.47	.33	.42	.47	.12	.34	.28	.27	.48	.47	.48
1D	.74	.36	.33	.54	.3	.09	.62	.31	.34	.09	.19	.21	.31	.31	.33
2D	.75	.32	.45	.49	.25	.18	.62	.26	.28	.19	.09	.1	.27	.28	.39
3D	.74	.32	.48	.48	.25	.2	.61	.25	.27	.21	.1	.09	.26	.28	.42
Circle	.93	.1	.45	.69	.08	.31	.82	.09	.48	.31	.27	.26	.09	.14	.4
GS (Bal.)	.91	.17	.41	.69	.14	.31	.79	.14	.47	.31	.28	.28	.14	.1	.35
GS (Cat.)	.73	.45	.12	.76	.41	.33	.68	.41	.48	.33	.39	.42	.4	.35	.06

Figure 4: Matrix of normalized positionwise distances between elections from the 100×100 dataset. The number in each cell gives the average distance between elections from respective cultures (cells on the diagonal give average distances between elections from the given culture).

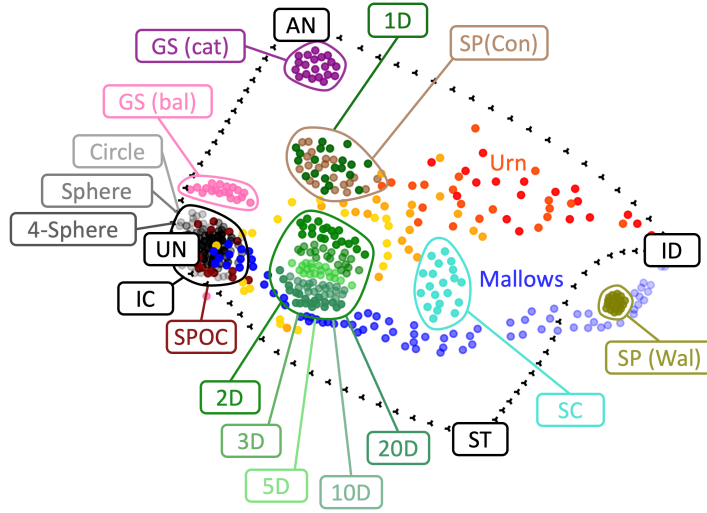


Figure 5: Map of elections obtained using the Kamada-Kawai algorithm (KK). The colors of the dots correspond to the statistical culture from which the elections are generated. Elections generated from the Mallows model use the blue color, and the more pale they are, the closer is the $\text{norm-}\phi$ parameter to 0. The urn elections use yellow-red colors, and the more red they are, the larger is the contagion parameter α .

is that elections coming from the same statistical culture are typically clustered together and do not have elections from other cultures in between (two main exceptions include elections that are located close to the UN matrix, which are quite mixed, and the 1D-Interval and single-peaked elections generated according to the Conitzer model; see our discussion below). Indeed, this clustering seems appropriate given the (underlying) positionwise distances between the elections, as shown in Figure 4: Elections from the same statistical cultures are, on average, closer to each other than to the other elections. Another general observation is that the compass matrices and the paths between them (mostly) encircle the other

elections (with the exception of the area close to the Walsh single-peaked elections). This suggests that, indeed, the compass matrices are quite extreme in the space of elections induced by the positionwise distance (or that our set of statistical cultures is missing some distinguished type of elections).

Throughout the rest of this section we discuss specific statistical cultures and areas of the map. We stress that the maps themselves are visualization tools and only provide intuitions. Accordingly, we verified all the comments and observations that we made below against the actual (underlying) positionwise distances.

4.2.1 Impartial Culture and Elections Around UN

The area near the UN matrix contains a number of very different elections, ranging from the completely unstructured ones, generated using the impartial culture model, to highly structured SPOC ones (and closely related Sphere ones). The reason why these very different elections take this position is an inherent flaw in the positionwise distance and frequency matrices. Indeed, both under IC and under SPOC, each candidate appears at each position in a generated vote with the same probability. The difference between IC and SPOC is that under IC there are almost no correlations between the positions of two given candidates in a single vote (except that they cannot be equal), whereas under SPOC the correlations can be quite strong (e.g., if two candidates are next to each other on the societal axis, then they are likely located nearby in the vote). Yet, the positionwise distance is blind to such correlations as they are not captured in election’s frequency matrices. This is the price that we need to pay for using a fast-to-compute distance (using, e.g., the isomorphic swap distance would avoid this issue, but would prevent us from considering large candidate sets). We point to the work of Boehmer et al. [20] for a detailed discussion of expected frequency matrices of various statistical cultures, and to the work of Boehmer et al. [22] for a comparison of several distances that one could use in the maps (including the positionwise one and the isomorphic swap one).

Another interesting issue is that balanced group-separable elections are near the UN matrix, but still at some distance from it. If the number of candidates were a power of two, then each candidate in a vote generated for a balanced group-separable election would be located at each possible position with the same probability and group-separable elections would be mixed together with the IC and SPOC ones. However, since we consider 100 candidates, the symmetry is broken to some extent and balanced group-separable elections are a bit further away.

Finally, we note that elections generated from the impartial culture model cover a relatively small area of the map. This confirms the well-accepted intuition that limiting one’s experiments to this model is likely to produce biased results, as we would ignore a huge number of possible elections that are not similar to the IC ones.

4.2.2 Urn and Mallows Elections

The elections generated using the urn and Mallows models form “paths” that link the UN and ID matrices. Importantly, these paths are, roughly, equally dense. For example, if we consider the urn “path” then irrespective of whether we are looking at the area near the UN matrix, or the area near the ID matrix, or anywhere in between, there is a similar number of elections in the vicinity. The same applies to the Mallows elections. This confirms that our way of generating the α and norm- ϕ parameters is reasonable (in Section 4.3.3 we will see that this property is maintained for different numbers of candidates).

4.2.3 Single-Peaked and 1D-Interval Elections

Single-peaked elections generated using the Conitzer model are nearly indistinguishable from those generated using the 1D-Interval model (as far as their positionwise distances go). This is because both models generate elections in a somewhat similar manner. Indeed, generating 1D-Interval elections, if

we draw the ideal points of the candidates and voters uniformly at random from an interval, then the process of forming the preference orders of the voters is similar to the one used in the Conitzer model. The difference is that in the 1D-Interval model there are more correlations: A given voter v ranks the candidate with the closest ideal point on top, the next ranked candidate is either to the left or to the right of the first one, and this happens with probability close to $1/2$, and so on (as in the Conitzer model). The correlations occur because the decisions regarding which candidate should be ranked next are not made independently for each voter, but are derived from the positions of the ideal points; still, apparently, these correlations are sufficiently small not to be easily detectable using the positionwise distances.

Elections generated using the Walsh model are very different from those generated using the Conitzer one. To get a feeling as to why this is a natural result, let us consider a candidate set $C = \{l_m, \dots, l_1, c, r_1, \dots, r_m\}$ and the corresponding societal axis $l_m \triangleleft \dots \triangleleft l_1 \triangleleft c \triangleleft r_1 \triangleleft \dots \triangleleft r_m$. Under the Conitzer model, the probability of generating a vote with a given candidate on top is $\frac{1}{2m+1}$ (by definition of the model), but under the Walsh's model these probabilities differ drastically. The probability of a vote with l_m on top (or, with r_m on top) is $\frac{1}{2^{2m}}$ (because there are 2^{2m} different single-peaked votes for this axis, each of them is drawn uniformly at random, and only one of them starts with l_m), whereas the probability of generating a vote with c on top is $\Theta(\frac{1}{\sqrt{m}})$ (we omit the calculations). Generally, Walsh's model generates votes that are similar to $c \succ \{l_1, r_1\} \succ \{l_2, r_2\} \succ \dots \succ \{l_m, r_m\}$; i.e., they are close to having a center order, as in the Mallows model. This explains both the distance of the Walsh elections from the Conitzer ones, and their proximity to some Mallows elections. Boehmer et al. [20] give a detailed analysis of the frequency matrices of Conitzer, Walsh, and Mallows distributions, which supports this observation. The differences between the Conitzer and Walsh elections are also very clearly visible in “microscope” maps provided by Faliszewski et al. [67], which depict inner structures of single elections.

4.2.4 Euclidean Elections

We observe that, for a given x , the x -dimensional hypercube elections are quite similar to each other and also fairly similar to hypercube elections generated for other dimensions. One exception is that the 1D-Interval elections are more different from the other hypercube ones. This is understandable since 1D-Interval elections are single-peaked and single-crossing, whereas the other hypercube elections are not. Interestingly, the computed positionwise distances were sufficient to recognize this difference. Generally, hypercube elections seem to form a large and diverse class, which means that they may be useful in experiments. Indeed, in Section 6 we observe that many real-life elections land in the same area of the map as high-dimensional hypercube ones.

Similar observations as for the hypercube elections apply to hypersphere ones, except that—as discussed before—they are quite similar to the impartial culture elections under the positionwise distance. This shows that the distribution of the ideal points in the Euclidean models has a strong impact on the generated elections. Further studies are needed to recommend distributions that should be used in experiments (as some may lead to particularly appealing classes of elections, or, perhaps, to elections that are close to those appearing in reality). The similarity between SPOC and hypersphere elections is reassuring. Indeed, Circle elections are, by their nature, a subset of SPOC ones, and for higher dimensions we would not expect big changes.

4.2.5 Single-Crossing Elections

Elections generated using our single-crossing model are fairly close to both the Mallows ones and the urn ones, but are at quite some distance from the 1D-Interval elections, which also are single-crossing. Indeed, the map certainly does not show all kinds of similarities between elections, but only those captured by the positionwise distance.

dataset	average PCC values Kamada-Kawai
4×100	0.9661 ± 0.0044
10×100	0.9686 ± 0.0061
20×100	0.9745 ± 0.0015
100×100	0.9735 ± 0.0115

Table 2: Average values of the PCC between the original and embedded distances for collections of datasets of various sizes. After the \pm signs we report the standard deviations.

4.3 Accuracy of the Maps

Now that we have seen that the maps can provide some interesting insights regarding the nature of the depicted elections, let us analyze how accurate is the map from Figure 5, in the sense of capturing the positionwise distances between the elections most precisely. To this end, we will evaluate it using three measures. First, in Section 4.3.1 we will evaluate the correlation between the positionwise distance between two elections and the Euclidean distance between their points in the embeddings. Second, in Section 4.3.2 we will have a closer look at the extent to which distances between elections are distorted. Finally, in Appendix B.2 we will consider whether relations between positionwise distances are preserved.

In this section, whenever we write *original distance* we refer to the positionwise distance between two elections, and whenever we write *embedded distance* we refer to the Euclidean distance between the points on a given map (which correspond to these elections). Whenever we write *normalized embedded (original) distance*, we refer to the embedded (original) distance divided by the embedded (original) distance between the ID and UN matrices (as it is the largest possible one). Further, we introduce the notion of an *embedding summary*: By an embedding summary $Q = (\mathcal{E}, d_{\mathcal{M}}, d_{\text{Euc}})$ we refer to a triple that consists of a set of elections \mathcal{E} , original distances $d_{\mathcal{M}}$ between these elections according to metric \mathcal{M} , and Euclidean distances d_{Euc} between these elections after the embedding.

In the analysis below, we will be interested in two kinds of results. Foremost, we will analyze the accuracy of the embedding shown in Figure 5. However, to also evaluate if the results are not due to random chance, for each dataset size (i.e., 4×100 , 10×100 , 20×100 , and 100×100) we generate 10 datasets (as described in Section 4.1) and report averages and standard deviations for them (given the low variance of the results we observed, we find using 10 datasets sufficient).

4.3.1 Correlation Between the Positionwise and Euclidean Distances

Given an embedding summary $Q = (\mathcal{E}, d_{\mathcal{M}}, d_{\text{Euc}})$ associated with some embedding, we would like to evaluate the correlation between the original distances and the Euclidean ones. To this end, we use the Pearson correlation coefficient (PCC), a classical measure of linear correlation used in statistics.

For two vectors $x = (x_1, \dots, x_t)$ and $y = (y_1, \dots, y_t)$, their PCC is defined as follows (\bar{x} is the arithmetic average of the values from x ; \bar{y} is defined analogously):

$$\text{PCC}(x, y) = \frac{(\sum_{i=1}^t (x_i - \bar{x})(y_i - \bar{y}))}{\sqrt{\sum_{i=1}^t (x_i - \bar{x})^2 \sum_{i=1}^t (y_i - \bar{y})^2}}.$$

PCC measures the level of linear correlation between two random variables and takes values between -1 and 1 (its absolute value gives the level of correlation and the sign indicates positive or negative correlation; in our case, the closer a value to 1 , the more correlation there is).

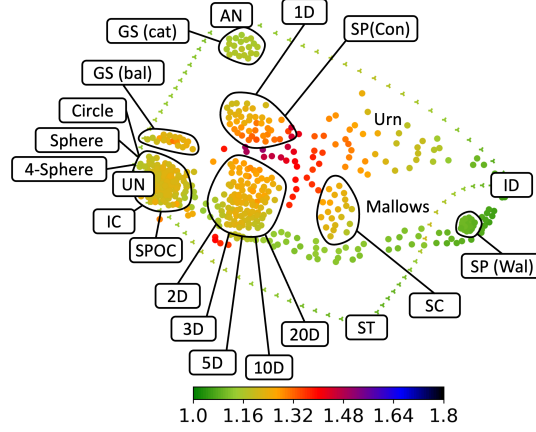


Figure 6: Distortion coloring for the embedding from Figure 5. Each election X (i.e., each point X) has a color reflecting its value $\text{AMR}(X)$ for the respective embedding.

For the embedding from Figure 5 we get very high PCC, equal to 0.9805. In Table 2 we report average PCC values and standard deviations for our datasets of various sizes (note that for our map in Figure 5 we chose a particularly fortunate embedding, so its PCC value is notably better than the average reported in Table 2). All in all, we see that the PCC values are very high for all datasets. In Appendix B.1 we compare the performance of Kamada-Kawai algorithm with that of FR and MDS and show that it has strong advantage over the former and slight over the latter.

4.3.2 Distortion

We analyze distortion of the distances introduced by the embedding. The intuition is that the normalized embedded distance between two points should be similar to the normalized original one. Formally, for a given pair of elections X and Y the *distortion* is defined as:

$$\text{MR}(X, Y) = \frac{\max(\bar{d}_{\text{Euc}}(X, Y), \bar{d}_{\mathcal{M}}(X, Y))}{\min(\bar{d}_{\text{Euc}}(X, Y), \bar{d}_{\mathcal{M}}(X, Y))},$$

where $\bar{d}(X, Y)$ means that the distance between X and Y is normalized by the distance between ID and UN. Note that $\text{MR}(X, Y) \geq 1$ for all elections X and Y . Its value can be interpreted as the relative error between the original and the embedded distance. For example, if $\text{MR}(X, Y) = 1.2$ then it means that the larger among the original and the embedded distance between X and Y is 20% larger than the other one. For a given embedding summary $Q = (\mathcal{E}, d_{\mathcal{M}}, d_{\text{Euc}})$ and a given election X , we define the average *distortion* of this election in this embedding summary as:

$$\text{AMR}_Q(X) = \frac{1}{|\mathcal{E}| - 1} \sum_{Y \in \mathcal{E} \setminus \{X\}} \text{MR}(X, Y).$$

The closer is the AMR value to one, the better—this means that the embedded distances are proportional to the original ones.

In Figure 6, we present the map from Figure 5 with elections colored according to their distortion (i.e., according to their AMR values). In Appendix B.3 we compare these distortion values to those achieved by FR and MDS and find that our KK embedding is superior. We see that urn elections, as well as 1D-Interval and Conitzer ones, have the highest average distortion. Another way of phrasing this observation would be that elections in the center of the map tend to have the highest distortion.

dataset	total average distortion values Kamada-Kawai
4×100	1.2612 ± 0.0158
10×100	1.2625 ± 0.0125
20×100	1.2406 ± 0.0060
100×100	1.2119 ± 0.0123

Table 3: Total average distortion values (i.e., AMR values) for collections of datasets of various sizes. After the \pm signs we report the standard deviations.

In Table 3 we present the average values of the average distortions for the KK embedding and datasets with different numbers of candidates. For each dataset, we compute the average AMR value for its elections, as well as the standard deviation. We observe that the more candidates there are, the lower is the distortion value. Overall, the distances in the embedding are, on average, off by 20 – 26%.

One reason why the distortion values may be high is that it is particularly difficult to represent distances between elections within a single statistical culture. For example, all elections in the 100×100 dataset generated from the impartial culture model are at roughly the same distance from each other, but it is impossible to reflect this accurately in an embedding. Hence, in Table 4 we report average total distortion values for elections from each of our statistical cultures, but computed only against elections that are sufficiently far away from them. Specifically, for each election X from a given statistical culture we consider only those other election Y from the dataset for which:

$$\text{POS}(X, Y) \geq 0.1 \cdot \text{POS}(\text{UN}, \text{ID}).$$

This way we disregard embedding errors that occur close to a given election and focus on the broader picture. We see that the distortion values in Table 4 are much lower than those reported in Table 3. For example, the overall result for the KK embedding is 1.159 and for some cultures (such as, e.g., the Mallows model or the high-dimensional Euclidean models) the results are notably lower. We interpret this as saying that, all in all, our maps are sufficiently accurate, but certainly not perfect.

4.3.3 Varying the Number of Candidates

Next, we check the robustness of the map with respect to varying the number of candidates in the depicted elections. In Figure 7 we compare the maps of the 4×100 , 10×100 , 20×100 , and 100×100 datasets, created using the KK algorithm. As we can see, the maps for 10, 20, and 100 candidates are surprisingly similar. The largest difference we can observe is for the balanced group-separable elections—for the case of 100 candidates they are clearly separated, while for 10 and 20 candidates they are mingling with the Circle elections (one possible explanation for this could be that, relatively speaking, for 100 candidates the underlying tree is closer to being balanced than for 10 and 20 candidates). In addition, Euclidean elections of different dimensions are better separated from each other for 100 candidates than for 10 or 20 candidates. Another interesting observation is that the Walsh elections are shifting toward the right side of the map as we increase the number of candidates. At the same time, the caterpillar group-separable elections are shifting toward AN (these two effects are symmetric as the frequency matrices of Walsh elections are transposed frequency matrices of the caterpillar group-separable ones; for details, see the work of Boehmer et al. [20]).

Only the map with four candidates is different, even if the main shape is still maintained. Note that for 4 candidates there are only 24 possible different votes, which likely explains why the map is not as meaningful. For example, Faliszewski et al. [69] have shown that if we generate two elections with 4 candidates and 50 voters using two, possibly different, statistical cultures (including many of

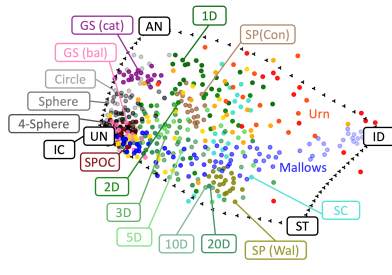
Model	average distortion values Kamada-Kawai
Impartial Culture	1.07
Single-Peaked (Conitzer)	1.244
Single-Peaked (Walsh)	1.071
SPOC	1.081
Single-Crossing	1.225
1D	1.233
2D	1.203
3D	1.146
5-Cube	1.114
10-Cube	1.094
20-Cube	1.097
Circle	1.101
Sphere	1.077
4-Sphere	1.072
Group-Separable (Balanced)	1.204
Group-Separable (Caterpillar)	1.14
Urn	1.285
Mallows	1.094
All	1.159

Table 4: Total average distortion values for elections from given cultures in the 100×100 dataset, where for each election X we compute the average distortion only with respect to elections whose distance from X is at least $0.1 \cdot \text{POS}(\text{ID}, \text{UN})$.

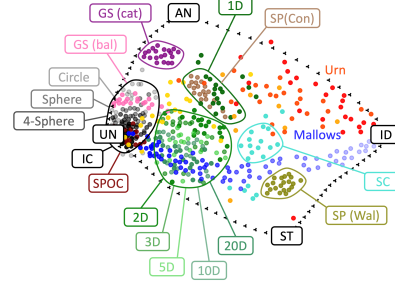
those that we consider), it often suffices to delete between 20% and 50% of the voters (from each of the elections) to make them isomorphic. For the case of 10 candidates, one would typically have to delete between 85% and 97% of the voters to achieve isomorphism. Hence it is not surprising that our map for 4 candidates is not as similar to the other ones (even if we use 100 voters and not 50).

4.3.4 Varying the Number of Voters

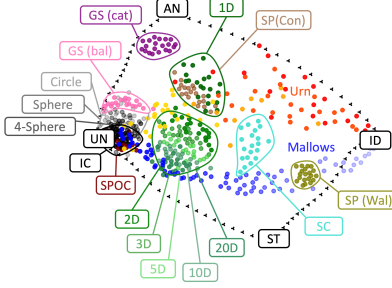
One may also ask about the influence of the number of voters on the shapes of our maps, especially in relation to the number of candidates. The answer to this question lies in the nature of the positionwise distance and the work of Boehmer et al. [20]: As the positionwise distance operates on elections' frequency matrices, the more voters there are, the closer are the frequency matrices of elections to the expected frequency matrices of the culture from which the elections were generated. As a result, the more voters there are, the more will our maps resemble the map of these expected matrices, provided by Boehmer et al. [20]. This map is very similar to those we show in Figure 7 (except for the one for four candidates). In particular, this implies that if we were to consider more and more voters, the location of the elections from the respective statistical cultures would converge to the locations of their expected frequency matrices. While this would result in lower spread of elections from one culture on the map, the general relations between the statistical cultures would be maintained. We confirm this in Figure 8, where we compare the map of the 100×100 dataset with maps of elections that have 100 candidates, but



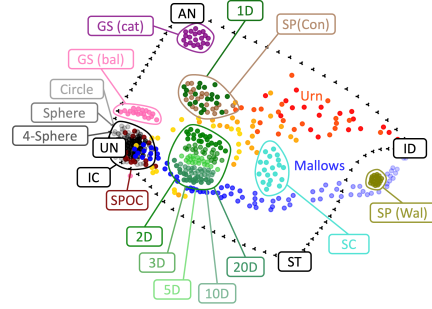
(a) 4 candidates and 100 voters



(b) 10 candidates and 100 voters

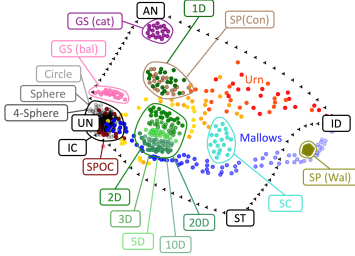


(c) 20 candidates and 100 voters

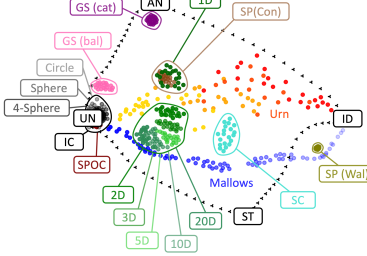


(d) 100 candidates and 100 voters

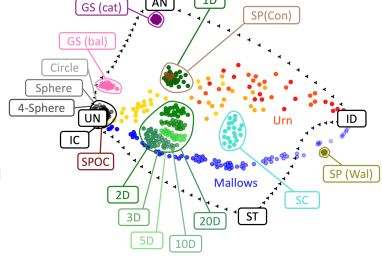
Figure 7: Maps of elections for datasets with different numbers of candidates.



(a) 100 candidates and 100 voters



(b) 100 candidates and 1000 voters



(c) 100 candidates and 2000 voters

Figure 8: Maps of elections for datasets with different numbers of voters.

where the numbers of voters are 1000 and 2000, respectively. We see that, indeed, elections generated from each culture (except for the urn one) are placed more compactly on maps for higher numbers of voters (this does not apply to the urn model because urn elections do not have an expected frequency matrix).

5 Examples of Experiments Using the Map

To demonstrate the usefulness of our map framework, we show its application in several experiments related to the analysis of voting rules. To this end, we use the 100×100 dataset from the previous section. Indeed, some of our experiments involve measuring running times and, hence, we need a dataset with large enough votes for the results to be meaningful. First, we focus on the scores obtained by winning

candidates for two prominent single-winner rules. Then, we look more closely at the running times of ILP-based algorithms for selected NP-hard rules. Finally, we analyze several approximation algorithms for finding high-scoring committees. Overall, the first two groups of experiments focus on the second use case described in Section 1.3 (*Visualizing Election Properties*), and the final group focuses on the third one (*Comparing Algorithm Performance*).

As each of our experiments regards a different collection of voting rules and/or algorithms, each of them includes a short description of the necessary preliminaries, where the preliminary part for the first experiment is also partially applicable to the other experiments.

5.1 Maps of Winner Scores: Borda and Copeland

In this section we visualize the scores of the winning candidates under the Borda and Copeland single-winner voting rules for the 100×100 dataset. Overall, we find that the positions on the map give relatively good information about the winner score that one might expect (however, as typical in experimental evaluation, nothing is perfect). Knowing the winner scores is useful as it confirms many natural intuitions (such as that the closer we are to the identity election, the higher scores we should expect) and, hence, provides additional arguments for the credibility of our map approach. We stress that the conclusions we get here about the scores are not necessarily universal: For other voting rules the results and conclusions might be quite different. Nonetheless, the presented experiments—especially for the Borda winners—show some of the most successful applications of the map (the running time experiment for Harmonic Borda in the next section is similar in this respect).

5.1.1 Borda and Copeland Rules

A single-winner voting rule is a function f that given an election $E = (C, V)$ outputs a set $W \subseteq C$ of the winners of E . Typically, we expect W to be a singleton, but ties may happen and then one needs some tie-breaking rule. Fortunately, in our analysis such tie-breaking will not be necessary. Below we describe Borda and Copeland voting rules, on which we focus in this experiment. Both rules are similar in the sense that we compute a score for each candidate and output those with the highest one:

Borda. Each voter assigns $m - 1$ points to the candidate that he or she ranks on the top position, $m - 2$ points to the second one, $m - 3$ to the third one, and so on, until the bottom-ranked candidate who receives 0 points from the voter.

Copeland. We examine all pairs of candidates. In each pair, the candidate who is preferred by more than half of the voters gets a point. If neither of the candidates is preferred to the other one by more than half of the voters, then both of them receive half a point.

Candidate c is a Condorcet winner if for every other candidate d , more than half of the voters rank c ahead of d . Note that if a Condorcet winner exists, then he or she will always be selected by the Copeland rule (such rules are called Condorcet extensions). The scores of the winning candidates can be computed in polynomial time for both our rules.

5.1.2 Score Maps

For each of the elections in our dataset, we computed the score of the winning candidate(s) for both Borda and Copeland. We present the results in Figure 9, where the color of each point corresponds to the score obtained by the winning candidate(s) in a given election. Note that for the Borda map, the paths, which consist of frequency matrices, are colored as well. This is so, because for Borda frequency matrices (together with the number of voters) contain enough information to compute the candidate

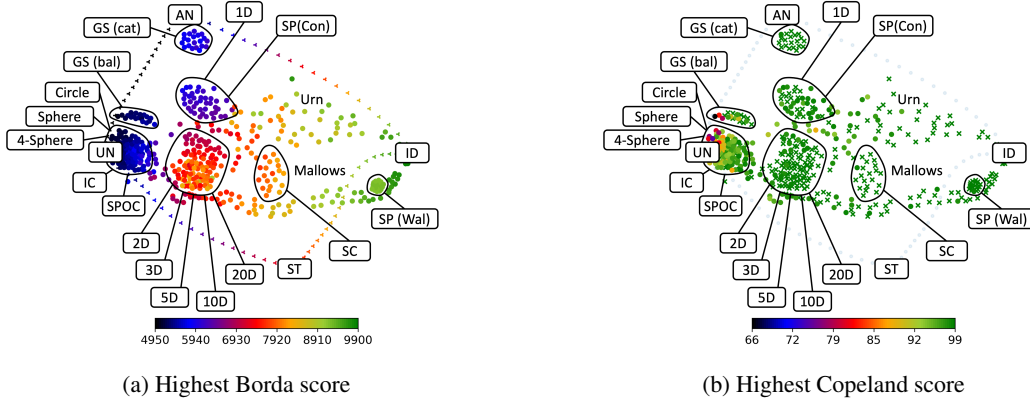


Figure 9: Maps of 100×100 elections colored according to the score obtained by the winner.

scores. For Copeland, we left the paths' uncolored because the frequency matrices are insufficient to determine the scores.

As for the Borda coloring, we observe that elections on the line between UN and AN have the same color. As we move from this line toward ID, we see a smooth shading. Consequently, Borda scores of the winners nicely correlate with the positions of our elections on the map. As we move closer to ID, the score of the Borda winner is increasing, and as we move toward UN/AN path, the score is decreasing. Indeed, the AN-UN path is interesting, as Borda winners have nearly the lowest possible scores for elections located there. This means that elections placed in this part of the map are very close to a tie according to the Borda rule.

Overall, the smooth shading and interpretability of the map for Borda is very appealing, but hardly surprising, as the Borda rule—and the score system it uses—seems particularly well aligned with the nature of the positionwise distance.

For the Copeland map, with crosses we mark elections that have a Condorcet winner. In our map 55% (264 out of 480) of the generated elections have a Condorcet winner.¹⁷ In particular, almost all the single-crossing, Walsh, caterpillar group-separable, 3-Cube, 5-Cube, 10-Cube, 20-Cube, and around half of 1D-Interval, 2D-Square, Conitzer, and balanced group-separable elections have a Condorcet winner. Even one IC election has a Condorcet winner. For the urn and Mallows elections, having a Condorcet winner is strongly related to their parameters. However, there are also elections without Condorcet winners that are located near those that have them. This is quite natural as relations between pairs of candidates are not reflected directly in frequency matrices. Yet, it is reassuring that for such elections Copeland scores of the winners still tend to be high (except for a few urn elections), so—in a certain formal sense—they are close to having Condorcet winners.

It is striking that for most elections the Copeland score of the winner is very high. Indeed, it is greater or equal to 90 in 449 elections out of the 480 present in the 100×100 dataset. The lowest Copeland score is witnessed by a balanced group-separable election. In general, the vast majority of lowest values are obtained by Circle, Sphere and 4-Sphere, as well as some SPOC and balanced group-separable elections. Note that all values are much larger than the lowest possible score, which is 49.5. Keeping all that in mind, the position on the map is still a good indication for the score of the Copeland winner: The score is very high, unless the election is very close to the UN compass matrix (however, a few of the urn elections have lower Copeland scores while being located at some distance from UN). Further, the elections in the vicinity of ID tend to have Condorcet winners (which is hardly surprising)

¹⁷Elections that are single-peaked, single-crossing, or group-separable, always have a Condorcet winner for an odd number of voters, and always have a weak Condorcet winner (or winners) for an even number of voters. A candidate c is a weak Condorcet winner if for every candidate d , at least half of the voters prefer c to d .

and even those as far as 3/4 of the UN-ID distance from ID are likely to have Condorcet winners (which is far more interesting).

5.2 Maps of ILP Running Times: Dodgson and Harmonic-Borda

Next, we consider two rules that are NP-hard to compute, namely the single-winner Dodgson rule and the multiwinner Harmonic Borda rule that we mentioned in our motivating example in Section 1.1. For both of these rules there are natural ILP formulations and we will evaluate how much time an ILP solver needs to compute Dodgson winners and Harmonic Borda winning committees on our elections. As throughout this section and most of the paper, we focus on the 100x100 dataset.

All the times that we report were obtained using the CPLEX ILP solver on a single thread (Intel(R) Xeon(R) Platinum 8280 CPU @ 2.70GH) of a 448 thread machine with 6TB of RAM.

5.2.1 Dodgson and Harmonic Borda

The score of a candidate under the Dodgson rule is the smallest number of swaps of adjacent candidates that need to be performed in the votes to make him or her the Condorcet winner. The candidate(s) for whom this value is lowest win(s). It is well-known that deciding if a given candidate is a Dodgson winner is NP-hard [6] and even Θ_2^P -complete [75]. However, one can compute Dodgson winners using an ILP solver and an ILP formulation [6, 36], or use one of the available FPT algorithms [14], or—if perfect precision is not required—use approximation algorithms [35, 36].

Harmonic Borda (HB) is a multiwinner voting rule, which means that given an election E and committee size k it outputs size- k candidate subsets as the (tied) winning committees. The rule proceeds as follows. Let $E = (C, V)$ be an election and let k be the committee size. For a committee S of k candidates and a vote v , we let the HB score that v assigns to S be the result of the following procedure:

For each candidate $c \in S$, we compute this candidate's position $\text{pos}_v(c)$ in v and sort these values from lowest to highest, obtaining vector (p_1, \dots, p_k) . The HB score assigned to S by v is $(p_1 - 1) + \frac{1}{2}(p_2 - 1) + \frac{1}{3}(p_3 - 1) + \dots + \frac{1}{k}(p_k - 1)$.

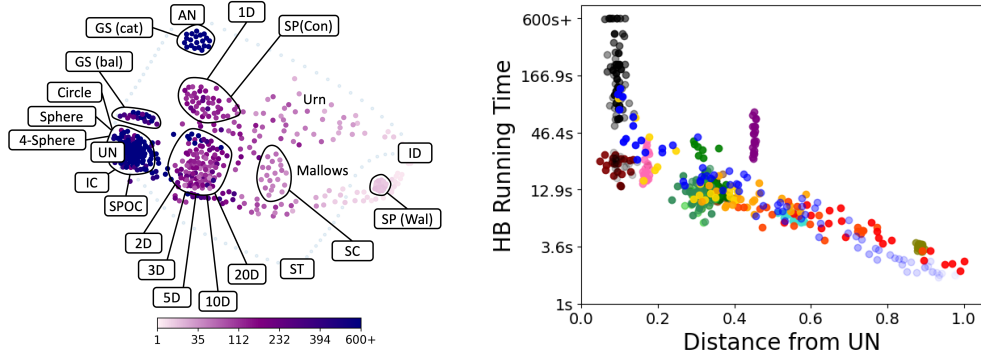
The HB score of committee S is the sum of the HB scores that each voter assigns to it. HB outputs all the size- k committees with the lowest HB score (the HB score we define here is sometimes called a *dissatisfaction* score, and some authors consider a *satisfaction* version instead, where we replace candidates' positions in the above computations with Borda scores and choose the committee with the highest score; both definitions are equivalent). HB is a variant of the Proportional Approval Voting rule (PAV) adapted to the setting of ordinal voting [82, 85, 122].

Example 5.1. Consider an election $E = (C, V)$ with committee size $k = 2$, where $C = \{a, b, c, d\}$, $V = (v_1, v_2, v_3, v_4)$, and the votes are:

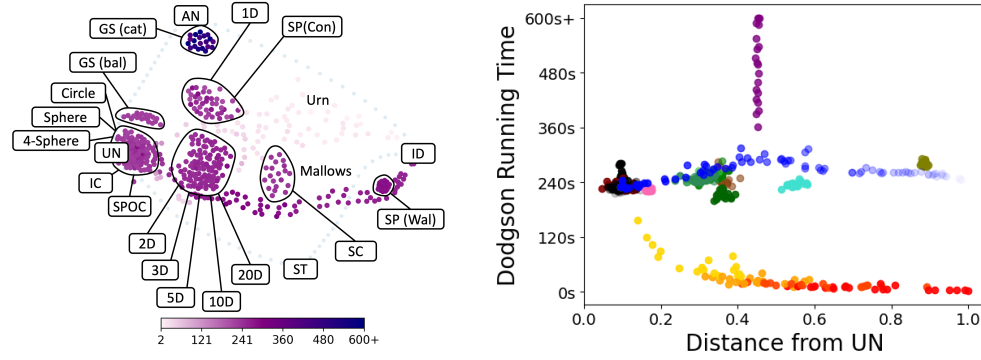
$$\begin{aligned} v_1: a \succ b \succ c \succ d \\ v_2: a \succ b \succ c \succ d, \\ v_3: a \succ b \succ c \succ d, \\ v_4: d \succ c \succ b \succ a. \end{aligned}$$

Under HB rule, $\{a, b\}$ is the unique winning committee with the score of 5: Each of the first three voters contributes score $1/2$, and the last one contributes $2 + 3/2$.

Unfortunately, identifying a winning committee under HB is NP-hard [63, 117]. We can try to overcome this issue, for example, by formulating the problem as an integer linear program (ILP) and solving it with an off-the-shelf ILP solver, or by using FPT algorithms [15, 32], or by designing efficient



(a) HB running time (the color scale on the left is quadratic; the y -axis on the right has logarithmic scale).



(b) Dodgson running time (the color scale on the left is linear; the y -axis on the right has linear scale).

Figure 10: ILP running times (in seconds) for Dodgson and HB for the 100×100 dataset. On the left, we show maps where each election is colored according to the time required by the ILP solver. On the right, each point is an election (colored according to its statistical culture; the color scheme is as in Figure 5) and its x/y coordinates indicate its normalized positionwise distance from ID and the time taken by the ILP solver.

approximation algorithms (see, e.g., the works of Skowron et al. [117], Faliszewski et al. [64] and Munagala et al. [100]). For the case of HB, it is also possible to use algorithms (both approximation or exact ones) designed for the PAV rule [34, 52, 61], which can be adapted to the case of HB using a trick described by Brederick et al. [32]. For a general overview of multiwinner rules we point to the work of Faliszewski et al. [62].

5.2.2 ILP Running Time Maps

We now analyze the time needed to compute the outcomes of the Dodgson and HB rules using ILP formulations and the CPLEX solver. We report the achieved running times in Figure 10. On the left we show maps, where the colors give the running times (the darker the color, the longer was the computation time). On the right, we plot the relation between the running times needed by particular elections (on the y axis) and their normalized positionwise distance from UN (on the x axis). The points in these plots are elections, colored according to the statistical culture from which they were generated, using the same color scheme as in Figure 5. Note that for HB in these plots the y -axis has logarithmic scale, but for Dodgson it is linear. We use the “presentation limit” of 600 seconds. All instances that required more time than the limit have the same color in our maps. Moreover, the coloring scale for the HB map

Culture	HB		Dodgson	
	avg. time	std. dev.	avg. time	std. dev.
Impartial Culture	155.7s	85.5	251.4s	17.2
Conitzer SP	12.2s	2.2	252.7s	14.9
Walsh SP	3.6s	0.2	281.1s	5.1
SPOC	22.3s	4.1	230.0s	8.0
Single-Crossing	7.1s	0.6	235.6s	4.4
1D	11.8s	1.4	213.2s	7.8
2D	20.6s	9.1	249.9s	7.3
3D	11.4s	1.8	254.1s	10.6
5-Cube	10.8s	2.0	251.0s	6.7
10-Cube	12.0s	3.4	249.3s	5.2
20-Cube	12.1s	3.0	249.7s	6.0
Circle	22.9s	3.7	222.3s	2.9
Sphere	126.8s	64.9	230.5s	5.0
4-Sphere	1614.1s	3912.1	232.3s	6.0
Balanced GS	22.2s	6.9	223.0s	2.1
Caterpillar GS	44.7s	14.3	513.0s	106.1
Urn	11.1s	13.1	30.0s	35.1
Mallows	17.3s	24.1	264.2s	19.7

Table 5: Analysis of ILPs running time for HB and Dodgson rules.

is quadratic, whereas for Dodgson it is linear.¹⁸ In Table 5 we present average running times and their standard deviations for each statistical culture and each rule that we considered.

We first consider the HB rule. The most challenging instance took five hours to solve (and, hence, exceeded the “presentation limit” and is reported as “600+” on the figure). The simplest instance required less than two seconds. Ten worst cases were witnessed by 4-Sphere elections, which suggests that it is particularly hard to find optimal winning committees under the HB rule for elections from this model. Perhaps the most visible phenomenon on the map is that the ILP solver tends to take most time on elections similar to those generated by the impartial culture, and the farther elections are away from UN, the less time is needed. Consequently, we see that in this experiment the position on the map is highly meaningful.

For the Dodgson rule the situation is quite different. Most instances need the same amount of time (i.e., around four minutes on average). Two exceptions are urn elections (which needed only half a minute per election on average) and caterpillar group-separable elections (which needed eight and a half minutes per election on average).

As we can see on the plots on the right side of Figure 10, for HB all of the hardest instances were very close to UN, while for the Dodgson rule this is not the case. Indeed, the Dodgson required most time on caterpillar group-separable elections. This is very interesting as these are highly structured elections and one would expect that finding winners for them would be easy. This is a clear indication that there is value in considering models producing elections with special structure that at first may seem quite arbitrary (indeed, it is unlikely that caterpillar group-separable preferences would ever arise in practice) and looking at maps containing elections that are as diverse as possible. On the downside, we have no guarantee that Dodgson (or any other of our rules) would not take even more time on yet different kinds of elections, not present in our dataset. Altogether, the Dodgson ILP running-time experiment illustrates a situation where elections’ positions on the map do not necessarily correspond to the analyzed feature,

¹⁸We would prefer to have the same scale for both pictures, but then it would have been hard to see anything interesting either on one or the other.

but the fact that maps encourage the use of diverse datasets helps in spotting interesting phenomena.

5.3 Maps of Approximation Ratios: Chamberlin–Courant

In our final example of an experiment in this section, we compare two approximation algorithms for the Chamberlin–Courant multiwinner rule. Here we will not see any particularly strong connection between experiment results and the positions of the elections on the map, but still the maps will be helpful in getting intuitions and observing the results.

5.3.1 Chamberlin–Courant

Chamberlin–Courant (CC) is a multiwinner voting rule that proceeds similarly to HB, but with a different notion of a score. Specifically, given an election $E = (C, V)$ and a committee S of size k , the CC score of S is defined as:

$$\sum_{v \in V} \min_{c \in S} (\text{pos}_v(c) - 1). \quad (1)$$

The intuition here is that each voter picks the member of the committee that he or she ranks highest (i.e., who has the lowest position) and views this candidate as his or her “representative.” The voter adds this candidate’s position (minus one) to the committee score. The rule selects the committee with the lowest score, i.e., each voter prefers to be represented by the candidate that he or she ranks as highly as possible. As in the case of HB, this is the dissatisfaction variant of the score and there is also a satisfaction variant, which leads to the same rule.

Example 5.2. *Consider the same election as in Example 5.1. According to the CC rule, $\{a, d\}$ is the winning committee with a score of 0 (which is the smallest possible in any election).*

Computing a CC winning committee is NP-hard [15, 89, 110], but as for HB, there are ILP formulations, FPT algorithms [15, 32], and efficient approximation algorithms (see, e.g., the works of Skowron et al. [117], Faliszewski et al. [64] and Munagala et al. [100]). In particular, we are interested in the following two algorithms:

Sequential CC. Sequential CC starts with an empty committee and works in k iterations, where in each of them it adds to the committee a single candidate, so that the resulting committee has as low total (dissatisfaction) score as possible. Munagala et al. [100] presents a detailed analysis of this algorithm, and Nemhauser et al. [101] give a general discussion of such algorithms (in particular, if we are interested in voter satisfaction rather than dissatisfaction, then the former paper shows that Sequential CC is a polynomial-time approximation scheme, PTAS, and the latter shows a general approximation ratio of $1 - 1/e$ of such greedy algorithms for a whole class of related problems). The first explicit mention of this algorithm in the context of CC was in the work of Lu and Boutilier [89].

Removal CC. Removal CC proceeds similarly to Sequential CC, but it starts with a committee containing all the candidates and works in $m - k$ iterations, in each of them removing a single candidate, so that the resulting committee has as low total dissatisfaction as possible. This algorithm belongs to the folklore.

Sequential CC and Removal CC, as well as their variants for other multiwinner rules, are well-known in the literature and are often used to compute winning committees [64, 89, 117, 118].

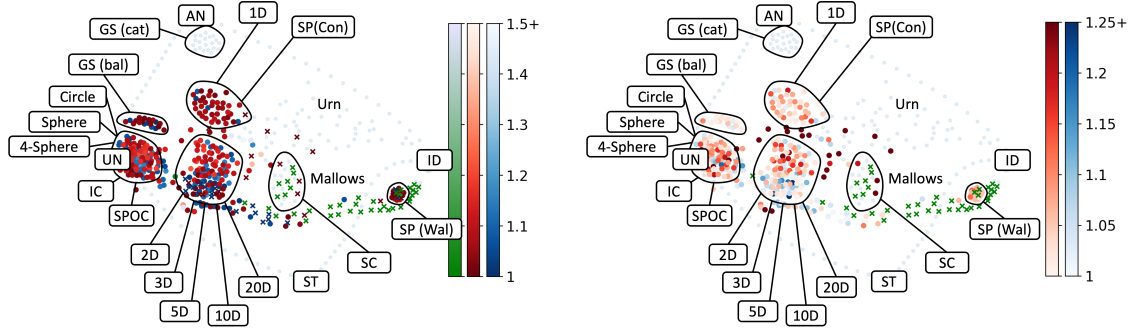
Model	average approximation ratio	
	Sequential CC	Removal CC
Impartial Culture	1.142	1.17
Single-Peaked (Conitzer)	1.108	1.061
Single-Peaked (Walsh)	1.084	1.028
SPOC	1.115	1.060
Single-Crossing	1.120	1.000
1D	1.121	1.056
2D	1.188	1.131
3D	1.228	1.126
5-Cube	1.150	1.135
10-Cube	1.048	1.101
20-Cube	1.052	1.084
Circle	1.108	1.081
Sphere	1.265	1.148
4-Sphere	1.263	1.174
Group-Separable (Balanced)	1.045	1.030
Group-Separable (Caterpillar)	–	–
Urn	2.375	1.192
Mallows	1.037	1.053

Table 6: Average approximation ratios achieved by two algorithms for the CC rule on the elections from the 100×100 dataset.

5.3.2 Approximation Quality Comparison Maps

We evaluate our two approximation algorithms by computing the approximation ratios that they achieve on each of the elections from the 100×100 dataset. The approximation ratio (that a given algorithm achieves on a given election for a given committee size) is the ratio between the (dissatisfaction) score of the committee provided by the algorithm and the lowest possible one. The smaller (and closer to 1) an approximation ratio is, the better. One complication is that for some elections the lowest possible dissatisfaction score is zero. We omit such elections in this experiment as they are easy to identify and it is unreasonable to use an approximation algorithm in their case. Indeed, to form optimal committees for such elections it suffices to take each voter’s top-ranked candidate and, possibly, arbitrary other candidates to fill-in the committee size.

We present the approximation ratios achieved by our algorithms in an aggregate form in Table 6. Generally, both algorithms perform very well, except for urn elections where Sequential CC is notably worse than Removal CC. Turning to a comparison between them, the results in Table 6 either suggest that both Sequential CC and Removal CC are, more or less, equally good, or point marginally in the direction of Removal CC (e.g., if one were to naively count the number of entries in the table where its approximation ratio is smaller than that of Sequential CC). It turns out that the truth is a bit more complicated. Indeed, while on many elections both algorithms perform comparably well, on a number of others their outcomes differ substantially. We illustrate this effect in Figure 11a, where the blue points refer to elections where Sequential CC is better at approximating CC, the red points mark the elections where Removal CC is better, and the green points depict elections where there is a draw (crosses indicate elections where the algorithms found optimal solutions). Removal CC often achieves



(a) Approximation ratios of the better among the Sequential CC (blue) and Removal CC (red) algorithms. Green points indicate elections where both algorithms achieved the same approximation ratios. Crosses indicate elections for which the respective algorithm found an optimal solution.

(b) Indication how much better was the algorithm that achieved lower (better) approximation ratio than the other. For each election, the intensity of the color corresponds to the value $\max(A, B) / \min(A, B)$, where A is the approximation ratio achieved by Sequential CC and B is the approximation ratio achieved by Removal CC. Colors specify which algorithm performed better (blue means Sequential CC, red means Removal CC, and green means that both algorithms achieved the same result).

Figure 11: Analysis of the approximation algorithms for CC.

better approximation ratios, even though theoretical arguments suggest that Sequential CC is a better algorithm (i.e., there are stronger guarantees for its approximation ratio in the satisfaction-based model). Further, we see that in the UN area, both algorithms are sometimes superior, and as far as hypercube elections are concerned, the higher dimension, the more successful Sequential CC becomes; indeed, this is also visible in Table 6. Finally, it is quite striking how often both algorithms give the same result. This is not as surprising close to ID, where all the votes are similar, but the phenomenon appears also at some nontrivial distance from ID.

Next, in Figure 11b, we present a different way for comparing the two algorithms. For each election we compute the value $\max(A, B) / \min(A, B)$, where A is the approximation ratio achieved by Sequential CC and B is the approximation ratio achieved by Removal CC, and color the elections according to this value (and the algorithm that performed better). This value indicates how much better the performance of the better approximation algorithm was. We see that while for many elections both algorithms achieve similar approximation ratios, there also are cases where either of the algorithms performs notably better than the other one (this is particularly visible for some urn elections and for Euclidean elections with higher dimensions).

Overall, we believe that the maps from Figure 11 add interesting insights that are not possible to observe in Table 6 (but, of course, one could spot them by looking at raw results or by a more careful statistical analysis). For example, we see that even though Removal CC is slightly better on elections from many statistical culture, Sequential CC still obtains better results in a nonnegligible number of cases.

5.4 Conclusions From Using the Map in Experiments

Let us take a moment to reflect on how the map approach was helpful in our experiments. While, in principle, each of the experiments could have been performed without the map, and could have led to

the same high-level conclusions, we believe that using the map it was far easier to reach them. Further, the sheer fact of being able to look at the results for all elections, in a non-aggregate way, motivated particular questions and further lines of inquiry. For example, if we were analyzing the running time of the ILP formulation for Dodgson in Section 5.2.2 without the map, it would be quite likely that we would have simply not thought of looking at caterpillar group-separable elections. This way, we would have lost the observation that they are much more challenging for the ILP solver than other, more typical models. The map aims to bring a varied set of elections together and, so, helps in finding special cases where algorithms behave in unusual ways. In particular, caterpillar group-separable elections are in the part of the map where no other elections reside, so if we looked at the map without them, we would be prompted to look for a way of generating data in this area. In Section 5.3.2 looking at the map helped in understanding and justifying that Sequential CC and Removal CC complement each other. Finally, the score maps from Section 5.1.2 gave quite some insight regarding the nature of the elections. For example, it is striking how many elections have very high Copeland winner scores and how many elections with Condorcet winners there are in our dataset, even quite far away from ID.

Overall, we found that if two elections were close on the map, then in all of our experiments—with the possible exception of the last one, in Section 5.3.2—they also had similar properties. Sometimes this was because positions on the maps had strong connection to the analyzed features, and sometimes this seemed more connected to the fact that the two elections were from the same statistical culture. We should also stress that this might be connected to us considering fairly high-level properties that are robust to small changes in the elections (for example, swapping two candidates can only affect their Borda scores in a fairly insignificant way, and may not change the Borda score of the election’s winner). If we considered more fragile properties, the outcome might be different. Nonetheless, even in such cases the maps could help in identifying general trends.

6 Map of Real-Life Elections

Our final goal is to demonstrate the usefulness of the map for analyzing real-life elections. To this end, we consider several datasets coming from Preflib [93] and collected by Boehmer and Schaar [17]. There are two main problems with real-life election data. One is that these elections typically involve only a few candidates. The second one is that in many cases numerous votes are incomplete. Thus we will first describe our general strategy of preprocessing the available data (e.g., how we extend incomplete preference orders) and, then, we will describe our datasets together with the exact preprocessing that we applied to each of them. Indeed, some datasets needed some special treatment. Next, we (i) present where these real-life elections land on our maps of elections, (ii) color these maps according to the Borda and Copeland scores and, finally, (iii) we find (norm- ϕ) parameters of the Mallows model that best approximate our real-life elections. Whenever we speak of real-life elections in this section, we mean elections from our datasets. Other “real-life” elections, from other sources, may behave differently (even if we hope that our datasets are at least somewhat representative, we cannot provide any guarantees).

6.1 Forming the Datasets

In Table 7, we present a detailed description of the real-life datasets that we decided to use. All of them are available in Preflib [93] (the TDF, GDI, and Speed Skating data was collected by Boehmer and Schaar [17]). We chose eleven real-life datasets of different types, and we divided them into three categories. The first group contains *political* elections: city council elections in Glasgow and Aspen [106], elections from Dublin North and Meath constituencies (Irish), and elections held by non-profit organizations, trade unions, and professional organizations (ERS). The second group consists of *sport* elections: Tour de France (TDF) [17], Giro d’Italia (GDI) [17], speed skating [19], and figure skating. The last group consists of *surveys*: preferences over Sushi [79], T-Shirt designs, and costs of living and population in

Category	Name	# Selected Elections	Avg. m	Avg. n	Description
Political	Irish	2	13	~ 54011	Elections from Dublin North and Meath
Political	Glasgow	13	~ 11	~ 8758	City council elections
Political	Aspen	1	11	2459	City council elections
Political	ERS	13	~ 12	~ 988	Various elections held by non-profit organizations, trade unions, and professional organizations
Sport	Figure Skating	40	~ 23	9	Figure skating
Sport	Speed Skating	13	~ 14	196	Speed skating
Sport	TDF	12	~ 55	~ 22	Tour de France
Sport	GDI	23	~ 152	20	Giro d'Italia
Survey	T-Shirt	1	11	30	Preferences over T-Shirt logo
Survey	Sushi	1	10	5000	Preferences over Sushi
Survey	Cities	2	42	392	Preferences over cities

Table 7: Each row contains a description of one of the real-life datasets we consider. In the column *# Selected Elections*, we denote the number of elections from the respective dataset that we consider.

different cities [37]. For TDF and GDI, each race is a vote, and each season is an election. For speed skating, each lap is a vote, and each competition is an election. For figure skating, each judge’s opinion is a vote, and each competition is an election.

We are interested in elections that have at least 10 candidates.¹⁹ As our map framework requires complete votes without ties, we are interested in instances where votes are as complete as possible and contain only a few ties. In some datasets, only parts of the data meets our criteria (i.e., complete votes without ties over at least 10 candidates). For example, in the dataset containing Irish elections, we have three different elections, but one of them (an election from the Dublin West constituency) contains only nine candidates. We remove all elections not meeting our criteria from consideration.

We further reduce the number of elections by considering only selected ones. We based our decisions on the number of voters and candidates. That is, for ERS, we only take elections with at least 500 voters, for Speed Skating with at least 80 voters, for TDF with at least 20 voters, and for Figure Skating with at least 9 (these numbers are in accordance with the sizes of the elections in the particular datasets). In addition to that, for TDF, we only selected elections with no more than 75 candidates. Naturally, these choices are somewhat arbitrary, but some such decisions are necessary to get a manageable collection of data. In Table 7, we include in the column *# Selected Elections* the number of elections we selected from each dataset.

6.1.1 Preprocessing of Datasets

There are two types of problems that we encounter in the selected datasets. First, some datasets include ties (i.e., pairs or larger sets of candidates that are reported as equally good by particular voters). We break any ties that appear by ordering the involved candidates uniformly at random. Second, many of the votes are incomplete in the sense that the reported preference orders do not rank all the candidates but only some top ones (note that while an incomplete vote can be seen as if the unranked candidates were tied on the bottom of the vote, we address the incompleteness differently than having a tie in a vote). Sometimes votes are both incomplete and include ties.

For all the elections from our selected datasets that contain incomplete votes, we need to fill-in all the missing data. For the decision how to complete each vote, we use the other votes as references, assuming that voters that rank the same candidates on top also continue to rank candidates similarly

¹⁹The more candidates, the more interesting is the data and the resulting maps. On the other hand, if we had required too many candidates, we would end up having very few election instances. In this sense, 10 candidates is a tradeoff between the number of candidates and the number of instances that include as many candidates.

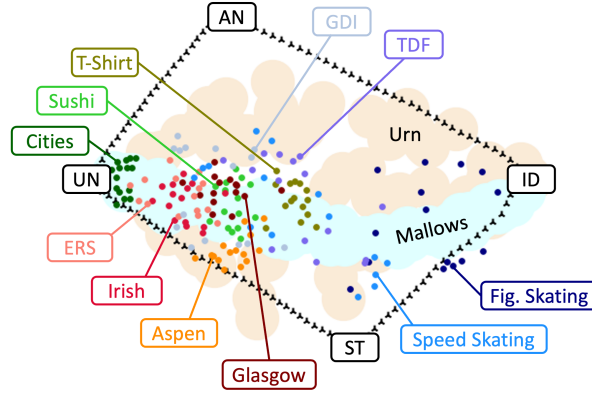


Figure 12: Map of real-life elections.

toward the bottom. For each incomplete vote v , we proceed as follows. Let us assume that vote v is over m candidates. Let V_P be the set of all original votes of which v is a prefix. We uniformly at random select one vote v_p from V_P and then at the end of vote v we add the candidate which appears in position $m + 1$ in vote v_p . We repeat the procedure until vote v is complete. If the set V_P is empty, then we choose c uniformly at random (from those candidates that are not part of v yet).

Our approach to filling-in missing information is reminiscent of what Doucette [51] calls *imputation plurality*. We point to his work for detailed analysis of various approaches to filling-in incomplete votes.

After applying these preprocessing steps, we arrive at a collection of datasets containing elections with ten or more candidates and complete votes without ties. As we focus on ten candidates, we need to select a subset of ten candidates for each election. In a given election, we compute each candidate’s average position in the votes and select ten candidates who, on average, are ranked highest (this is equivalent to choosing ten candidates with the highest Borda scores). The rationale is that these are the most relevant candidates in the elections. In case there is a tie, we break it randomly. We refer to the datasets resulting from this preprocessing as *intermediate* datasets. Each intermediate dataset internally contains one or more elections (e.g., the Sushi dataset contains only one election, whereas TDF contains twelve).

6.1.2 Sampling Elections from the Intermediate Datasets

We treat each of our intermediate datasets as a separate election model from which we sample 15 elections to create the final dataset that we use. For each intermediate dataset, we sample elections as follows. First, we randomly select one of the elections present internally in it. Notably, we may select the same election multiple times. Second, we sample 100 votes from this election uniformly at random with replacement (this implies that for elections with less than 100 votes, we select some votes multiple times, and for elections with more than 100 votes, we do not select some votes at all). We do so to make full use of elections with far more than 100 votes. For instance, our Sushi intermediate dataset contains only one election consisting of 5000 votes. Sampling an election from the Sushi intermediate dataset thus corresponds to drawing 100 votes uniformly at random from the set of 5000 votes. On the other hand, for intermediate datasets containing a higher number of elections, e.g., the Tour de France intermediate dataset, most of the sampled elections come from different original elections.

After executing this procedure, we arrive at eleven sets, each containing 15 elections consisting of 100 complete and strict votes over 10 candidates, which we use for our experiments.

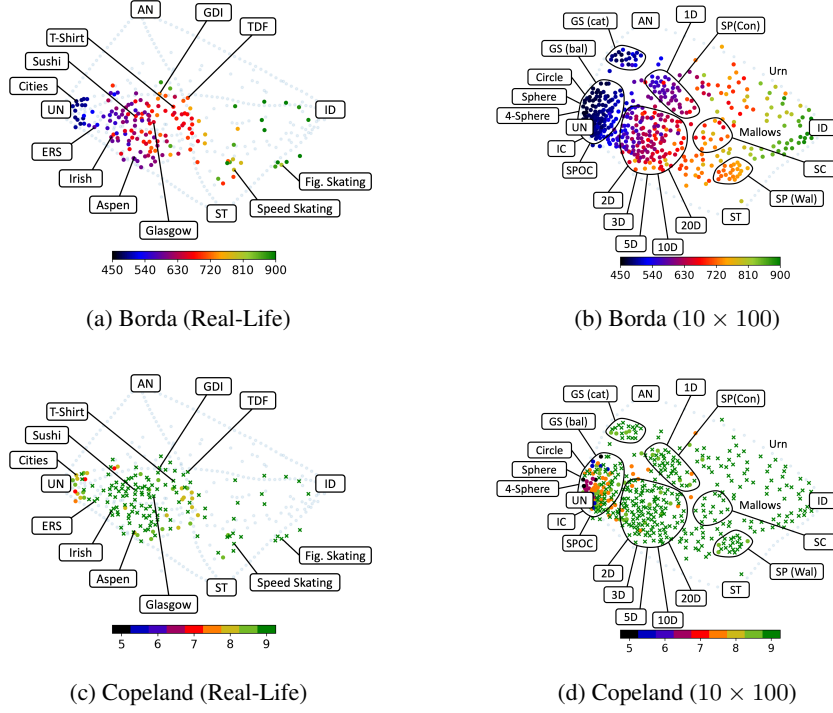


Figure 13: Maps of the real-life elections (on the left) and the 10×100 dataset (on the right), colored according to the scores of the winning candidate under Borda and Copeland. On the real-life elections map, urn and Mallows elections are depicted as pale blue points, in the same way as the paths between the compass matrices.

6.2 Real-Life Elections on the Map

In Figure 12, we show a map of our real-life elections along with the compass, Mallows, and urn elections. For readability, we present the Mallows and urn elections as large, pale-colored areas. Not all real-life elections form clear clusters, hence the labels refer to the largest compact groupings.

While the map is not a perfect representation of distances among elections (see Section 4.3), analyzing it nevertheless leads to many conclusions. Most strikingly, real-life elections occupy a very limited area of the map. This is especially true for political elections and surveys, which appear in the bottom-left quarter of the map. Except for several sport elections, all elections are closer to UN than to ID, and none of the real-life elections falls in the top-right part of the map. Another observation is that Mallows elections go right through the real-life elections, while urn elections are on average further away. This means that for most real-life elections there exists a parameter ϕ such that elections generated according to the Mallows model with that parameter are relatively close (see Section 6.4 for specific recommendations).

Most of the political elections lie close to each other and are located next to the Mallows elections (and high-dimensional hypercube ones, had we shown them on the map). At the same time, sport elections are spread over a larger part of the map and, with the exception of GDI, are shifted toward ID. Regarding the surveys, the Cities survey is very similar to a sample from IC.²⁰ The Sushi survey is surprisingly similar to political elections. The T-Shirt surveys are located in the middle of the Mallows cloud, closer to ST than to AN. We mention that Boehmer and Schaar [17] show maps of many further survey and sport-based elections. They find that the former are occasionally closer to AN, whereas the latter often appear in the vicinity of ID (they also consider “ground-truth” elections, where the votes can

²⁰In the survey people were casting votes in the form of truncated ballots, ranking only their six favorite options. Hence, our completion method filled-in the rest of the votes uniformly at random. This is partly the reason why it is so similar to IC. Nevertheless, we have not observed any particular structure within these votes, hence its similarity to IC is not only accidental.

Type of elections	Value of $\text{norm-}\phi$	Avg. Norm. Distance	Norm. Std. Dev.	Num. of Elections
Political elections	0.750	0.15	0.036	60
Sport elections	0.534	0.27	0.080	60
Survey elections	0.730	0.20	0.034	45
All real-life elections	0.700	0.22	0.106	165

Table 8: Values of $\text{norm-}\phi$ such that elections generated with the Mallows model for $m = 10$ are, on average, as close as possible to elections from the respective dataset. We include the average positionwise distance of the elections generated with the Mallows model for this parameter $\text{norm-}\phi$ from the elections from the dataset as well as the standard deviation, both normalized by the positionwise distance between the uniformity and identity. The last column gives the number of elections in the respective real-life dataset.

be viewed as noisy estimates of the objectively correct rankings, and these elections are even closer to ID).

6.3 Winner Scores Under Borda and Copeland

In Section 5.1 we have shown maps of the 100×100 dataset where each election was colored according to the score of the winner under Borda and Copeland. In Figure 13 we show analogous maps for the real-life elections and, for comparison, for the 10×100 dataset of synthetic elections. We make two observations. First, generally the colorings of the maps for the 10×100 dataset are very similar to the ones for the 100×100 dataset. Second, the colorings of the real-life maps are consistent with the colorings of the respective 10×100 maps, in the sense that similar colors appear in similar areas of the maps.

All in all, this is yet another argument that the maps provide some useful information regarding the elections they include and their absolute positions on the map carry some inter-map meaning.

6.4 Capturing Real-Life Elections

As we have observed that real-life data is scarce and naturally hard to control, we now make some recommendations on how the Mallows model can be used to generate semi-realistic data. For this, we now analyze how to choose the $\text{norm-}\phi$ parameter so that elections generated using the Mallows model with our normalization resemble the real-life ones. In this section we include only a fairly simple experiment. In a follow-up work, we have explored the possibility of learning Mallows parameters using the map framework more deeply [20].

We consider four different datasets, each consisting of elections with 10 candidates and 100 voters (created as described in Section 6.2): the set of all political elections, the set of all sport elections, the set of all survey elections, and the combined set, i.e., the union of the three preceding ones. For each of these four datasets, to find the value of $\text{norm-}\phi$ that produces elections that are as similar as possible to the respective real-life elections, we conducted the following experiment. For each $\text{norm-}\phi \in \{0, 0.001, 0.002, \dots, 0.999, 1\}$, we generated 100 elections with 10 candidates and 100 voters from the Mallows model with the given $\text{norm-}\phi$ parameter. Subsequently, we computed the average distance between these elections and the elections from the respective dataset. Finally, we selected the value of $\text{norm-}\phi$ that minimized this distance. We present the results of this experiment in Table 8.

Recall that in the previous section we have observed that a majority of real-life elections are close to some elections generated from the Mallows model with a certain dispersion parameter. However, we have also seen that the real-life datasets consist of elections that differ to a certain extent from one another (in particular, this is very visible for the sports elections). Thus, it is to be expected that elections drawn from the Mallows model for a fixed dispersion parameter are at some nonzero (average) distance from

the real-life ones. Indeed, this is the case here. However, the more homogeneous political elections and survey elections can be captured quite well using the Mallows model with parameter $\text{norm-}\phi = 0.750$ and $\text{norm-}\phi = 0.730$, respectively. Generally speaking, if one wants to generate elections that should be particularly close to elections from the real world, then choosing a $\text{norm-}\phi$ value between 0.7 and 0.8 seems like a good strategy. If, however, one wants to capture the full spectrum of real-life elections, then we recommend using the Mallows model with different values of $\text{norm-}\phi$ from the interval $[0.5, 0.8]$.

7 Conclusions and Future Work

Our main conclusion is that the map of elections framework is both credible and useful. In particular, regarding the credibility of the map, in Section 4 we have shown that the Euclidean distances between points representing elections on the map are similar to the positionwise distances between these elections, and that relations between the distances are often preserved. This is reinforced by the fact that elections located close to each other on the map often have similar high-level properties, such as, e.g., the scores of the winning candidates and committees (see Section 5). Regarding the usefulness of the map, in Section 5 and in Section 6 we have shown a number of experiments where our framework proved to be helpful.

Generally speaking, the strategy of using the map of elections in one’s own experiments is as follows: Take a particular dataset of elections (e.g., our 100×100 dataset), compute the feature of interest for each of the elections, and then draw the map, coloring each election according to its computed feature. This way it is possible to get a bird’s eye view at the space of elections and see how the considered feature depends on the election’s position on the map. Importantly, this way we see results for all the elections at the same time, without the need to, e.g., compute average values or other similar statistics, which often lose important information. These results can then guide more focused experiments. For example, one may realize which statistical cultures lead to the most extreme values of the feature, or which statistical cultures lead to elections with the most diverse values.

7.1 Advantages and Shortcomings of the Maps

The most important conclusions of our paper relate to the advantages and disadvantages of using the maps. Below we list a number of observations that we either made throughout the paper or that become apparent when looking at our work as a whole. We start with the advantages of using the map framework:

1. Maps allow us to see relations between particular elections or groups of elections and, maybe even more importantly, with respect to compass elections. This helps to understand the nature of the elections that we have in our datasets. For example, we were able to see that elections generated from particular statistical cultures tend to be quite similar to each other. The two exceptions here are the urn and Mallows elections that cover large areas, where their placement is largely controlled by their parameters.
2. The maps allow us to form general intuitions about the features of our elections, by looking at the colorings according to these features. Looking at a map, we get a comprehensible bird’s eye view of individual results for all the elections in the dataset. We saw this in essentially all the experiments in Section 5 (we also describe more specific conclusions from these experiments in Section 7.2 below).
3. The maps facilitate and motivate experiments conducted on elections from multiple, diverse data sources (such as different statistical cultures or different datasets from Preflib). While, in principle, this is not a feature of the maps—one could simply choose to use diverse datasets without

knowing about maps at all—maps help one realize that given datasets are not diverse. For example, if one only considered one or two statistical cultures/data sources, a map of such data would make it apparent that there are areas in the election space that are not covered. Moreover, by observing which parts of the map remain unoccupied, one can get a good sense of what type of elections one’s dataset is missing. On a practical level, we also offer ready-made diverse datasets. We believe this is quite important, especially since Boehmer et al. [26] observed that papers in computational social choice often use very limited data.

The maps also have a number of shortcomings. We do not necessarily perceive these shortcomings as reasons for not using the maps, but we stress that one should take them into account. Below we list a few of the issues:

1. The maps, at least when using the positionwise distance introduced and considered in this paper, are limited to datasets where all elections have the same number of candidates. Similarly, the current map framework for ordinal elections does not handle the case where some preference orders are partial.
2. The maps, by necessity, are approximate. On the one hand, in this paper, we use the positionwise distance to measure the distance between two elections which, due to focusing on frequency matrices, disregards some information about the input elections. On the other hand, embedding algorithms introduce additional errors in the visualizations. While we put effort into evaluating the credibility of our maps, some errors are always present and one has to double-check the intuitions one gets from the maps.
3. As the positionwise distance focuses on elections’ frequency matrices, it is incapable of differentiating elections whose frequency matrices are very similar. While in most cases this does not lead to significant issues, it should for instance be taken into account when analyzing elections close to the UN matrix—i.e., elections where each candidate appears at each position in a vote with close to equal probability. For example, this is the case for elections generated using IC and SPOC statistical cultures. These elections are of very different nature—with the former one being quite chaotic and the latter one having a rather rigid structure—but generate nearly identical frequency matrices and, consequently, take similar positions on the maps based on the positionwise distance.
4. Due to the embedding algorithms used, the exact arrangement of elections in a map may be affected by the composition of the dataset used. If we add a large number of elections of a particular type, the area where these elections land on the map may be overinflated, with these elections taking a larger part of the picture. Hence, we repeat our warning about verifying the intuitions that one gets from the maps. That said, in our maps we do have many more elections close to UN than close to ID, but it does not seem to affect the visualizations strongly under the KK embedding (but for other embeddings—such as the Fruchterman-Reingold—this effect is stronger, see Appendix B).
5. The maps of elections with just a few candidates—such as four or five—do not seem to be particularly informative (see Section 4.3.3). Indeed, as shown by Faliszewski et al. [69], elections with such few candidates simply tend to be quite similar to each other irrespective of which data source they come from. As a result, maps that rely on analyzing election similarity cannot distinguish them well.
6. The results of various experiments may show, e.g., that elections that are close on the map have very different features. In some sense, this is not a disadvantage of the maps per se, but rather it is an indication that a given feature depends on much more subtle properties of elections than those

captured by the considered distance measure. While such cases are interesting in themselves, they may require the use of other tools than maps.²¹

7.2 Specific Conclusions

Our work also leads to a number of more specific conclusions. For example, we have found that elections generated according to particular statistical cultures are fairly similar to each other. This is a strong argument that when performing numerical experiments using synthetic data, one should use a set of statistical cultures that is as diverse as possible. This was further confirmed, e.g., by our experiments regarding the running time of ILP-based winner determination procedures for NP-hard voting rules. We observed that while for the HB rule the time needed to find a winning committee in a given election is correlated with its distance from ID (or, on a higher level of abstraction, it is correlated with the diversity of the votes in the election), for Dodgson this relation is less clear. In particular, we have observed that computing the Dodgson winner for caterpillar group-separable elections usually takes much more time than for elections from other statistical cultures. This illustrates that even if some statistical culture does not seem particularly likely to generate realistic elections, it is still useful to include it in experiments to get a sense for all possible behaviors that might occur.

Further, in our experiments regarding approximation algorithms, we have compared the Sequential CC and Removal CC algorithms for the CC rule. In the satisfaction-based model, the former algorithm has much stronger approximation guarantees than the latter, yet our experiments show that Removal CC performs very well on some data, more often than not achieving better results than Sequential CC.²² This illustrates the value of experimental evaluation, which can give quite different insights than theoretical studies. More importantly from our point of view, we have shown that the map of elections is very useful in analyzing for which elections a particular algorithm performs better.

Finally, in Section 6 we have shown that the map of elections framework can also be used for learning parameters of statistical cultures that lead to elections most similar to real-life ones. The idea is that we seek such a parameter of a given culture under which the average distance between the generated elections and the input real-life ones is as small as possible. In particular, we have shown which normalized dispersion parameters for the Mallows model are best for generating political, sport, and survey elections. This idea is further developed in the work of Boehmer et al. [20].

7.3 Follow-Up and Future Work

The work presented in this paper has already lead to a number of follow-up works, which we have discussed in Section 1.4. One of the most pressing directions for future research is to extend the map framework with the ability to deal with elections of different sizes and with partial preference data. In other words, instead of filling in incomplete votes, as we did in Section 6, it would be far better to have distances that could work with partial preference orders “natively.” Consequently, it would be possible to prepare a map of all elections from Preflib [93] and see how they relate to each other. It would be very interesting to see if, for example, there are particularly many elections in certain areas of the map, if nearby elections have similar features, and if conclusions we found regarding real-life elections would still hold.

²¹As a mild form of this phenomenon, it may be the case that the value of a particular election feature is more closely tied to, e.g., the statistical culture from which the election was generated than to its position on the map. As statistical cultures are typically clustered on the maps, in such a case the maps are still useful, but the particular conclusions that one may draw may not be as strong as otherwise.

²²Interestingly, there are two other approximation algorithms for CC, namely Ranging CC and Banzhaf CC, that also have equally strong approximation guarantees as Sequential CC. Our initial results, not shown in the paper, indicate that in practice they perform notably worse than the other two algorithms on our datasets.

It would also be interesting to extend the framework beyond ordinal elections. This has already been done for approval elections [121], stable roommates and stable marriages problems [25], voting rules [68], and to visualize internal structure of elections [67]. However, there are many more types of objects studied in computational social choice (and beyond) for which appropriate maps could help in designing and conducting experiments.

Acknowledgments

We are very grateful to the AAMAS and IJCAI reviewers who provided comments on the papers on which this work is based, and to the AIJ reviewers. Their comments greatly helped in improving this paper. This project has received funding from the European Research Council (ERC) under the European Union’s Horizon 2020 research and innovation programme (grant agreement No 101002854), and from the French government under the management of Agence Nationale de la Recherche as part of the France 2030 program, reference ANR-23-IACL-0008. Niclas Boehmer was supported by the DFG project MaMu (NI 369/19). In part, Stanisław Szufa was supported by the Foundation for Polish Science (FNP).



References

- [1] R. Ahuja, T. Magnanti, and J. Orlin. *Network Flows: Theory, Algorithms, and Applications*. Prentice-Hall, 1993. (see page 17, 19)
- [2] C. Alós-Ferrer and D. Granić. Two field experiments on approval voting in Germany. *Social Choice and Welfare*, 39(1):171–205, 2012. (see page 9)
- [3] A. Anand and P. Dey. Distance restricted manipulation in voting. *Theoretical Computer Science*, 891:149–165, 2021. (see page 8)
- [4] M. Ayadi, N. Ben Amor, J. Lang, and D. Peters. Single transferable vote: Incomplete knowledge and communication issues. In *Proceedings of AAMAS-19*, pages 1288–1296, 2019. (see page 2)
- [5] N. Barrot, J. Lang, and M. Yokoo. Manipulation of hamming-based approval voting for multiple referenda and committee elections. In *Proceedings of AAMAS-17*, pages 597–605, 2017. (see page 1)
- [6] J. Bartholdi, III, C. Tovey, and M. Trick. Voting schemes for which it can be difficult to tell who won the election. *Social Choice and Welfare*, 6(2):157–165, 1989. (see page 37)
- [7] J. Barzilai and J. Borwein. Two-Point Step Size Gradient Methods. *IMA Journal of Numerical Analysis*, 8(1):141–148, 1988. (see page 5)
- [8] A. Baujard and H. Igersheim. Framed-field experiment on approval voting and evaluation voting. some teachings to reform the french presidential electoral system. In *In Situ and Laboratory Experiments on Electoral Law Reform*, pages 69–89. 2010. (see page 9)
- [9] A. Baujard, H. Igersheim I. Lebon, F. Gavrel, and J.-F. Laslier. Who’s favored by evaluative voting? an experiment conducted during the 2012 french presidential election. *Electoral Studies*, 34:131–145, 2014. (see page 9)

- [10] D. Baumeister, T. Hogrebe, and L. Rey. Generalized distance bribery. In *Proceedings of AAAI-2019*, pages 1764–1771, 2019. (see page 8)
- [11] G. Benade, S. Nath, A. Procaccia, and N. Shah. Preference elicitation for participatory budgeting. In *Proceedings of AAAI-2017*, pages 376–382, 2017. (see page 1)
- [12] M. Bentert and P. Skowron. Comparing election methods where each voter ranks only few candidates. In *Proceedings of AAAI-2020*, pages 2218–2225, 2020. (see page 2)
- [13] S. Berg. Paradox of voting under an urn model: The effect of homogeneity. *Public Choice*, 47(2):377–387, 1985. (see page 2, 12)
- [14] N. Betzler, J. Guo, and R. Niedermeier. Parameterized computational complexity of Dodgson and Young elections. *Information and Computation*, 208(2):165–177, 2010. (see page 37)
- [15] N. Betzler, A. Slinko, and J. Uhlmann. On the computation of fully proportional representation. *Journal of Art. Int. Research*, 47:475–519, 2013. (see page 37, 40)
- [16] D. Black. *The Theory of Committees and Elections*. Cambridge University Press, 1958. (see page 2, 9, 10)
- [17] N. Boehmer and N. Schaar. Collecting, classifying, analyzing, and using real-world ranking data. In *Proceedings of AAMAS-23*, pages 1706–1715, 2023. (see page 2, 4, 8, 43, 46)
- [18] N. Boehmer, R. Bredereck, P. Faliszewski, and R. Niedermeier. Winner robustness via swap- and shift-bribery: Parameterized counting complexity and experiments. In *Proceedings of IJCAI-2021*, pages 52–58, 2021. (see page 1, 7)
- [19] N. Boehmer, R. Bredereck, P. Faliszewski, R. Niedermeier, and S. Szufa. Putting a compass on the map of elections. In *Proceedings of IJCAI-2021*, pages 59–65, 2021. (see page 1, 6, 7, 26, 43)
- [20] N. Boehmer, R. Bredereck, E. Elkind, P. Faliszewski, and S. Szufa. Expected frequency matrices of elections: Computation, geometry, and preference learning. In *Proceedings of NeurIPS-2022*, 2022. (see page 6, 7, 8, 28, 29, 32, 33, 47, 50)
- [21] N. Boehmer, R. Bredereck, P. Faliszewski, and R. Niedermeier. A quantitative and qualitative analysis of the robustness of (real-world) election winners. In *Proceedings of EAAMO-2022*, pages 7:1–7:10, 2022. (see page 7)
- [22] N. Boehmer, P. Faliszewski, R. Niedermeier, S. Szufa, and T. Was. Understanding distance measures among elections. In *Proceedings of IJCAI-2022*, pages 102–108, 2022. (see page 5, 8, 14, 17, 21, 23, 24, 28)
- [23] N. Boehmer, J.-Y. Cai, P. Faliszewski, A. Fan, Ł. Janeczko, A. Kaczmarczyk, and T. Wąs. Properties of position matrices and their elections. In *Proceedings of AAAI-2023*, pages 5507–5514, 2023. (see page 8, 15)
- [24] N. Boehmer, P. Faliszewski, and S. Kraiczy. Properties of the Mallows model depending on the number of alternatives: A warning for an experimentalist. In *Proceedings of ICML-2023*, 2023. (see page 6, 12, 26)
- [25] N. Boehmer, K. Heeger, and S. Szufa. A map of diverse synthetic stable roommates instances. In *Proceedings of AAMAS-23*, pages 1003–1011, 2023. (see page 8, 51)

- [26] N. Boehmer, P. Faliszewski, L. Janeczko, A. Kaczmarczyk, G. Lisowski, G. Pierczynski, S. Rey, D. Stolicki, S. Szufa, and T. Was. Guide to numerical experiments on elections in computational social choice. In *Proceedings of IJCAI-2024*, pages 7962–7970, 2024. (see page 2, 3, 6, 49)
- [27] N. Boehmer, P. Faliszewski, L. Janeczko, D. Peters, G. Pierczynski, S. Schierreich, P. Skowron, and S. Szufa. Evaluation of project performance in participatory budgeting. In *Proceedings of IJCAI-2024*, pages 2678–2686, 2024. (see page 1)
- [28] S. Bouveret, R. Blanch, A. Baujard, F. Durand, H. Igersheim, J. Lang, A. Laruelle, J.-F. Laslier, I. Lebon, and V. Merlin. Voter autrement 2017 for the french presidential election. working paper or preprint, November 2019. (see page 9)
- [29] F. Brandt, V. Conitzer, U. Endriss, J. Lang, and A. Procaccia, editors. *Handbook of Computational Social Choice*. Cambridge University Press, 2016. (see page 1)
- [30] F. Brandt, C. Geist, and M. Strobel. Analyzing the practical relevance of voting paradoxes via ehrhart theory, computer simulations, and empirical data. In *Proceedings of AAMAS-16*, pages 385–393, 2016. (see page 2, 3)
- [31] R. Bredereck, J. Chen, R. Niedermeier, and T. Walsh. Parliamentary voting procedures: Agenda control, manipulation, and uncertainty. In *Proceedings of IJCAI-2015*, page 164–170, 2015. (see page 1)
- [32] R. Bredereck, P. Faliszewski, A. Kaczmarczyk, D. Knop, and R. Niedermeier. Parameterized algorithms for finding a collective set of items. In *Proceedings of AAAI-2020*, pages 1838–1845, 2020. (see page 37, 38, 40)
- [33] M. Brill, U. Schmidt-Kraepelin, and W. Suksompong. Margin of victory in tournaments: Structural and experimental results. In *Proceedings of AAAI-2021*, pages 5228–5235, 2021. (see page 1)
- [34] J. Byrka, P. Skowron, and K. Sornat. Proportional approval voting, harmonic k -median, and negative association. In *Proceedings of ICALP-2018*, pages 26:1–26:14, 2018. (see page 38)
- [35] I. Caragiannis, C. Kaklamanis, N. Karanikolas, and A. Procaccia. Socially desirable approximations for Dodgson’s voting rule. In *Proceedings of EC-2010*, pages 253–262. ACM Press, June 2010. (see page 37)
- [36] I. Caragiannis, J. Covey, M. Feldman, C. Homan, C. Kaklamanis, N. Karanikolas, A. Procaccia, and J. Rosenschein. On the approximability of Dodgson and Young elections. *Artificial Intelligence*, 187:31–51, 2012. (see page 37)
- [37] I. Caragiannis, X. Chatzigeorgiou, G. Krimpas, and A. Voudouris. Optimizing positional scoring rules for rank aggregation. *Artificial Intelligence*, 267:58–77, 2019. (see page 8, 44)
- [38] L. Celis, L. Huang, and N. Vishnoi. Multiwinner voting with fairness constraints. In *Proceedings of IJCAI-2018*, pages 144–151, 2018. (see page 2)
- [39] B. Chamberlin and P. Courant. Representative deliberations and representative decisions: Proportional representation and the Borda rule. *American Political Science Review*, 77(3):718–733, 1983. (see page 7)
- [40] V. Conitzer. Eliciting single-peaked preferences using comparison queries. *Journal of Artificial Intelligence Research*, 35:161–191, 2009. (see page 12)

- [41] C. Contet, U. Grandi, and J. Mengin. Abductive and contrastive explanations for scoring rules in voting. In *Proceedings of ECAI-2024*, volume 392, pages 3565–3572, 2024. (see page 6)
- [42] T. Csar, M. Lackner, and R. Pichler. Computing the schulze method for large-scale preference data sets. In *Proceedings of IJCAI-2018*, pages 180–187, 2018. (see page 1)
- [43] J. Davies, G. Katsirelos, N. Narodytska, T. Walsh, and L. Xia. Complexity of and algorithms for the manipulation of borda, nanson’s and baldwin’s voting rules. *Artificial Intelligence*, 217: 20–42, 2014. (see page 1)
- [44] J. de Leeuw. Modern multidimensional scaling: Theory and applications. *Journal of Statistical Software*, 14:1–2, 2005. (see page 5, 9, 26, 62)
- [45] T. Delemazure and D. Peters. Generalizing instant runoff voting to allow indifferences. Technical Report arXiv:2404.11407 [cs.GT], arXiv.org, 2024. (see page 7)
- [46] L. Van der Maaten. Fast optimization for t -SNE. In *NeurIPS-2010 Workshop on Challenges in Data Visualization*, volume 100, 2010. (see page 9)
- [47] L. Van der Maaten and G. Hinton. Visualizing data using t -SNE. *Journal of Machine Learning Research*, 9(11), 2008. (see page 9)
- [48] P. Dey. Local distance constrained bribery in voting. *Theoretical Computer Science*, 849:1–21, 2021. (see page 8)
- [49] M. M. Deza and E. Deza. *Encyclopedia of Distances*. Springer, 2009. (see page 8)
- [50] D. Donoho and C. Grimes. Hessian eigenmaps: Locally linear embedding techniques for high-dimensional data. *Proceedings of the National Academy of Sciences*, 100(10):5591–5596, 2003. (see page 9)
- [51] J. Doucette. *Social Choice for Partial Preferences Using Imputation*. PhD thesis, University of Waterloo, 2016. (see page 45)
- [52] S. Dudycz, P. Manurangsi, J. Marcinkowski, and K. Sornat. Tight approximation for proportional approval voting. In *Proceedings of IJCAI-2020*, pages 276–282. ijcai.org, 2020. (see page 38)
- [53] E. Elkind and A. Slinko. Rationalizations of voting rules. In F. Brandt, V. Conitzer, U. Endriss, J. Lang, and A. D. Procaccia, editors, *Handbook of Computational Social Choice*, chapter 8, pages 169–196. Cambridge University Press, 2016. (see page 8)
- [54] E. Elkind, P. Faliszewski, and A. Slinko. Rationalizations of condorcet-consistent rules via distances of hamming type. *Social Choice and Welfare*, 39(4):891–905, 2012. (see page 8)
- [55] E. Elkind, P. Faliszewski, J. Laslier, P. Skowron, A. Slinko, and N. Talmon. What do multiwinner voting rules do? An experiment over the two-dimensional euclidean domain. In *Proceedings of AAAI-2017*, pages 494–501, 2017. (see page 2)
- [56] E. Elkind, M. Lackner, and D. Peters. Preference restrictions in computational social choice: A survey. Technical Report arXiv.2205.09092 [cs.GT], arXiv.org, 2022. (see page 9)
- [57] J. Enelow and M. Hinich. *The Spatial Theory of Voting: An Introduction*. Cambridge University Press, 1984. (see page 2, 12)
- [58] J. Enelow and M. Hinich. *Advances in the Spatial Theory of Voting*. Cambridge University Press, 1990. (see page 2, 12)

- [59] G. Erdélyi, M. Fellows, J. Rothe, and L. Schend. Control complexity in Bucklin and fallback voting: An experimental analysis. *Journal of Computer and System Sciences*, 81(4):661–670, 2015. (see page 1, 2)
- [60] Ö. Egecioğlu and A. Giritligil. The impartial, anonymous, and neutral culture model: A probability model for sampling public preference structures. *Journal of Mathematical Sociology*, 37(4): 203–222, 2013. (see page 12)
- [61] P. Faliszewski, P. Skowron, A. Slinko, and N. Talmon. Multiwinner analogues of the plurality rule: Axiomatic and algorithmic views. In *Proceedings of AAAI-2016*, pages 482–488, 2016. (see page 38)
- [62] P. Faliszewski, P. Skowron, A. Slinko, and N. Talmon. Multiwinner voting: A new challenge for social choice theory. In U. Endriss, editor, *Trends in Computational Social Choice*. AI Access Foundation, 2017. (see page 38)
- [63] P. Faliszewski, P. Skowron, A. Slinko, and N. Talmon. Multiwinner rules on paths from k -Borda to Chamberlin–Courant. In *Proceedings of IJCAI-2017*, pages 192–198, 2017. (see page 2, 37)
- [64] P. Faliszewski, M. Lackner, D. Peters, and N. Talmon. Effective heuristics for committee scoring rules. In *Proceedings of AAAI-2018*, pages 1023–1030, 2018. (see page 1, 2, 38, 40)
- [65] P. Faliszewski, A. Slinko, K. Stahl, and N. Talmon. Achieving fully proportional representation by clustering voters. *Journal of Heuristics*, 24(5):725–756, 2018. (see page 1, 2)
- [66] P. Faliszewski, A. Karpov, and S. Obraztsova. The complexity of election problems with group-separable preferences. *Autonomous Agents and Multi-Agent Systems*, 36(1):18, 2022. (see page 11)
- [67] P. Faliszewski, A. Kaczmarczyk, K. Sornat, S. Szufa, and T. Was. Diversity, agreement, and polarization in elections. In *Proceedings of IJCAI-2023*, pages 2684–2692, 2023. (see page 8, 29, 51)
- [68] P. Faliszewski, M. Lackner, K. Sornat, and S. Szufa. An experimental comparison of multiwinner voting rules on approval elections. In *Proceedings of IJCAI-2023*, pages 2675–2683, 2023. (see page 8, 51)
- [69] P. Faliszewski, K. Sornat, and S. Szufa. The complexity of subelection isomorphism problems. *Journal of Artificial Intelligence Research*, 80:1343–1371, 2024. (see page 32, 49)
- [70] P. Faliszewski, P. Skowron, A. Slinko, K. Sornat, S. Szufa, and N. Talmon. How similar are two elections? *Journal of Computer and System Sciences*, 150:103632, 2025. (see page 5, 14, 23)
- [71] T. Fruchterman and E. Reingold. Graph drawing by force-directed placement. *Software: Practice and Experience*, 21(11):1129–1164, 1991. (see page 5, 9, 26, 62)
- [72] R. Gandhi, S. Khuller, S. Parthasarathy, and A. Srinivasan. Dependent rounding and its applications to approximation algorithms. *Journal of the ACM*, 53(3):324–360, 2006. (see page 18)
- [73] J. Goldsmith, J. Lang, N. Mattei, and P. Perny. Voting with rank dependent scoring rules. In *Proceedings of AAAI-2014*, pages 698–704, 2014. (see page 1, 2)
- [74] B. Hadjibeyli and M. Wilson. Distance rationalization of anonymous and homogeneous voting rules. *Social Choice and Welfare*, 52(3):559–583, 2019. (see page 8)

- [75] E. Hemaspaandra, L. Hemaspaandra, and J. Rothe. Exact analysis of Dodgson elections: Lewis Carroll’s 1876 voting system is complete for parallel access to NP. *Journal of the ACM*, 44(6): 806–825, 1997. (see page 37)
- [76] K. Inada. A note on the simple majority decision rule. *Econometrica*, 32(32):525–531, 1964. (see page 3, 11)
- [77] K. Inada. The simple majority decision rule. *Econometrica*, 37(3):490–506, 1969. (see page 3, 11)
- [78] T. Kamada and S. Kawai. An algorithm for drawing general undirected graphs. *Information Processing Letters*, 31(1):7–15, 1989. (see page 5, 9, 23, 26, 62)
- [79] T. Kamishima. Nantonac collaborative filtering: Recommendation based on order responses. In *Proceedings of KDD-2003*, pages 583–588, 2003. (see page 8, 43)
- [80] A. Karpov. On the number of group-separable preference profiles. *Group Decision and Negotiation*, 28(3):501–517, 2019. (see page 11)
- [81] O. Keller, A. Hassidim, and N. Hazon. New approximations for coalitional manipulation in scoring rules. *Journal of Artificial Intelligence Research*, 64:109–145, 2019. (see page 1, 2)
- [82] M. Kilgour. Approval balloting for multi-winner elections. In *Handbook on Approval Voting*, pages 105–124. Springer, 2010. Chapter 6. (see page 2, 37)
- [83] J. Kruskal. Multidimensional scaling by optimizing goodness of fit to a nonmetric hypothesis. *Psychometrika*, 29(1):1–27, 1964. (see page 5, 9, 26, 62)
- [84] M. Lackner. Perpetual voting: Fairness in long-term decision making. In *Proceedings of AAAI-2020*, pages 2103–2110, 2020. (see page 2)
- [85] M. Lackner and P. Skowron. *Multi-Winner Voting with Approval Preferences*. Springer, 2023. (see page 37)
- [86] J.-F. Laslier and K. Van Der Straeten. A live experiment on approval voting. *Experimental Economics*, 11(1):97–105, 2008. (see page 9)
- [87] D. Leep and G. Myerson. Marriage, magic, and solitaire. *The American Mathematical Monthly*, 106(5):419–429, 1999. (see page 18, 60)
- [88] J. Lu, D. Zhang, Z. Rabinovich, S. Obraztsova, and Y. Vorobeychik. Manipulating elections by selecting issues. In *Proceedings of AAMAS-19*, pages 529–537, 2019. (see page 1)
- [89] T. Lu and C. Boutilier. Budgeted social choice: From consensus to personalized decision making. In *Proceedings of IJCAI-2011*, pages 280–286, 2011. (see page 1, 40)
- [90] T. Lu and C. Boutilier. Robust approximation and incremental elicitation in voting protocols. In *Proceedings of IJCAI-2011*, pages 287–293, 2011. (see page 1)
- [91] T. Lu and C. Boutilier. Effective sampling and learning for mallows models with pairwise-preference data. *Journal of Machine Learning Research*, 15(1):3783–3829, 2014. (see page 12)
- [92] C. Mallows. Non-null ranking models. *Biometrika*, 44:114–130, 1957. (see page 2, 12)

- [93] N. Mattei and T. Walsh. Preflib: A library for preferences. In *Proceedings of ADT-2013*, pages 259–270, 2013. (see page 2, 4, 43, 50)
- [94] N. Mattei, J. Forshee, and J. Goldsmith. An empirical study of voting rules and manipulation with large datasets. In *Proceedings of COMSOC-2012*, 2012. (see page 2)
- [95] J. McCabe-Dansted and A. Slinko. Exploratory analysis of similarities between social choice rules. *Group Decision and Negotiation*, 15:77–107, 2006. (see page 2, 12)
- [96] T. Meskanen and H. Nurmi. Closeness counts in social choice. In M. Braham and F. Steffen, editors, *Power, Freedom, and Voting*. Springer-Verlag, 2008. (see page 8)
- [97] E. Micha and N. Shah. Can we predict the election outcome from sampled votes? In *Proceedings of AAAI-2020*, pages 2176–2183, 2020. (see page 1, 2)
- [98] T. Minka. Automatic choice of dimensionality for PCA. *Proceedings of NIPS-2000*, 13, 2000. (see page 9)
- [99] J. Mirrlees. An exploration in the theory of optimal income taxation. *Review of Economic Studies*, 38:175–208, 1971. (see page 3, 10)
- [100] K. Munagala, Z. Shen, and K. Wang. Optimal algorithms for multiwinner elections and the chamberlin-courant rule. In *Proceedings of EC-2021*, pages 697–717, 2021. (see page 38, 40)
- [101] G. Nemhauser, L. Wolsey, and M. Fisher. An analysis of approximations for maximizing submodular set functions. *Mathematical Programming*, 14(1):265–294, December 1978. (see page 40)
- [102] S. Nitzan. Some measures of closeness to unanimity and their implications. *Theory and Decision*, 13(2):129–138, 1981. (see page 8)
- [103] S. Obraztsova and E. Elkind. Optimal manipulation of voting rules. In *Proceedings of AAAI-2012*, pages 2141–2147, 2012. (see page 8)
- [104] S. Obraztsova, E. Elkind, P. Faliszewski, and A. Slinko. On swap-distance geometry of voting rules. In *Proceedings of AAMAS-13*, pages 383–390, 2013. (see page 8)
- [105] S. Obraztsova, E. Elkind, and P. Faliszewski. On swap convexity of voting rules. In *Proceedings of AAAI-2020*, pages 1910–1917, 2020. (see page 8)
- [106] J. O’Neill. Open STV, www.openstv.org. 2013. (see page 8, 43)
- [107] J. Oren, Y. Filmus, and C. Boutilier. Efficient vote elicitation under candidate uncertainty. In *Proceedings of the 23rd International Joint Conference on Artificial Intelligence*, page 309–316, 2013. (see page 1)
- [108] D. Peters and M. Lackner. Preferences single-peaked on a circle. *Journal of Artificial Intelligence Research*, 68:463–502, 2020. (see page 10)
- [109] L. Pospisil, M. Hasal, J. Nowakova, and J. Platos. Computation of kamada-kawai algorithm using barzilai-borwein method. In *International Conference on Intelligent Networking and Collaborative Systems*, pages 327–333, 2015. (see page 5)
- [110] A. Procaccia, J. Rosenschein, and A. Zohar. On the complexity of achieving proportional representation. *Social Choice and Welfare*, 30(3):353–362, 2008. (see page 40)

- [111] C. Puppe and A. Slinko. Condorcet domains, median graphs and the single-crossing property. *Economic Theory*, 67(1):285–318, 2019. (see page 10)
- [112] K. Roberts. Voting over income tax schedules. *Journal of Public Economics*, 8(3):329–340, 1977. (see page 3, 10)
- [113] Y. Rubner, C. Tomasi, and L. Guibas. The earth mover’s distance as a metric for image retrieval. *International Journal of Computer Vision*, 40(2):99–121, 2000. (see page 16)
- [114] K. Sapała. Algorithms for embedding metrics in euclidean spaces. Master’s thesis, AGH University of Science and Technology, 2022. (see page 5, 9, 23)
- [115] T. Service and J. Adams. Strategyproof approximations of distance rationalizable voting rules. In *Proceedings of the 11th International Conference on Autonomous Agents and Multiagent Systems*, pages 569–576, 2012. (see page 8)
- [116] P. Skowron, P. Faliszewski, and A. Slinko. Achieving fully proportional representation: Approximability result. *Artificial Intelligence*, 222:67–103, 2015. (see page 1, 2)
- [117] P. Skowron, P. Faliszewski, and J. Lang. Finding a collective set of items: From proportional multirepresentation to group recommendation. *Artificial Intelligence*, 241:191–216, 2016. (see page 2, 37, 38, 40)
- [118] P. Skowron, M. Lackner, M. Brill, D. Peters, and E. Elkind. Proportional rankings. In *Proceedings of IJCAI-2017*, pages 409–415, 2017. (see page 40)
- [119] S. Szufa. *Map of Elections*. PhD thesis, AGH University, 2024. (see page 1, 7)
- [120] S. Szufa, P. Faliszewski, P. Skowron, A. Slinko, and N. Talmon. Drawing a map of elections in the space of statistical cultures. In *Proceedings of AAMAS-20*, pages 1341–1349, 2020. (see page 1, 7, 14)
- [121] S. Szufa, P. Faliszewski, L. Janeczko, M. Lackner, A. Slinko, K. Sornat, and N. Talmon. How to sample approval elections? In *Proceedings of IJCAI-2022*, pages 496–502, 2022. (see page 2, 8, 51)
- [122] T. Thiele. Om flerfoldssvalg. In *Oversigt over det Kongelige Danske Videnskabernes Selskabs Forhandlinger*, pages 415–441. 1895. (see page 2, 37)
- [123] T. Tideman and F. Plassmann. Modeling the outcomes of vote-casting in actual elections. In D. Felsenthal and M. Machover, editors, *Electoral Systems: Paradoxes, Assumptions, and Procedures*, pages 217–251. Springer, 2012. (see page 2)
- [124] T. Walsh. Where are the really hard manipulation problems? The phase transition in manipulating the veto rule. In *Proceedings of IJCAI-2009*, pages 324–329. AAAI Press, July 2009. (see page 1)
- [125] T. Walsh. Where are the hard manipulation problems. *Journal of Artificial Intelligence Research*, 42(1):1–29, 2011. (see page 1, 2)
- [126] T. Walsh. Generating single peaked votes. Technical Report arXiv:1503.02766 [cs.GT], arXiv.org, March 2015. (see page 12, 13)
- [127] J. Wang, S. Sikdar, T. Shepherd, Z. Zhao, C. Jiang, and L. Xia. Practical algorithms for multi-stage voting rules with parallel universes tiebreaking. In *Proceedings of AAAI-2019*, pages 2189–2196, 2019. (see page 1, 2)

- [128] B. Wilder and Y. Vorobeychik. Controlling elections through social influence. In *Proceedings of AAMAS-18*, pages 265–273, 2018. (see page 1)
- [129] Z. Zhang and J. Wang. MLLE: Modified locally linear embedding using multiple weights. *Proceedings of NIPS-2006*, 19, 2006. (see page 9)

Appendix

A Missing Proofs

Proposition 3.3 (★). *Given a position matrix $X \in \mathcal{P}(m)$, one can compute in $O(m^{4.5})$ time an election E that contains at most $m^2 - 2m + 2$ different votes such that $\#\text{pos}(E) = X$.*

Proof. Let X be our input $m \times m$ matrix and let $C = \{c_1, \dots, c_m\}$ be a set of candidates. Our algorithm creates an election $E = (C, V)$ iteratively, as follows. In each iteration we first create a bipartite graph G with vertex sets $A = \{a_1, \dots, a_m\}$ and $B = \{b_1, \dots, b_m\}$. For each $i, j \in [m]$, if $x_{i,j}$ is nonzero, then we put an edge between a_i and b_j (vertices in A correspond to rows of X and vertices in B correspond to the columns). Next, we compute a perfect matching M in G (we will see later that it is guaranteed to exist). Let v be the vote that ranks c_j on position i exactly if $M(a_i) = b_j$ (v is well-defined because M is a perfect matching). Let P be the position matrix corresponding to vote v , i.e., to election $(C, (v))$, and let z be the largest integer such that $X - zP$ contains only non-negative entries. Then, we add z copies of v to V and set $X := X - zP$. We proceed to the next iteration until X becomes the zero matrix.

To prove the correctness of the algorithm, we show that at each iteration the constructed graph G has a perfect matching. Let us assume that this is not the case. Note that each row and each column in the current X sums up to the same integer, say n' . Since there is no perfect matching, by Hall's theorem, there is a subset of vertices $A' \subseteq A$ such that the neighborhood $B' \subseteq B$ of A' in G contains fewer than $|A'|$ vertices. Yet, we have that $\sum_{a_i \in A', b_j \in B'} x_{i,j} = n'|A'|$, as we sum up all the nonzero entries of each row corresponding to a vertex from A' . However, this implies that $|B'| \geq |A'|$ because each column corresponding to a vertex from B' sums up to n' , but we do not necessarily include all its nonzero entries. This is a contradiction.

The algorithm terminates after at most $m^2 - m + 1$ steps (in each step at least one more entry of X becomes zero, and in the last step, m entries become zero). Each step requires $\mathcal{O}(m^{2.5})$ time to compute the matching, so the overall running time is $\mathcal{O}(m^{4.5})$. This implies that V contains at most $m^2 - m + 1$ different votes; indeed, using a similar argument as in Leep and Myerson [87] it can be shown that the algorithm always terminates after at most $m^2 - 2m + 2$ steps. \square

Proposition 3.5 (★). *If m is divisible by 4, then it holds that:*

1. $\text{POS}(\text{ID}_m, \text{UN}_m) = \frac{1}{3}(m^2 - 1)$,
2. $\text{POS}(\text{ID}_m, \text{AN}_m) = \text{POS}(\text{UN}_m, \text{ST}_m) = \frac{m^2}{4}$,
3. $\text{POS}(\text{ID}_m, \text{ST}_m) = \text{POS}(\text{UN}_m, \text{AN}_m) = \frac{2}{3}(\frac{m^2}{4} - 1)$,
4. $\text{POS}(\text{AN}_m, \text{ST}_m) = \frac{13}{48}m^2 - \frac{1}{3}$.

Proof. ID_m and UN_m: We start by computing the distance between ID_m and UN_m . Note that UN_m always remains the same matrix independent of how its columns are ordered. Thus, we can compute the distance between these two matrices using the identity permutation between the columns of the two matrices: $\text{POS}(\text{ID}_m, \text{UN}_m) = \sum_{i=1}^m \text{emd}((\text{ID}_m)_i, (\text{UN}_m)_i) = \sum_{i=1}^m (\sum_{j=1}^{i-1} \frac{j}{m} + \sum_{j=1}^{m-i} \frac{j}{m})$
 $= \frac{1}{m} \sum_{i=1}^m (\frac{1+(i-1)}{2}(i-1) + \frac{1+(m-i)}{2}(m-i))$
 $= \frac{1}{2m} \sum_{i=1}^m (2i^2 - 2i - 2mi + m^2 + m)$
 $= \frac{1}{2m} (2 \frac{m(m+1)(2m+1)}{6} - m(m+1) - m^2(m+1) + m(m^2 + m))$

$$\begin{aligned}
&= \frac{1}{2m} \left(\frac{(m^2+m)(2m+1)}{3} - (m+1)(m+m^2) + m(m^2+m) \right) \\
&= \frac{m+1}{2} \left(\frac{(2m+1)}{3} - (m+1) + m \right) = \frac{(m+1)(m-1)}{3} = \frac{1}{3}(m^2-1).
\end{aligned}$$

In the following, we use (*) when we omit some calculations analogous to the calculations for $\text{POS}(\text{ID}_m, \text{UN}_m)$.

UN_m and ST_m: Similarly, we can also directly compute the distance between UN_m and ST_m using the identity permutation between the columns of the two matrices. In this case, all column vectors of the two matrices have indeed the same emd distance to each other:

$$\text{POS}(\text{UN}_m, \text{ST}_m) = m \cdot \left(\frac{1}{2} + 2 \cdot \sum_{i=1}^{\frac{m}{2}-1} \frac{i}{m} \right) = \frac{m}{2} + \frac{m}{2} \left(\frac{m}{2} - 1 \right) = \frac{m^2}{4}.$$

UN_m and AN_m: Next, we compute the distance between UN_m and AN_m using the identity permutation between the columns of the two matrices. Recall that AN_m can be written as:

$$\text{AN}_m = 0.5 \begin{bmatrix} \text{ID}_{m/2} & \text{rID}_{m/2} \\ \text{rID}_{m/2} & \text{ID}_{m/2} \end{bmatrix}.$$

Thus, it is possible to reuse our ideas from computing the distance between identity and uniformity:

$$\text{POS}(\text{UN}_m, \text{AN}_m) = 4 \sum_{i=1}^{\frac{m}{2}} \left(\sum_{j=1}^{i-1} \frac{j}{m} + \sum_{j=1}^{\frac{m}{2}-i} \frac{j}{m} \right) = (*) = \frac{2}{3} \left(\frac{m^2}{4} - 1 \right).$$

ID_m and ST_m: There exist only two different types of column vectors in ST_m , i.e., $\frac{m}{2}$ columns starting with $\frac{m}{2}$ entries of value $\frac{2}{m}$ followed by $\frac{m}{2}$ zero-entries and $\frac{m}{2}$ columns starting with $\frac{m}{2}$ zero entries followed by $\frac{m}{2}$ entries of value $\frac{2}{m}$. In ID_m , $\frac{m}{2}$ columns have a one entry in the first $\frac{m}{2}$ rows and $\frac{m}{2}$ columns have a one entry in the last $\frac{m}{2}$ rows. Thus, again the identity permutation between the columns of the two matrices minimizes the emd distance:

$$\text{POS}(\text{ID}_m, \text{ST}_m) = 2 \cdot \text{POS}(\text{ID}_{\frac{m}{2}}, \text{UN}_{\frac{m}{2}}) = \frac{2}{3} \left(\frac{m^2}{4} - 1 \right)$$

AN_m and ST_m: We now turn to computing the distance between $\text{AN}_m = (\text{an}_1, \dots, \text{an}_m)$ and $\text{ST}_m = (\text{st}_1, \dots, \text{st}_m)$. As all column vectors of AN_m are palindromes, each column vector of AN_m has the same emd distance to all column vectors of ST_m , i.e., for $i \in [m]$ it holds that $\text{emd}(\text{an}_i, \text{st}_j) = \text{emd}(\text{an}_i, \text{st}_{j'})$ for all $j, j' \in [m]$. Thus, the distance between AN_m and ST_m is the same for all permutation between the columns of the two matrices. Thus, we again use the identity permutation. We start by computing $\text{emd}(\text{an}_i, \text{st}_i)$ for different $i \in [m]$ separately distinguishing two cases. Let $i \in [\frac{m}{4}]$. Recall that an_i has a 0.5 at position i and position $m-i+1$ and that st_i has a $\frac{2}{m}$ at entries $j \in [\frac{m}{2}]$. We now analyze how to transform an_i to st_i . For all $j \in [i-1]$, it is clear that it is optimal that the value $\frac{2}{m}$ moved to position j comes from position i . The overall cost of this is $\sum_{j=1}^{i-1} \frac{2j}{m}$. Moreover, the remaining surplus value at position i (that is, $\frac{1}{2} - \frac{2i}{m}$) needs to be moved toward the end. Thus, for $j \in [i+1, \frac{m}{4}]$, we move value $\frac{2}{m}$ from position i to position j . The overall cost of this is $\sum_{j=1}^{\frac{m}{4}-i} \frac{2j}{m}$. Lastly, we need to move value $\frac{2}{m}$ to positions $j \in [\frac{m}{4}+1, \frac{m}{2}]$. This needs to come from position $m-i+1$. Thus, for each $j \in [\frac{m}{4}+1, \frac{m}{2}]$, we move value $\frac{2}{m}$ from position $m-i+1$ to position j . The overall cost of this is $\frac{1}{2} \cdot \left(\frac{m}{2} - i \right) + \sum_{j=1}^{\frac{m}{4}} \frac{2j}{m} = \frac{1}{2} \left(\frac{m}{2} - i \right) + \frac{m}{16} + \frac{1}{4}$.

Now, let $i \in [\frac{m}{4}+1, \frac{m}{2}]$. For $j \in [\frac{m}{4}]$, we need to move value $\frac{2}{m}$ from position i to position j . The overall cost of this is $\frac{1}{2} \cdot \left(i - \frac{m}{4} - 1 \right) + \sum_{j=1}^{\frac{m}{4}} \frac{2j}{m} = \frac{1}{2} \cdot \left(i - \frac{m}{4} - 1 \right) + \frac{m}{16} + \frac{1}{4}$. For $j \in [\frac{m}{4}+1, \frac{m}{2}]$, we need to move value $\frac{2}{m}$ from position $m-i+1$ to position j . The overall cost of this is $\frac{1}{2} \cdot \left(\frac{m}{2} - i \right) + \sum_{j=1}^{\frac{m}{4}} \frac{2j}{m} = \frac{1}{2} \cdot \left(\frac{m}{2} - i \right) + \frac{m}{16} + \frac{1}{4}$.

Observing that the case $i \in [\frac{3m}{4}+1, m]$ is symmetric to $i \in [\frac{m}{4}]$ and the case $i \in [\frac{m}{2}+1, \frac{3m}{4}]$ is symmetric to $i \in [\frac{m}{4}+1, \frac{m}{2}]$ the emd distance between AN_m and ST_m can be computed as follows:

$$\begin{aligned}
\text{POS}(\text{AN}_m, \text{ST}_m) &= 2 \cdot \left(A + \frac{1}{2} \cdot \left(\sum_{i=1}^{\frac{m}{4}} \frac{m}{2} - i \right) + \frac{m}{4} \cdot \left(\frac{m}{16} + \frac{1}{4} \right) + \frac{1}{2} \cdot \left(\sum_{i=\frac{m}{4}+1}^{\frac{m}{2}} \left(i - \frac{m}{4} - 1 \right) \right) + \frac{m}{4} \cdot \left(\frac{m}{16} + \frac{1}{4} \right) \right. \\
&\quad \left. + \frac{1}{2} \cdot \left(\sum_{i=\frac{m}{2}+1}^{\frac{3m}{4}} \frac{m}{2} - i \right) + \frac{m}{4} \cdot \left(\frac{m}{16} + \frac{1}{4} \right) \right)
\end{aligned}$$

dataset	FR	average PCC values	
		MDS	KK
4×100	0.9226 ± 0.0083	0.9664 ± 0.0031	0.9661 ± 0.0044
10×100	0.9095 ± 0.0098	0.9649 ± 0.0032	0.9686 ± 0.0061
20×100	0.9135 ± 0.0105	0.9657 ± 0.0036	0.9745 ± 0.0015
100×100	0.9174 ± 0.0088	0.9731 ± 0.0051	0.9735 ± 0.0115

Table 9: Average values of the PCC between the original and embedded distances for collections of datasets of various sizes. After the \pm signs we report the standard deviations.

$$\begin{aligned}
&= \frac{m^2}{48} - \frac{1}{3} + \frac{3m^2-4m}{32} + \frac{m}{2} \cdot \left(\frac{m}{16} + \frac{1}{4}\right) + \frac{m^2-4m}{32} + \frac{m}{2} \cdot \left(\frac{m}{16} + \frac{1}{4}\right) + \frac{m^2-4m}{32} + \frac{m}{2} \cdot \left(\frac{m}{16} + \frac{1}{4}\right) \\
&= \frac{m^2}{48} - \frac{1}{3} + \frac{3m^2-4m}{32} + \frac{3m}{2} \left(\frac{m}{16} + \frac{1}{4}\right) + \frac{m^2-4m}{16} = \left(\frac{1}{48} + \frac{3}{32} + \frac{3}{32} + \frac{1}{16}\right)m^2 + \left(-\frac{4}{32} + \frac{3}{8} - \frac{4}{16}\right)m = \frac{13}{48}m^2 - \frac{1}{3}m
\end{aligned}$$

with

$$A = \sum_{i=1}^{\frac{m}{4}} \left(\sum_{j=1}^{i-1} \frac{2j}{m} + \sum_{j=1}^{\frac{m}{4}-i} \frac{2j}{m} \right) = (*) = \frac{1}{6} \left(\frac{m^2}{16} - 1 \right) = \frac{1}{2} \left(\frac{m^2}{48} - \frac{1}{3} \right)$$

ID_m and AN_m: Lastly, we consider $ID_m = (id_1, \dots, id_m)$ and $AN_m = (an_1, \dots, an_m)$. Note that, for $i \in [m]$, id_i contains a 1 at position i and an_i contains a 0.5 at position i and position $m-i$. Note further that for $i \in [\frac{m}{2}]$ it holds that $an_i = an_{m-i+1}$. Fix some $i \in [\frac{m}{2}]$. For all $j \in [i, m-i+1]$ it holds that $\text{emd}(an_i, id_j) = \frac{m-2i+1}{2}$ and for all $j \in [1, i-1] \cup [m-i+2, m]$ it holds that $\text{emd}(an_i, id_j) > \frac{m-2i+1}{2}$. That is, for every $i \in [m]$, an_i has the same distance to all column vectors of ID_m where the one entry lies in between the two 0.5 entries of an_i but a larger distance to all column vectors of ID_m where the one entry is above the top 0.5 entry of an_i or below the bottom 0.5 entry of an_i . Thus, it is optimal to choose a mapping of the column vectors such that for all $i \in [m]$ it holds that an_i is mapped to a vector id_j where the one entry of id_j lies between the two 0.5 in an_i . This is, among others, achieved by the identity permutation, which we use to compute:

$$\text{POS}(ID_m, AN_m) = 2 \sum_{i=1}^{\frac{m}{2}} \left(\frac{1}{2} (m - 2i + 1) \right) = \frac{m}{2}m - \frac{m}{2} \left(\frac{m}{2} + 1 \right) + \frac{m}{2} = \frac{m^2}{4} \quad \square$$

B Different Embeddings and Their Robustness

In this section, we provide the results of the accuracy experiments from Section 4.3 for the embedding algorithms of Fruchterman-Reingold (FR) [71], Kamada-Kawai (KK) [78], and for Multidimensional Scaling algorithm (MDS) [44, 83]. The results for KK from the main body of the paper are repeated in this section, for comparison. Overall, we find that KK is either superior or nearly as good as each of the other ones.

In Figure 14 we show maps of elections of the 100x100 dataset from Section 4 obtained using the three embedding algorithms. While the three maps in Figure 14 are different in some ways, for example, the MDS one has the most compact clusters of points and the FR one has the most scattered ones, on the high level they are similar. For example, they all have IC, SPOC, and 4-Sphere elections very close to the UN matrix, they all have a path of Mallows elections forming an arc between the UN and ID matrices, and they all have hypercube elections in the same area and in the same relation with respect to each other (and with respect to the other elections).

B.1 Correlation Between the Positionwise and Euclidean Distances

For each of the maps from Figure 14, we have computed the PCC between the vector of the original distances and the vector of the embedded ones. For the KK method the PCC is the highest and is equal to 0.9805, for the MDS method it is equal to 0.9748 and for the FR method it is equal 0.9364. In Table 9 we report average PCC values and standard deviations for the three embedding algorithms and

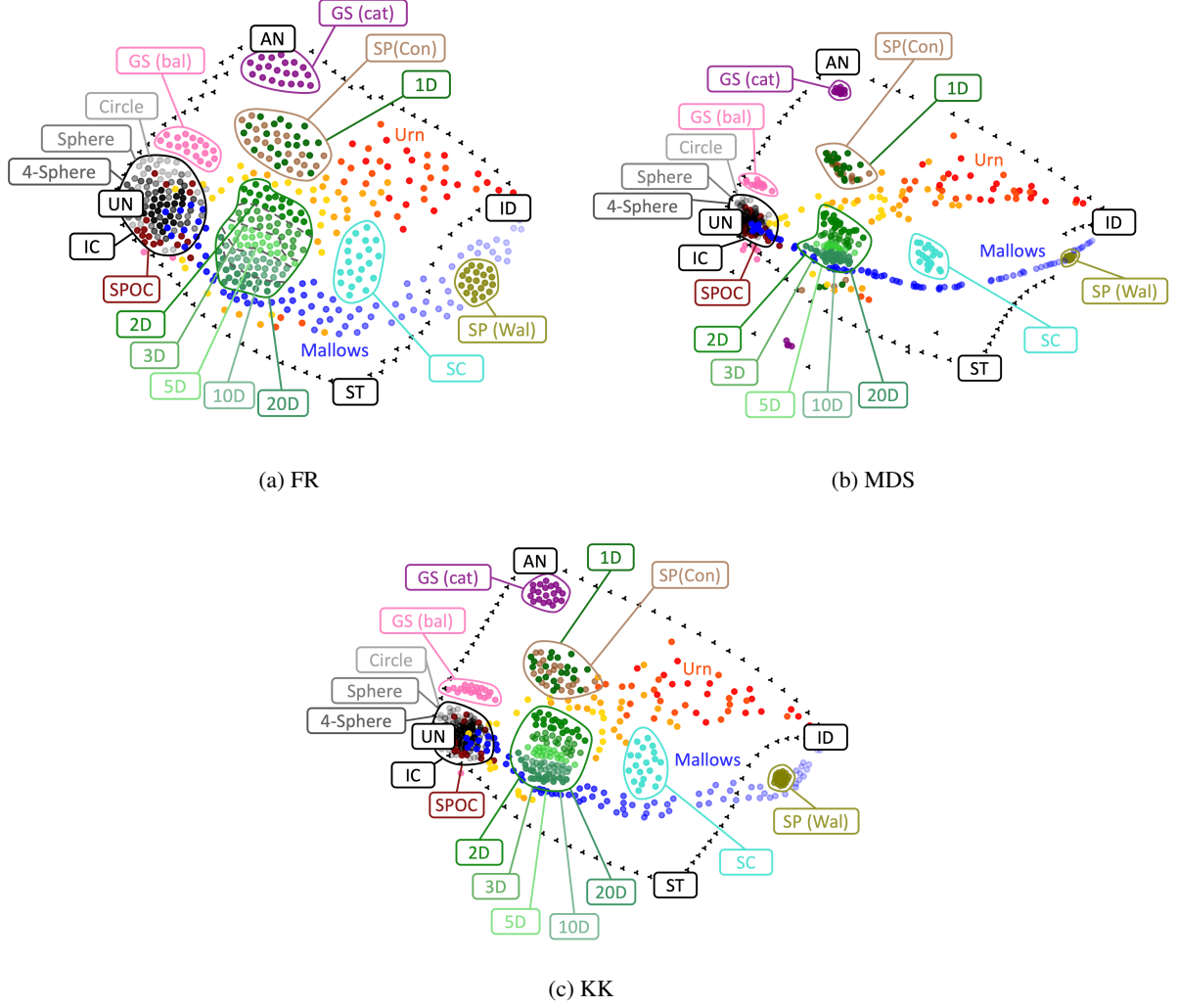


Figure 14: Maps of elections obtained using the (a) Fruchterman-Reingold algorithm (FR), (b) the Multidimensional Scaling algorithm (MDS), and the Kamada-Kawai algorithm (KK). The colors of the dots correspond to the statistical culture from which the elections are generated. Elections generated from the Mallows model use the blue color, and the more pale they are, the closer is the norm- ϕ parameter to 0. The urn elections use yellow-red colors, and the more red they are, the larger is the contagion parameter α .

collections of datasets of various sizes (for our three maps of the 100×100 dataset we chose very good embeddings, whose PCC values are superior to the averages reported in Table 2).

B.2 Monotonicity

Our next evaluation metric is what we call *monotonicity*. The intuition is that if the original distance between elections X and Y is larger than the original distance between elections X and Z , then we expect that the same will hold for the embedded distances.

Formally, for a given embedding summary $Q = (\mathcal{E}, d_{\mathcal{M}}, d_{\text{Euc}})$ and a given election $X \in \mathcal{E}$, we define the average monotonicity of this election in the embedding summary to be:

$$\mu_Q(X) = \frac{1}{|\binom{\mathcal{E}-1}{2}|} \sum_{Y, Z \in \mathcal{E} \setminus X} \Delta_X(Y, Z),$$

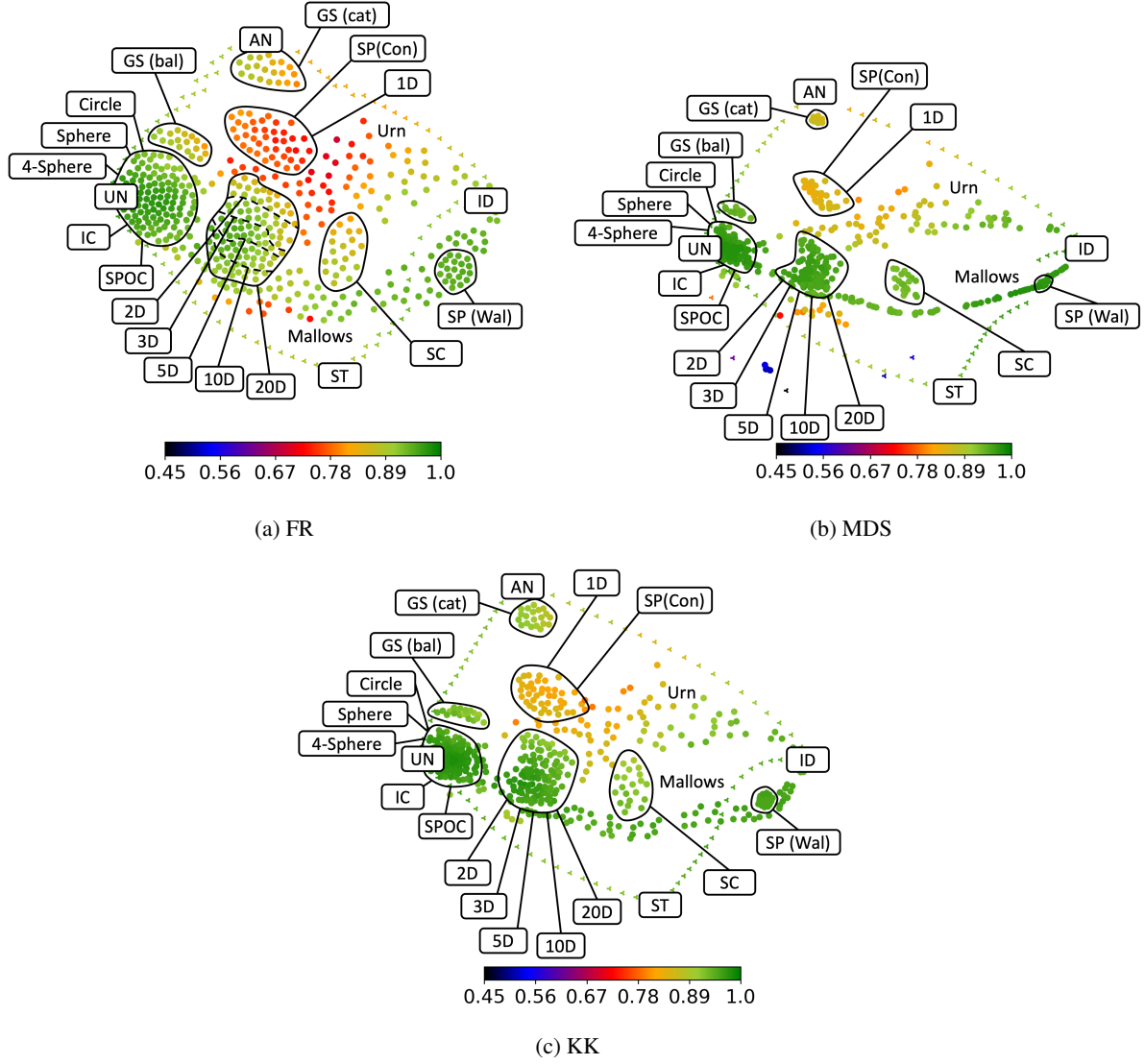


Figure 15: Monotonicity coloring for the three embeddings from Figure 5. Each election X (i.e., each point X) has a color reflecting its value $\mu(X)$ for the respective embedding.

where $\Delta_X(Y, Z)$ is equal to 1, if

$$\text{sgn}(d_{\text{Euc}}(X, Y) - d_{\text{Euc}}(X, Z)) = \text{sgn}(d_{\mathcal{M}}(X, Y) - d_{\mathcal{M}}(X, Z)),$$

and is equal to 0 otherwise. Positive (negative) signs in the above equation mean that both the original and the embedded distances between X and Y were larger (smaller) than the distances between X and Z . The larger is the average monotonicity, the better.

In Figure 15 we present the three maps from Figure 5 where each point (election) is colored accordingly to its monotonicity value. The larger (the closer to green) the value, the better, and the lower (the closer to black) the value, the worse. Monotonicity equal to 1 means that all inequalities are maintained after the embedding. For all three maps, the main message is the same: Elections from the IC, SPOC, Mallows, Walsh, and multidimensional Euclidean models are nicely embedded. Then, elections from the single-crossing and group-separable models are still fine, but on average worse than the previously mentioned models. Finally, we have elections from the 1D-Interval, Conitzer, and urn models, which are the worst embedded ones (not counting some caterpillar group-separable elections for MDS embedding, which are obviously wrong).

dataset	total average monotonicity values		
	FR	MDS	KK
4×100	0.8684 ± 0.0051	0.8936 ± 0.0044	0.8968 ± 0.0068
10×100	0.8637 ± 0.0112	0.9045 ± 0.0054	0.9130 ± 0.0065
20×100	0.8649 ± 0.0105	0.9091 ± 0.0062	0.9207 ± 0.0040
100×100	0.8689 ± 0.0065	0.9224 ± 0.0076	0.9225 ± 0.0096

Table 10: Total average monotonicity values for collections of datasets of various sizes. After the \pm signs we report the standard deviations.

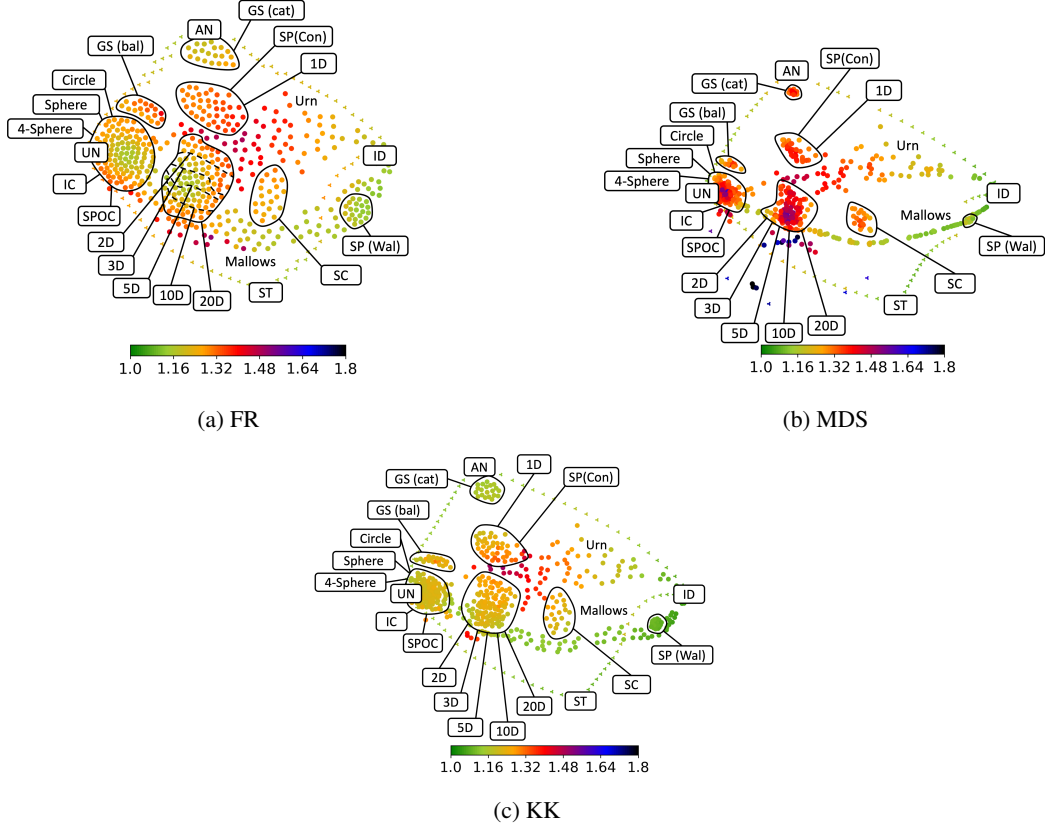


Figure 16: Distortion coloring for the three emdeddings from Figure 5. Each election X (i.e., each point X) has a color reflecting its value $\text{AMR}(X)$ for the respective embedding.

In Table 10 we provide the total average monotonicity values for our collections of dataset. We see that with respect to monotonicity, KK and MDS embeddings perform best, followed by FR. This is in sync with the results regarding the Pearson correlation coefficient.

We mention that instead of defining monotonicity for triples of elections, we could have defined it for quadruples. Given elections X and Y and elections A and B , we could ask if the fact that the original distance between X and Y is smaller than the original distance between A and B implies the same relation between the embedded distances. This would have lead to a somewhat more accurate analysis, but would require significant amount of computation without providing a clear advantage (in each of our datasets, we would have to analyze nearly $480^4 \approx 53 \cdot 10^9$ quadruples of elections).

dataset	total average distortion values		
	FR	MDS	KK
4×100	1.3213 ± 0.0157	1.3099 ± 0.0076	1.2612 ± 0.0158
10×100	1.3119 ± 0.0194	1.3531 ± 0.0108	1.2625 ± 0.0125
20×100	1.2979 ± 0.0195	1.3545 ± 0.0126	1.2406 ± 0.0060
100×100	1.3006 ± 0.0256	1.3225 ± 0.0194	1.2119 ± 0.0123

Table 11: Total average distortion values (i.e., AMR values) for collections of datasets of various sizes. After the \pm signs we report the standard deviations.

B.3 Distortion

In Figure 16, we present the map from Figure 14 with elections colored according to their distortion (i.e., according to their AMR values; recall Section 4.3.2). The best distortion is witnessed by the KK embedding, followed by those for FR and MDS. In the cases of KK and FR, urn elections, as well as 1D-Interval and Conitzer ones, have the highest average distortion. This is in sync with the results regarding monotonicity. In case of MDS, we additionally see elections with high average distortion in the middle of the impartial culture cluster and within the highly dimensional Euclidean clusters.

In Table 11 we present the average values of the average distortions for the three embedding methods and datasets with different numbers of candidates. For each dataset, we compute the average AMR value for its elections, as well as the standard deviation. We observe two patterns. The first one is related to the embedding methods: KK is always the best, followed by FR, with MDS being the worst (except for the 4×100 dataset). The second pattern is that for KK the more candidates there are, the lower is the distortion value. For MDS and FR this relation is not as clear. Overall, for each method the distances in the embedding are, on average, off by 20 – 30%.

C Selection of Preflib Datasets

In Table 12 we list the datasets that were available on Preflib when conducting our experiment on real-life elections (at the end of 2020), including information whether we chose to include it in our study and the reason for rejection (in case we deemed a given dataset unsuitable).

Preflib ID	Name	Inst.	m	Type	Selected	Reason to reject
1	Irish	3	9,12,14	soi	yes	-
2	Debian	8	4-9	toc	no	Too few candidates
3	Mariner	1	32	toc	no	Too many ties
4	Netflix	200	3,4	soc	no	Too few candidates
5	Burlington	2	6	toi	no	Too few candidates
6	Skate	48	14-30	toc	yes	-
7	ERS	87	3-29	soi	yes	-
8	Glasgow	21	8-13	soi	yes	-
9	AGH	2	7,9	soc	no	Too few candidates
10.1	Formula	48	22-62	soi	no	Incomplete and few votes
10.2	Skiing	2	~50	toc	no	Few votes and many ties
11.1	Webimpact	3	103, 240, 242	soc	no	Too many candidates and too few votes (~5)
11.2	Websearch	74	100-200, ~2000	soi	no	
12	T-shirt	1	11	soc	yes	-
13	Anes	19	3-12	toc	no	Too many ties
14	Sushi	1	10	soc	yes	-
15	Clean Web	79	10-50, ~200	soc	no	Too few votes (~4)
16	Aspen	2	5,11	toc	yes	-
17	Berkeley	1	4	toc	no	Too few candidates
18	Minneapolis	4	7,9,379,477	soi	no	Incomplete votes
19	Oakland	7	4-11	toc	no	Incorrect data (votes like: 1,1,1)
20	Pierce	4	4,5,7	toc	no	Too few candidates
21	San Francisco	14	4-25	toc	no	Incorrect data (votes like: 1,1,1)
22	San Leonardo	3	4,5,7	toc	no	Too few candidates
23	Takoma	1	4	toc	no	Too few candidates
24	MT Dots	4	4	soc	no	Too few candidates
25	MT Puzzles	4	4	soc	no	Too few candidates
26	Fench Presidential	6	16	toc	no	Approval ballots
27	Proto French	1	15	toc	no	Approval ballots
28	APA	12	5	soi	no	Too few candidates
29	Netflix NCW	12	3,4	soc	no	Too few candidates
30	UK labor party	1	5	soi	no	Too few candidates
31	Vermont	15	3-6	toc	no	Approval ballots
32	Cujae	7	6,32	soc/soi/toc	no	Multiple issues
33	San Sebastian Poster	2	17	toc	no	Approval ballots
34	Cities survey	2	36, 48	soi	yes	-

Table 12: Overview of all election datasets that are part of the Preflib database (as of the end of 2020). “Inst.” stands for the number of elections in the dataset, “ m ” for the number of candidates and “Type” for the type of the votes in the dataset (“soc” means that all votes are strict complete orders; “soi” means that all votes are strict incomplete orders; “toc” means that all votes are weak incomplete orders).